SUBMILLIMETER SOURCES FOR RADIOMETRY USING HIGH POWER INDIUM PHOSPHIDE GUNN DIODE OSCILLATORS

FINAL REPORT
FOR
CONTRACT NO. NAS7-996

February 9, 1990

PREPARED FOR:

NASA RESIDENT OFFICE - JPL
4800 Oak Grove Drive
Pasadena, CA 91109

PREPARED BY:

MILLITECH CORPORATION
South Deerfield Research Park
P.O. Box 109
South Deerfield, MA 01373
(413) 665-8551

TABLE OF CONTENTS

1.0 INTRODUCTION

1.1 Overview

This final report presents the work performed in a research and development program for millimeter-wave and submillimeter-wave local oscillator sources for radiometry in the frequency range of 60-1000 GHz. This second phase effort was focused on Indium Phosphide Gunn diode oscillators and Schottley-barrier varactor multipliers. The scope of the investigation is outlined in Section 1.2, together with its key objectives. The design criteria and relevant requirements for the local oscillators are summarized in Chapter 2. Theoretical considerations for the design and mode-of-operation are also included. Various options for realizing the source performance for this development are discussed on a comparative basis.

Chapter 3 deals with the construction details and fabrication aspects of various source components examined in this study. Mechanical and electrical parameters of critical importance are described in the context of physical realization of these oscillators and frequency multipliers.

The results of measurements and experimental characterization of the sources implemented in this program are elaborated upon in Chapter 4. An extensive evaluation and measurement program that addressed various elements or aspects of millimeter and submillimeter wave power generation was conducted as an essential part of this study. The results of this effort are also presented in this chapter. The performance of the complete source subsystem is discussed in Chapter 5, which also deals with the experimental characterization of other peripheral components associated with high-frequency millimeter wave sources.

Finally, the prime conclusions of this investigation are summarized in Chapter 6. Future trends in the realm of solid-state sources for radiometry receivers are projected together with some estimations of expected performance. Recommendations for additional work to further this development in this effort are also made here.

1.2 Scope of the Research Program

The research program was multifaceted, and addressed many different aspects of high frequency local oscillator power generation. The primary objectives of the investigation are outlined below:

    (i)   The design, fabrication and performance optimization of exceptionally high power, high frequency Gunn diode oscillators using Indium Phosphide Gunn devices. These are used as pumps or drivers for a new class of multipliers, which are capable of handling a high fundamental input power.

    (ii)   Development of a new generation of frequency multipliers, which can provide high output power at relatively high harmonic conversion efficiencies. These

multipliers (doublers and triplers) will produce useful levels of output power in the 500-700 GHz range when pumped by the Gunn device sources mentioned above.

(iii)   Development of higher-order harmonic extraction oscillators to provide usable local oscillator power at frequencies up to 183 GHz and beyond, where unmultiplied primary solid-state sources are generally not available.

(iv)   Qualification of these newly-developed Indium Phosphide sources and multipliers for spaceborne applications. This includes both device character-ization (qualification), as well as an examination of mechanical considerations for reliable operation of spaceborne active componentry.

(v)   Extending the general capabilities of Gunn diode oscillators and other sources in terms of tunability and power output. In particular, multi-device power combining, injection locking, and broadband mechanical tuning were experimentally investigated quite extensively.

In addition to these goals, this program was also aimed at realizing several additional objectives: Some of these are:

(a)   Characterization of semiconductor devices for millimeter wave power generation applications,

(b)   Establishing design information and database for the implementation of sources in the 60-1000 GHz range. A handbook of sources for radiometric receivers was expected to be a natural offshoot of this research program.

(c)   Examination of various aspects of commercial production of high frequency millimeter wave sources for spaceborne applications was a necessary objective of this endeavor.

1.3   Work Plan

Some of the specific activities of the program are described next. Submillimeter wave receivers employing the newly-developed SIS mixer devices require a moderately low local oscillator power at frequencies in the range of 300 to 1000 GHz. The typical pump requirements are in the range of 1 to 10 μW. Hence, solid-state semiconductor devices were targeted for the L.O. generation at these frequencies.

The chief purpose of this development endeavor was to devise schemes to generate reasonable power anywhere in the 300 - 1000 GHz range through the use of high-power Gunn diode sources and a chain of frequency multipliers. Experimental demonstration of this technique was focussed for 500 GHz. When used in conjunction with either a quasi-optical frequency doubler, or with a subharmonically-pumped mixer, this source can provide

local oscillator power for a receiver at 1000 GHz, the typical highest frequency of interest for Explorer Spectrometer or similar instruments. The baseline approach was to use a 83.3 GHz Indium Phosphide Gunn diode oscillator to drive a balanced doubler cascaded with a tripler to produce X6 multiplication to 500 GHz.

Indium Phosphide Gunn diode oscillators are of considerable significance in radiometry applications, as they provide the necessary pump power for frequency multipliers, as well as subharmonically-pumped mixers. A fairly extensive examination of these oscillators utilizing various modes of operations, and every commercially available device-type was carried out. The main objectives were:

(i)   to characterize various devices for oscillator and amplifier applications,

(ii) develop a design guideline and databank for producing a source at practically any frequency of interest,

(iii) to extend the capability of present oscillators well beyond the established performance levels in terms of their frequency and power.

New configurations and novel circuit structures were developed to achieve the above objectives. Commercially-available devices have standard packages and rather rigid electrical parameters selected by the manufacturer, which impose a severe limitation on their ultimate performance. This study was aimed at extracting the maximum performance potential using standard devices for the targeted applications. Device modifications and their influence on the eventual performance was studied theoretically, since the time and cost considerations prohibited any major effort in the area of new device or package development. The commercially-available devices and their characteristics will be described in Chapter 4.

2.0 SOURCE DESIGN CONSIDERATIONS

2.1 Introduction

The design of high performance submillimeter source subsystems involves a multitude of technical considerations and factors. Several options or alternate implementation architectures are available for a particular local oscillator requirement. Generally, a tradeoff study is required to determine the optimal scheme for the realization of a source at a specific frequency of operation.

The critical considerations for the overall scheme of configuring a source are as follows:

      (1)   Cascaded multipliers versus higher-order harmonic generator,

      (2)   Multiplier factor selection,

      (3)   Efficiency, power output, bandwidth tradeoffs,

      (4)   Individual multiplier capabilities and limitations,

      (5)   Pump power availability,

      (6)   Versatility of operation.

Once a particular scheme has been selected, the individual source components must be specified with ranges of acceptable performance for meeting the overall source subsystem requirements. In the following section, the design deliberations for the 500 GHz source are presented in detail.

2.2 Source Scheme for 500 GHz Operation

The objective of this development was to implement a 500 GHz local oscillator with the following performance characteristics:

Center Frequency of Operation	500 GHz
Power Output	0.5 mW min.
Bandwidth	4 GHz
Efficiency (pump to output)	1% min.

In the submillimeter-wave range, typically only higher-order multipliers (X4, X6) or harmonic generators have been available. These are relatively simple to implement, easy to operate, and offer low to moderate power levels. However, in order to produce higher power at these high frequencies, it is advantageous to use cascaded multipliers for the following reason. In two (or more) stages of multiplication, it is possible to optimize each multiplier for its specific operating conditions, and hence obtain an overall superior

performance in comparison to a higher-order multiplier. For a two-stage case, the first multiplier uses relatively higher capacitance diodes, optimized for higher power handling capability. The second stage, which operates at a lower power level, can utilize a lower capacitance varactor diode to achieve highest cutoff frequency, and an optimal efficiency of multiplication. It should be noted that the overall harmonic conversion efficiency of the cascaded multipliers and higher-order multipliers is comparable, while cascaded versions offer significantly higher power handling capacity, and hence a greater output power at these submillimeter wave frequencies.

The lower-order multipliers used in cascaded multiplication scheme require fewer or no idler circuits at intermediate harmonic frequencies in order to obtain optimal results. Consequently, their design and construction (and overall operation) is simpler than that of higher-order multipliers with many idlers.

Newly-developed multiplying varactors now offer a very wide range of capacitances and breakdown voltages, making it possible to achieve truly optimal operation in conjunction with the multiplier designs developed in this research effort. High input power handling capacity of these newly developed varactors is the key factor in attaining the objectives of this source development program.

The baseline design for the 500 GHz source subsystem is shown in Figure 2.1. The power levels and frequencies associated with this scheme are also indicated. The prime pump power is supplied by an Indium Phosphide high power Gunn diode oscillator, which is described in Section 2.3 in considerable detail. The basic operating features of this oscillator are:

Frequency Range of operation:	79-84 GHz
Power output	80-140 mW
Bias tunability	100 MHz
Technical approach	Dual diode combiner

The first doubler, which operates under high power pump conditions was developed with the following design goals:

Frequency range of operation	158-168 GHz
Input power handling capacity	100 mW min.
Efficiency of second-harmonic conversion	33%
Output power level	20 mW min.
Instantaneous bandwidth	2 GHz

The output tripler was developed with a view to achieve highest possible efficiency at moderately high input power levels. The design objectives for this frequency tripler in this cascaded source are:

|	
Output frequency range	500 GHz
Output power	0.5 mW
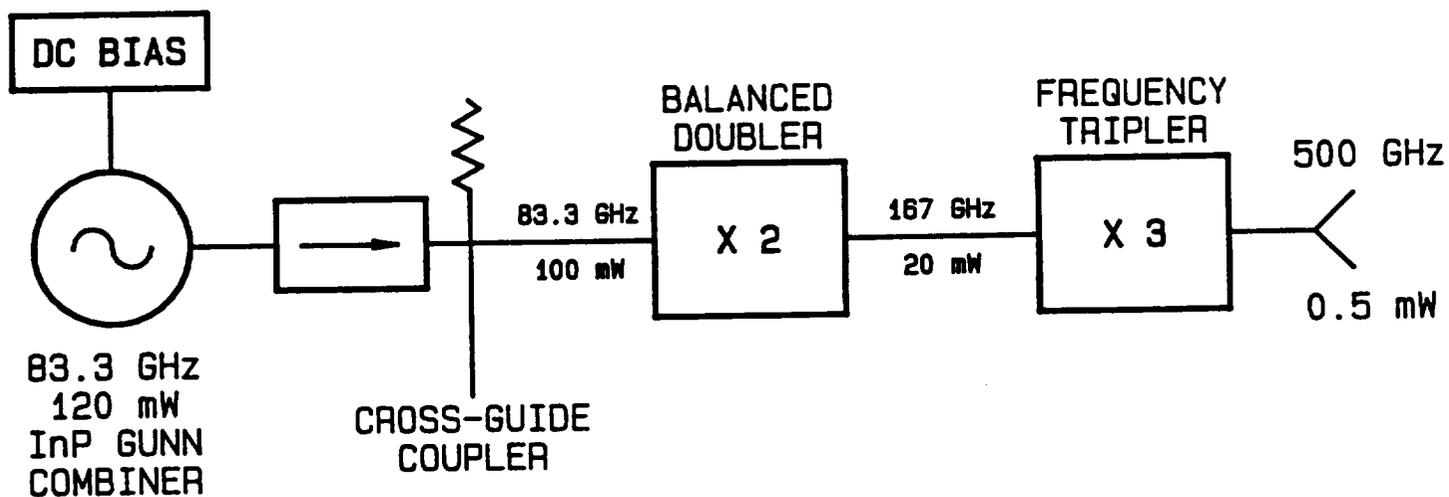
Figure 2.1 500 GHz source baseline architecture.

Efficiency of harmonic generation	2-5%
Instantaneous bandwidth	5 GHz

The details of design and construction of individual source components are given in the following sections.

2.3   High Power InP Oscillator Design

The high power source to drive the first stage doubler posed many technical challenges. The performance requirements, as listed above in Section 2.2, mandate a new source design, since existing sources using available devices were unable to achieve the required power levels. Typical commercial devices are rated in the 80-90 mW power output region. Development of a superior device was considered, but determined to be non-viable, both from technical and economic standpoints. The most appropriate option was to employ some power-combining scheme which could meet all the desired characteristics. A wide variety of Gunn diode power-combining techniques are applicable to the present situation. The most significant and practical options for this requirement are as follows:

(i)   In-line or series combining using multiple Gunn diodes with independent resonators and bias circuits.

(ii)   Multi-device chip level combining to produce a single diode package for use in a "standard" design oscillator.

(iii)   Radial combiners, which utilize several diodes located along radially distributed resonators, and power combined at the central junction.

(iv)   Vertically stacked diodes using a single resonator.

These schemes are depicted in Figure 2.2, and have been described in reference [1] in considerable detail. From the power output requirement standpoint, only two Indium Phosphide Gunn devices were determined to be adequate. Hence, a radial combiner was unnecessary. While multi-chip combining was a very attractive technical option, there were practical difficulties in securing devices which were specially fabricated for this requirement. Multi-device combining on a single package necessitated additional development, and long deliveries from qualified vendors. Therefore, this approach was not pursued beyond the theoretical design stage.

A vertically-stacked device combiner has the advantage of potentially offering a very wide mechanically adjustable operating bandwidth, and a relatively trouble-free operation. These advantages stem from the fact that the two devices are in the same phase plane, and share a common resonator. Hence, the "mutual locking" is virtually assured and broadband. However, their construction is somewhat complex and difficult to implement.
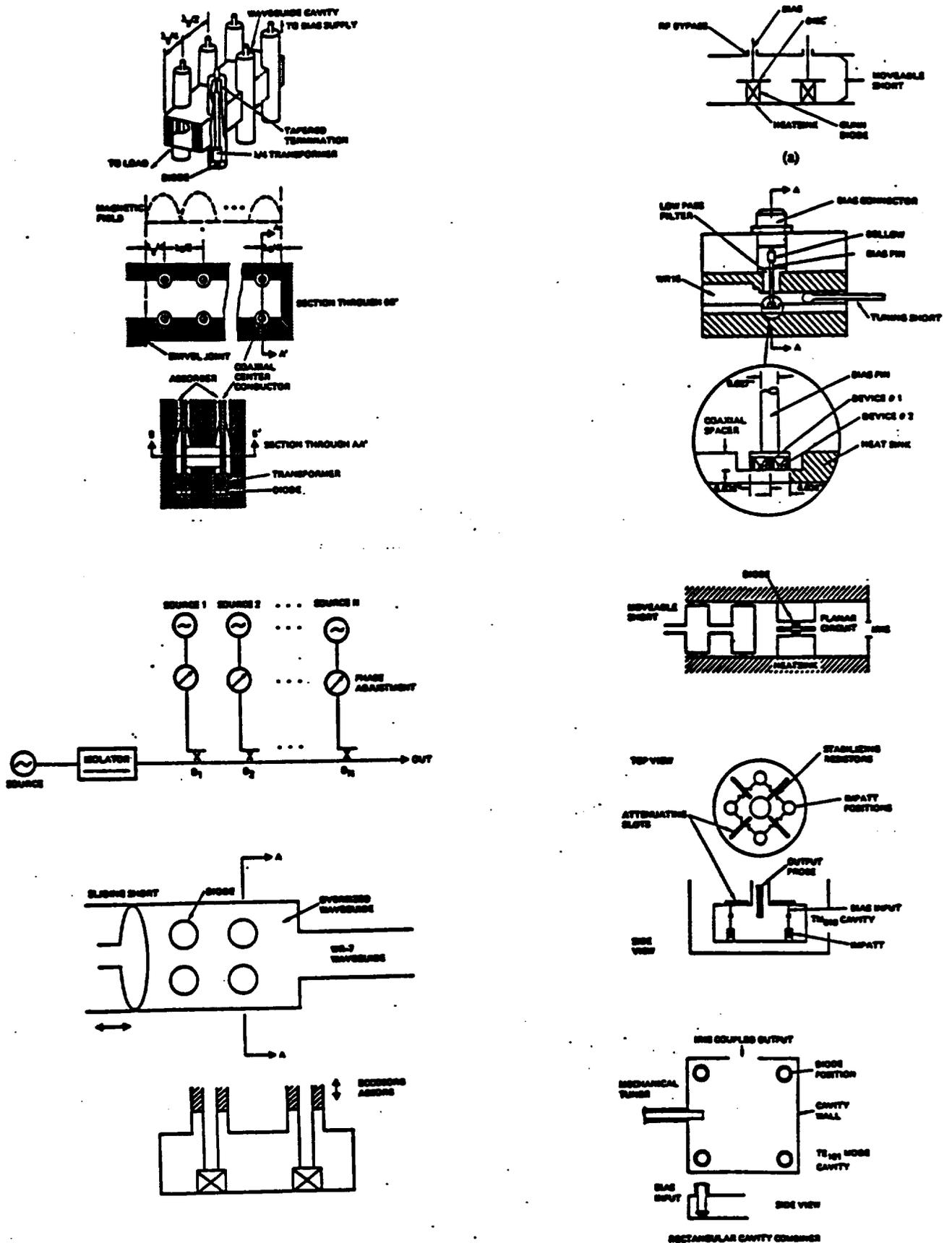
Figure 2.2 Various schemes for power combining using Gunn diodes (Ref.1)
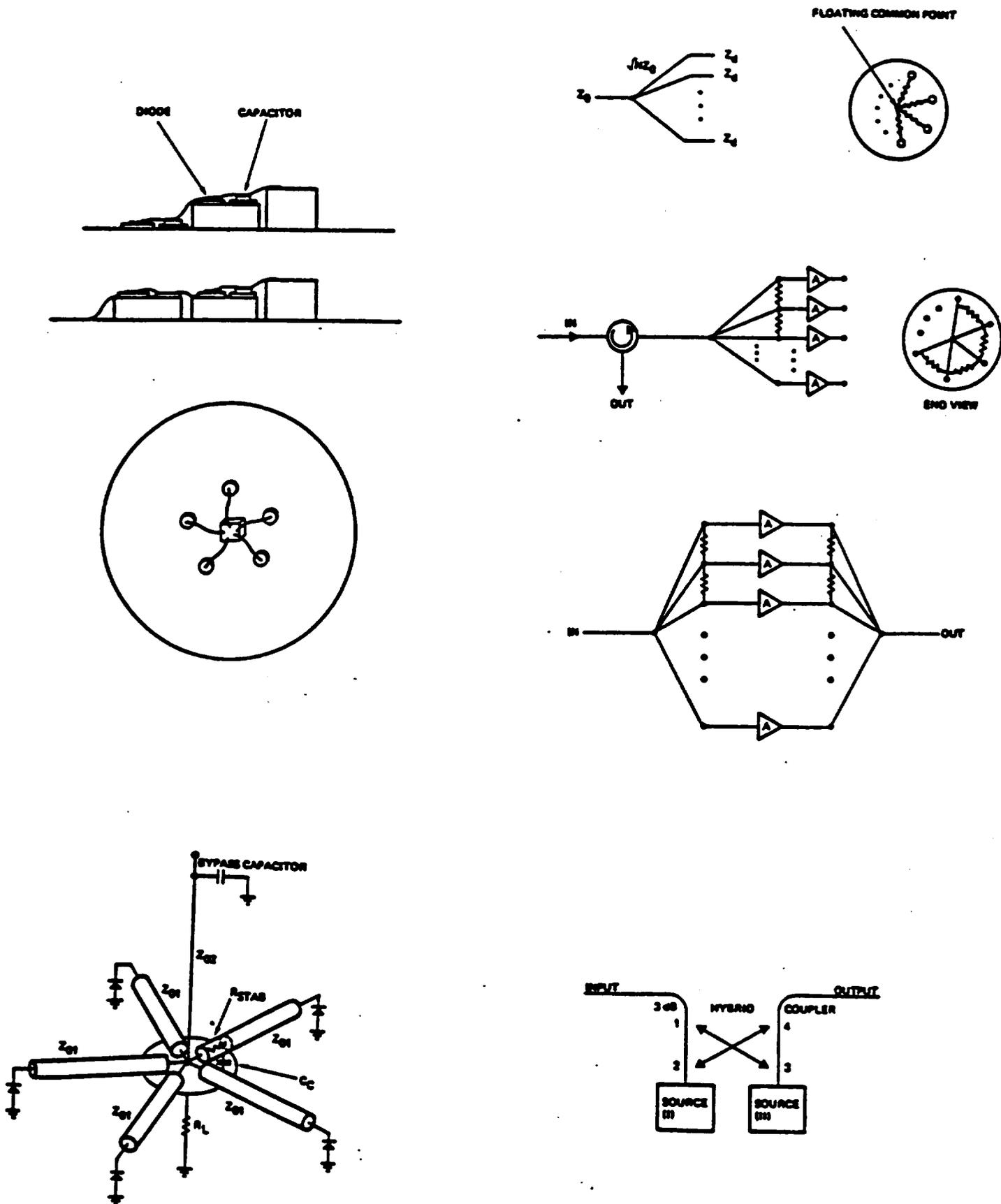
Figure 2.2 Various schemes for power combining using Gunn diodes (Ref.1)

In-line or series combining technique was selected as the primary method of achieving power combining for the pump oscillators, even though many experimental sources using other techniques were evaluated. For the present application, the in-line combiners can be designed using either a fundamental mode or second-harmonic extraction mode of operation. In this program, both types of power combiners were examined in a comparative study. The detailed electrical design of this type of oscillator (power combiners) is shown in Figure 2.3. Some of the theoretical considerations and design guidelines are presented next.

In this combiner scheme, the individual "oscillators" (Gunn device and resonator pairs) must be located an integral multiple of half-wavelength apart. However, from bandwidth considerations, they should be as close to each other as mechanically possible, one-half wavelength being the ideal situation. Additionally, the devices must have relatively similar electrical characteristics. It is highly desirable to have identical dc bias characteristics as well, to allow common biasing of the oscillator using a single power supply. To accomplish this, a test cavity which contains a single resonator at the desired center frequency can be employed to characterize a batch of diodes, under identical operating conditions. Devices exhibiting relatively similar rf characteristics can be paired for the combiner.

For the present source realization, the operating frequency range of the combiner is 78-86 GHz at a power level of 120-180 mW. The fundamental oscillator version of the combiner uses a post-coupled design, in which the frequency of operation is established by the Gunn diode parameters, post dimensions, and the distance to the backwall, or short-circuit. In this combiner configuration, the devices are one full wavelength apart. The frequency of the oscillator in the front is determined by this distance, while the backshort establishes the operating frequency of the oscillator in the rear.

To obtain power combining by mutual injection-locking, the two sources must operate relatively close in frequency, and with proper phase relationship. Theoretically, a 100% efficiency of power combining can be achieved when fully optimized. Phase shifters are generally necessary between the two oscillators to obtain the desired center frequency, synergistic power combining and mechanical tunability.

The second-harmonic version of this in-line combiner uses disc resonator-type oscillator design, where the operating frequency is largely dictated by the diameter of the disc and the post length. In this scheme, the two sources can run at independent frequencies, since the mutual interaction between them is negligible due to their second-harmonic operation. Consequently, the combiner instantaneous bandwidth is relatively narrow. However, each oscillator unit can be independently tuned, and hence a large mechanically adjustable operating bandwidth may be obtained. Since a single backshort is employed, eventual performance limit is reached when the power output from the front unit, which has an essentially fixed backshort, drops down significantly.

The fabrication details of the various combiners built in this program are described in Chapter 3. The performance summary is presented in Chapter 4, together with a discussion of their operating features.
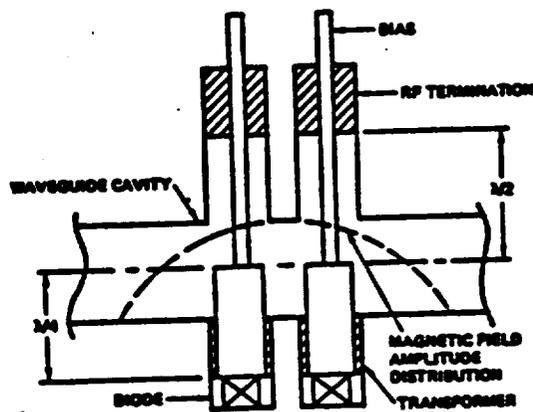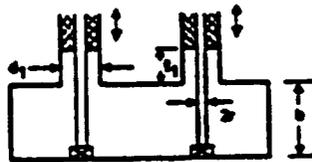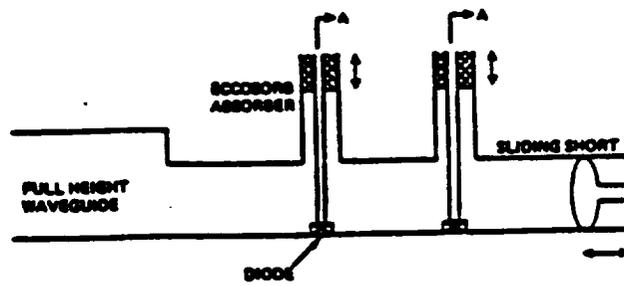
Figure 2.3 Dual-Gunn diode power combiner.

2.4   First Stage Doubler Design

The most critical consideration in the design of this first stage doubler was input power handling capability of the varactor, and the associated circuit. Hence, a systematic examination of available multiplier varactors was made. The three key electrical parameters of interest are: zero bias capacitance, series resistance, and the breakdown voltage. For the frequency range of interest, i.e., 80 GHz input, the circuit model was analyzed with various varactor parameters as variables. The results of this analysis indicated that the most suitable varactor for 160 GHz output frequency had the following specifications:

Zero bias capacitance, C_{jo}	21ff
Series resistance, R_s	10 ohms
Breakdown Voltage, V_B	20 V
Theoretical optimal input pump power	30 mW
Designation (Univ. of Virginia)	6P4

Experimental work indicated that these devices could actually withstand 60 mW of input power without damage at a somewhat diminished efficiency of harmonic conversion. The performance objective for this first stage doubler, however, require much greater input power handling capability. This basic design has previously exhibited a very high efficiency at a somewhat lower frequency of operation (94 GHz, 48% efficiency). It demonstrated a significant potential for use at higher frequencies as well. Hence, it was decided to select a dual-diode balanced construction, which utilizes two varactors, doubling the power handling capacity. The advantageous features of this novel approach are:

(a)   A single varactor chip is utilized by making contact with two of the multiplying diodes on the chip.

(b)   Input power handling capacity is virtually doubled in this configuration.

(c)   Balanced configuration does not require any filter structures to separate the input and output circuits.

(d)   Relatively simple design, which avoids using power splitters and combiners with two independent sources as in a conventional power combiner scheme.

In this design, the two diodes are electrically in series across the input waveguide, and are parallel-coupled via a probe into the output waveguide. A cross section of this doubler is shown in Figure 2.4. Both varactor diodes are actually on the same 0.25 mm square chip, which is contacted on two anodes.

The input circuit is a simple shunt of the two back-to-back series diodes across the reduced height waveguide, which ends in a shorted wall. The bias pin has little effect at the input frequency except to lower the guide impedance and the cutoff frequency. The output circuit, driven by the two diodes in parallel, is a "strip" transmission line up to the end of the input guide, where it becomes coaxial as it passes through the back wall of the waveguide, and

REDUCED
HEIGHT
WAVEGUIDE

CIRCULAR HOLE

BACKSHORT

BIAS PIN

INPUT
WAVEGUIDE

DIODE

COAXIAL
BIAS FILTER

WHISKER
PIN
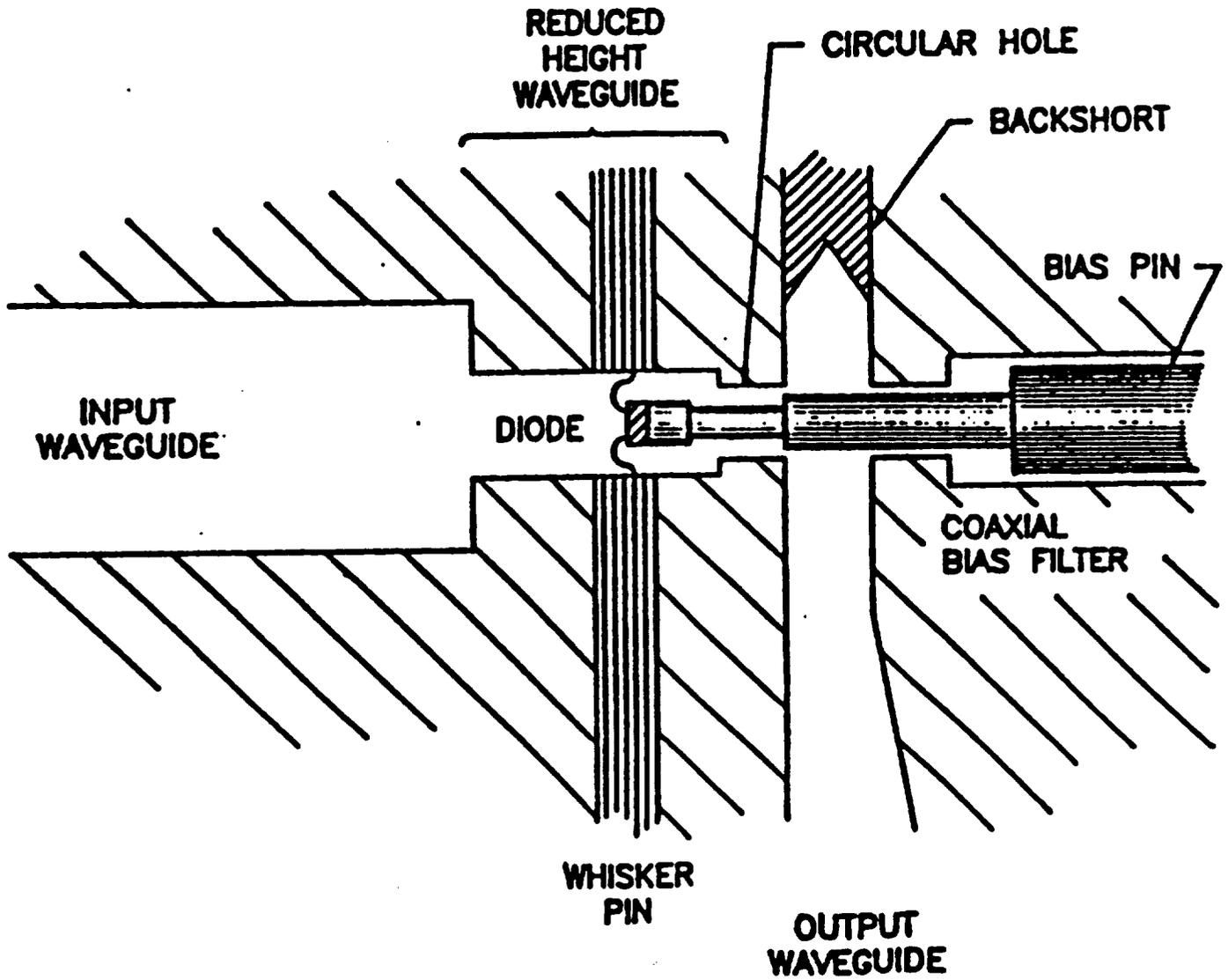
OUTPUT
WAVEGUIDE

Figure 2.4 Balanced doubler design.

then couples across the output waveguide. The output waveguide circuit may be tuned with a backshort, but the input tuning is fixed.

The several mode transitions and discontinuities involved in the input and output circuits make designing this circuit tedious, and require some scale modeling for best results. In addition, the circuit design suffers from a number of constraints. The input circuit is complicated by the need to suppress the TM_{11} mode at the output frequency, which has the symmetry to be strongly excited in the input waveguide if the height is too great. Thus, the reduced height section where the diode is mounted must continue toward the input for a sufficient length to cut off this mode. The output matching is affected by the transmission line length up to the end of the input guide, which must be short enough to allow a reasonable bandwidth at the output. Adjusting the input waveguide width provides one variable which has little effect on the output circuit, and in addition a step in height or an impedance transformer may be used ahead of the mode suppression section to produce a good match. In lower frequency models, a nearly optimal match has been achieved over a bandwidth of ~15% although that was not the goal of this work.

2.5   Submillimeter Wave Tripler Design

The tripler for 500 GHz uses a single diode design, similar to that used in a 230 GHz tripler [2]. Unfortunately, no two diode tripler designs seem practical at this frequency, so the diode should be quite overdriven. This type of design has been refined considerable using theory and modeling to improve the wideband input impedance match to the diode. In addition, there are a number of innovations in the electrical/mechanical design to simplify the fabrication and allow the use of split block construction, even at this frequency. One objective of this work was to design a circuit which could be entirely machined, primarily on a CNC mill, without the use of electroformed parts. A cross section of the tripler is shown in Figure 2.5. Both waveguides are machined as channels, with one broadwall of each waveguide formed by a third wafer. This wafer contains the coaxial filter joining the two waveguides.

Modeling was used to help produce an equivalent circuit of the varactor as mounted in the output waveguide and driven by the coaxial filter, based on physically expected circuit elements, together with some empirically determined discontinuity capacitances. Next, the transition from the input waveguide to the coaxial filter was modeled to drive the input impedance. A five section filter was then computer optimized to allow an input match from 160 to 173 GHz with no backshort tuning, while simultaneously presenting a short circuit at the second and third harmonics. The coaxial impedances in this filter were allowed to range only from 16 to 54 Ω in order to avoid extreme machining tolerances. Only the final two sections of this filter are small enough to suppress higher modes at the output frequency. The wafer containing this filter is too thin to machine accurately, if a choke of minimum length is used. To add thickness, an extra half wave long section with 40 Ω impedance was added to the input end of the filter, and the design then reoptimized. This addition has very little effect on theoretical performance.

DC
BIAS

ANODIZED
COLLET

BIAS FILTER

INPUT GUIDE
(REDUCED
HEIGHT)

LOW PASS FILTER
(AIR DIELECTRIC)

BACKSHORT

VARACTOR DIODE

COAXIAL
RESONATOR

OUTPUT
WAVEGUIDE

WHISKER
PIN
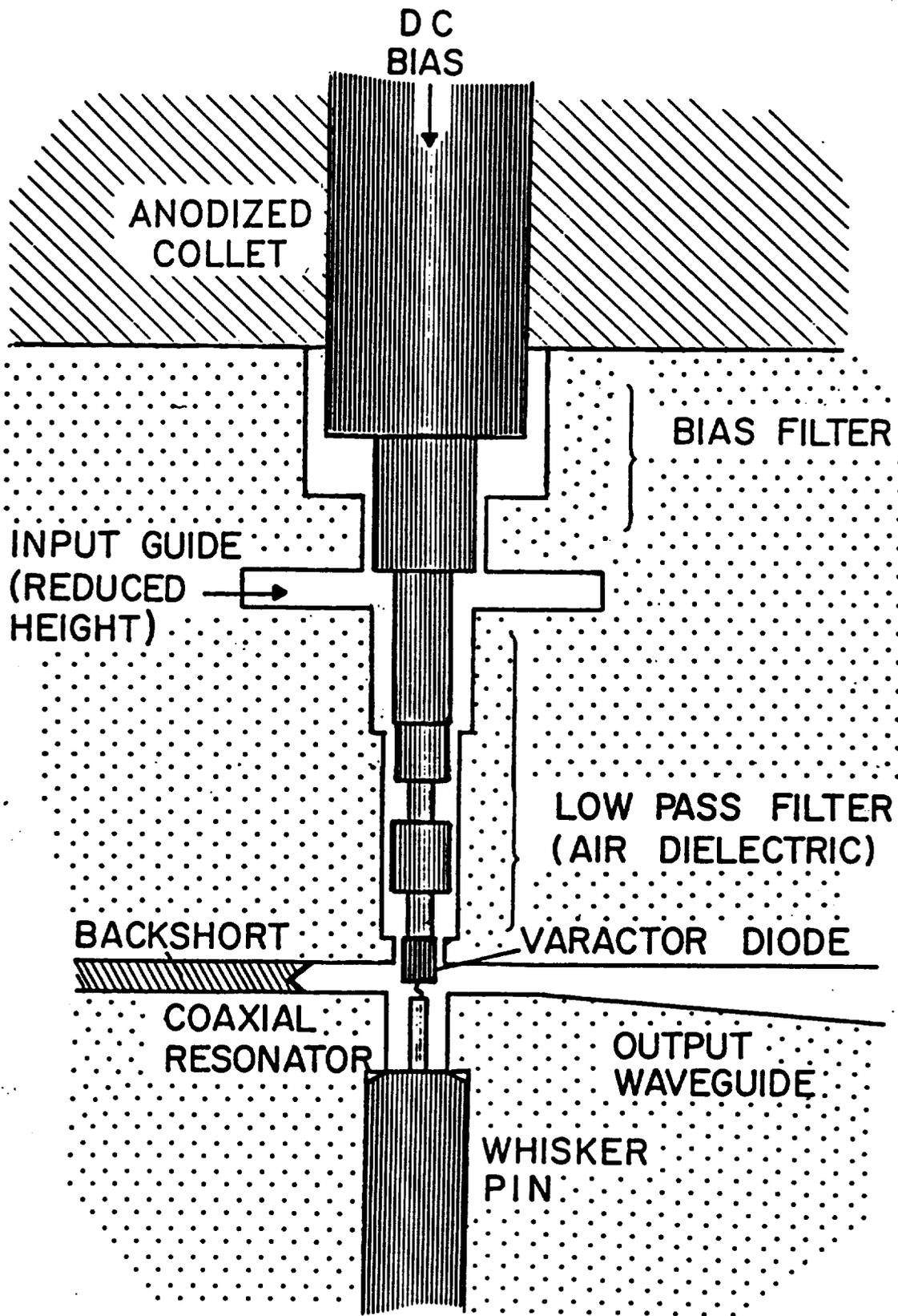
Figure 2.5 High frequency tripler design.

The input match is aided as in a previous design with a coaxial resonator, $\lambda/6$ long at the input frequency, in series with the diode [2]. This resonator adds input inductance without affecting the output match. At the second harmonic idler, the effect is capacitive, which partially cancels the effective inductance of the whisker. Poor contact at the end of this resonator is a potential source of loss, and is reduced in this design by having the shorted end of this pin meet the outer wall at a shoulder where contact can be assured. This makes pressing the whisker pin into the diode less practical as a means of contacting an anode, as is commonly done in such devices. To avoid this problem, the position of filter choke was made adjustable by allowing it to slide in a tight fitting anodized aluminum collet, which replaces the previous ceramic support at this location.

To minimize the output waveguide losses, a conical horn was machined directly into the block. This requires a novel transition, based on shapes that are easily machined. The circular to rectangular transition consists of an abrupt step from round to square guide of the same cutoff frequency, in this case 0.53 mm square to 0.62 mm diameter. This introduces no impedance discontinuity, except for the step susceptance which is small. This step is followed by an asymmetric linear taper to reduced height rectangular guide. The final reduced height dimensions are 0.076 mm X 0.42 mm. Making this taper at least 5 λ long keeps the higher mode excitation to a low level causing little perturbation in the feed horn beam patterns. This transition is fabricated by milling the rectangular waveguide taper into one piece of the split block, while the conical horn is bored into the block after the pieces are assembled. The conical horn diameter at the aperture is 1.45 mm.

3.0 CONSTRUCTION OF SOURCE COMPONENTS

3.1 Introduction

The electrical design of the individual source components used in the 500 GHz local oscillator assembly has been described in Chapter 2 in considerable detail. The physical realization of these components requires significant mechanical design, and careful assembly procedures. Due to the high frequency of operation, the machining tolerances, surface finish requirements, etc., are rather stringent. Mechanical design of these components takes into consideration the requirements for dimensional accuracy, physical alignment, assembly constraints, and small size of devices. The structural integrity of the unit is also very important, since the reliability of operation largely depends upon the unit's ruggedness and thermal stability of the whisker-contact to the device.

The construction technique must also provide for mechanical tuning or adjustability of critical dimensions or geometrical parameters. Moveable backshorts, phase trimmers, impedance matching transformers, etc., must be incorporated in the design to allow performance optimization without requiring major rework or refabrication of the unit. Hence, appropriate mechanisms and mechanical features were devised into each of the source components. Moveable backshorts present a particularly difficult problem at these high frequencies. Both contacting and non-contacting backshort designs were examined for various frequency ranges. Typically, a contacting backshort was employed for these high frequencies.

The device biasing arrangement presents a serious challenge in all these source components, regardless of whether it is a multiplier or an oscillator. Thermal considerations and device ruggedness are both factors in designing a suitable bias/contacting arrangement. For whisker-contacted devices, the application of optimal pressure and contact integrity represent difficult challenges in the assembly process. Considerable amount of experimentation and practice were necessary to achieve reliable, repeatable contacts. Similarly, for InP Gunn devices, the biasing scheme was standardized and carefully executed to avoid device failures.

All the components for this development program were fabricated at Millitech in their entirety. The machining of all the parts was carried out on CNC machines, or specialized machine tools consistent with the accuracy and tolerance requirements. Gold plating and other chemical processes also demand precise control, and hence were generally carried out at Millitech. Significant experience has been accumulated by the assembly and fabrication personnel in handling this class of components in the past. New assembly techniques were devised wherever needed, to achieve the desired results. Special fixtures were employed to facilitate the final assembly of the source components.

The technical details of the construction and physical implementation are provided in the remainder of this chapter.

3.2   Doubler Fabrication Details

The mechanical structure of the balanced doubler is shown in Figure 3.1. Basic split-block waveguide construction is used in implementing this multiplier. For convenience, the input tuning was fixed, while the output circuit is tunable by means of a movable backshort.

The doubler is fabricated in three pieces. The input waveguide is milled into the first as a pocket, and the output waveguide is milled as a channel into the next, which also holds the bias pin in a ceramic insulator. The third part simply adds length to the input guide to make the block larger. All parts are gold plated after machining. The 0.25 mm square varactor diode is soldered to the end of the bias pin. Contacting an anode in this geometry has proven to be simple since it is possible to view the diode face-on with a high power microscope while contacting. The whisker is made so that rotating the whisker pin will bring it into contact with the diode. Input impedance matching is aided by sliding a quarter wave transformer made of a suitable dielectric in the input waveguide to a point where an optimum match is achieved.

3.3   Tripler Fabrication Details

The electrical design of the submillimeter wave tripler has been described in considerable detail in Section 2.5, which includes some of the mechanical fabrication considerations. For example, the wafer containing the filter was determined to be too thin to machine accurately. Hence, an extra one-half wavelength was added to the input side of the filter to reach reasonable wafer thickness.

Figure 3.2 shows the construction details of this tripler. The waveguide channels are machined in wafers, with one broadwall of each waveguide formed by a third wafer. This wafer incorporates the coaxial filter which interconnects the input and the output waveguide. The filter choke positioning arrangement used in this tripler to contact the varactor anode has been modified with respect to a standard tripler design. An anodized aluminum collet with sliding fit was employed in the place of a ceramic support which fits very tightly around the choke. Hence, the choke could be adjustable by sliding it in the anodized collet.

All parts were machined from brass, and the wafers then lapped to assure perfectly flat surfaces for good mating. Parts where then gold plated. The varactor forms the center conductor of the final low impedance section of the filter choke, and was cut down to the exact diameter needed for the correct impedance. This requires that the diode be soldered to a post smaller than the diode itself. The diode is contacted by an electrosharpened NiAu wire 3.5 μm. Contacting backshorts are used for tuning.

A conical output horn was directly machined in the block containing the output waveguide. A novel transition from the rectangular guide to the circular horn input cross section was incorporated. To avoid complex fabrication steps, a three-step cross-section transformation is carried out.
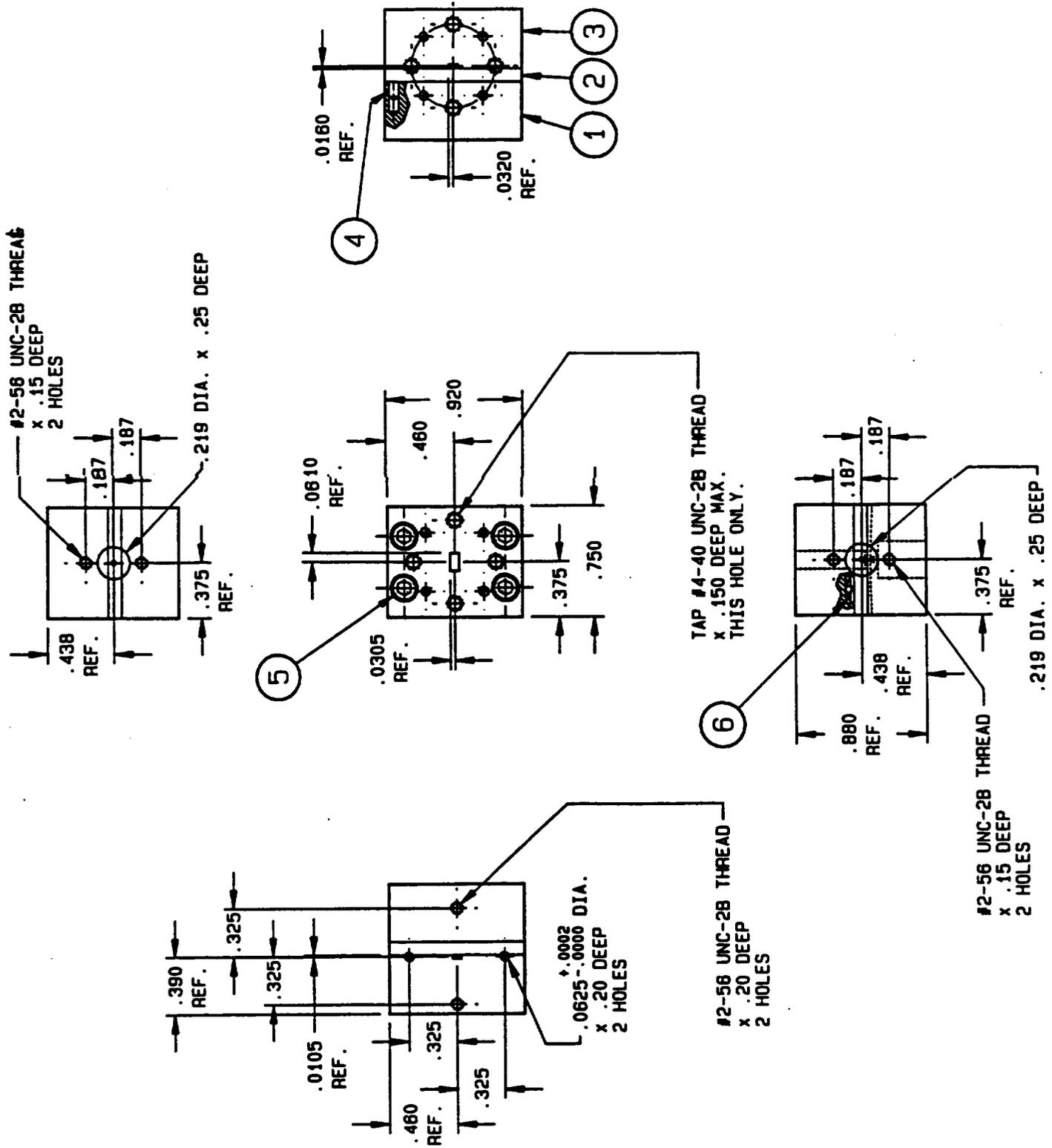
Figure 3.1 Balanced doubler outline and construction detail.
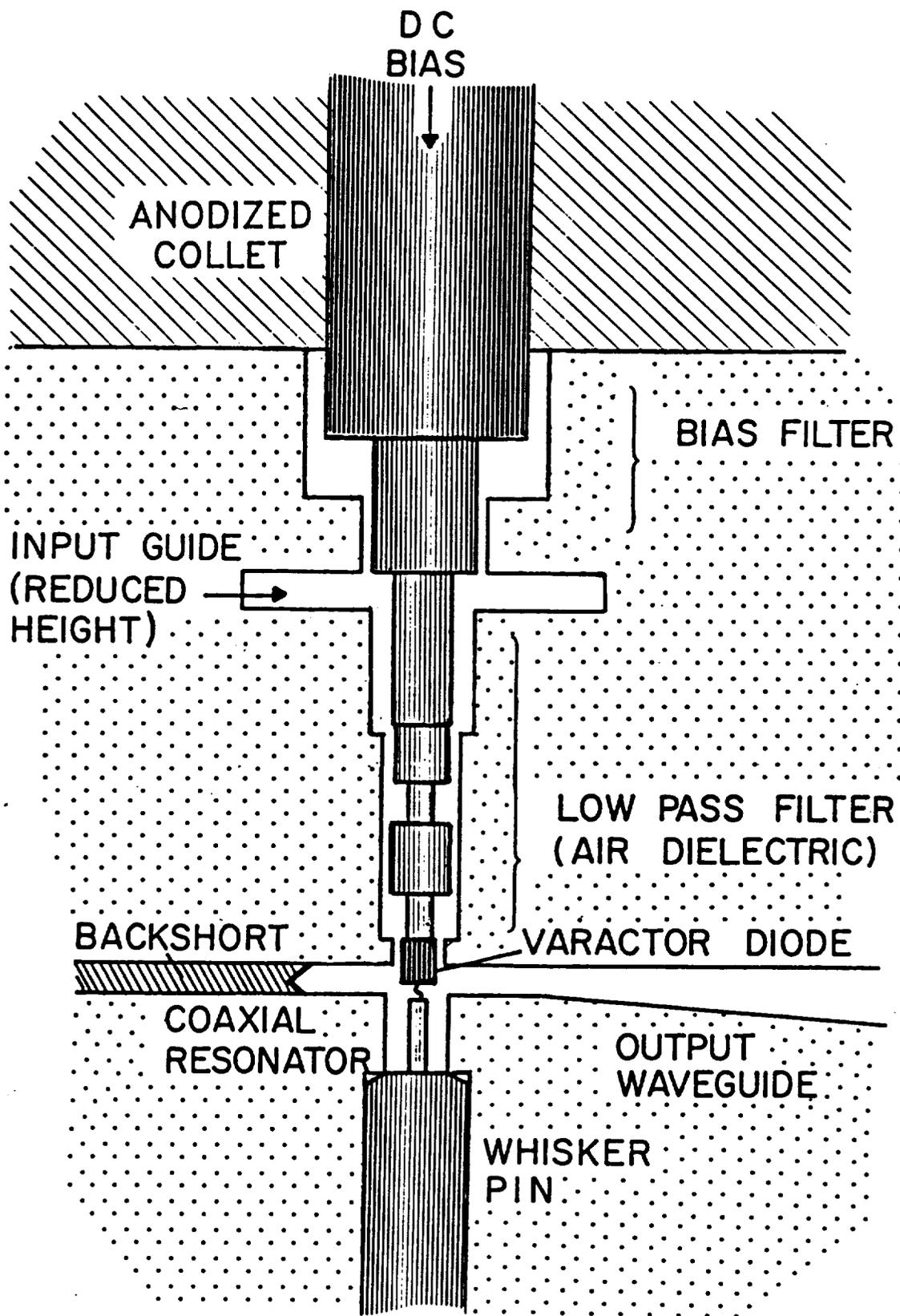
Figure 3.2 High frequency tripler construction detail.

3.4   Gunn Oscillator Construction Details

All the Gunn oscillators used for power combining in the 78-84 GHz range utilized a standard Millitech Gunn oscillator body. This consists of three individual blocks: the diode block, the bias choke block, and the cover. The waveguide (WR-12) channel is directly machined in the diode block, which also contains the hole to accommodate a packaged Gunn diode mounted in a diode holder. The diode can be raised up or lowered by altering the diode holders, and can be rotated by simply rotating the entire diode holder.

The choke block contains cylindrical holes (0.116 inch diameter) to insert the bias chokes directly in line with the Gunn diodes. A simple leaf spring is used to provide adequate choke contact pressure to the diode. Figure 3.3 depicts a typical Gunn diode oscillator which has been modified to accept two Gunn devices in the same body. Bias filter and suppression network is incorporated in a circuit located within the choked block (top side). A cover, which incorporated the bias connector, etc., is used to enclose the bias circuit and choke pressure adjustment mechanism. Rectangular non-contacting backshorts were produced to permit manual adjustment and optimization of combiner performance.

CHOKE PIN

SAPPHIRE ROD (REF)
BACKSHORT
DIODE

DIODE HOLDER
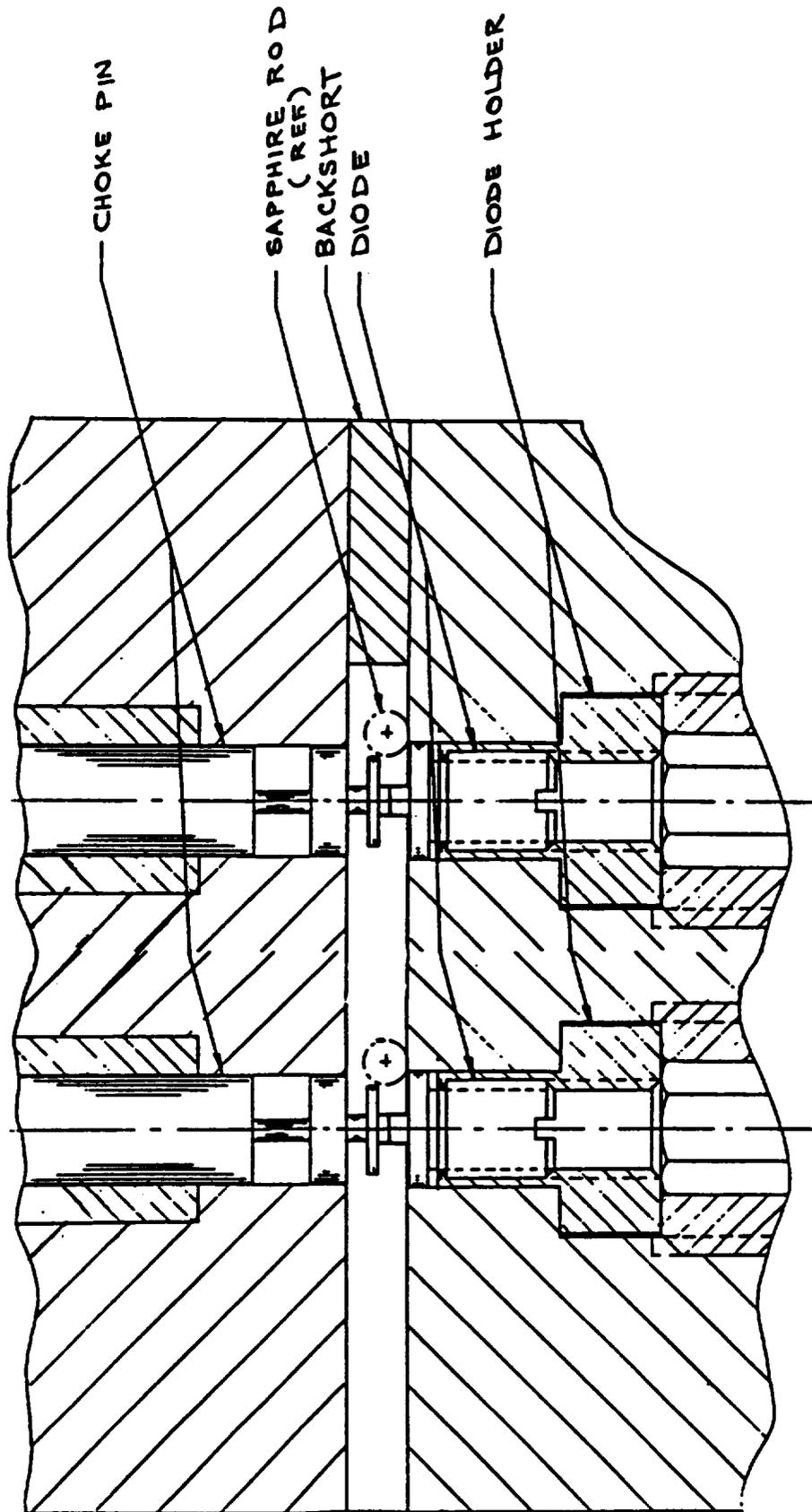
Figure 3.3 Dual-diode combiner cross-sectional view.

4.0 MEASUREMENTS AND RESULTS

4.1 Source Evaluation

The individual source components developed under this program were rigorously characterized and optimized to extract the best operating performance for the present application. The test and evaluation program generally utilized standard test equipment and procedures established at Millitech Corporation. Wherever possible, cross-calibration and indirect verification of measured results were carried out to enhance the confidence level in the results. A standard test arrangement for oscillators and multipliers is shown in Figure 4.1.

In this chapter, the results of measurement of performance characteristics of the prototype units of the individual source elements are presented first. This is followed by a detailed description of an investigation of Indium Phosphide Gunn diode-based sources for general local oscillator applications to radiometry. A significant effort was directed toward the examination of the InP devices for high-reliability applications. Hence, a systematic characterization of these devices in terms of their thermal properties and failure modes was carried out. The results of this endeavor are also included in this chapter.

4.2 Power Combining Results

A number of prototypes were built to demonstrate power combining in the frequency range of 34 to 95 GHz. Most of the experimental work has concentrated on power combining using an in-line combining geometry. Both fundamental and second-harmonic power combining schemes were studied. A summary of the final results is presented in Table 4-1.

TABLE 4-1
POWER COMBINING RESULTS (DUAL DIODE SOURCES)

| Experiment Number	Individual Device Characteristics				Combiner Characteristics			Comments and Observations
	First Device		Second Device		Freq. GHz	Power mW	Combiner Efficiency	
	GHz	mW	GHz	mW				
00A565N	79.2	68	79.4	70	81.1	152	110%	Combiner at higher freq. than devices
00A565E	80.2	70	79.4	70	70.4	190	156%	Combiner at lower freq. excellent bias tuning
00A182N	94	62	93.8	63	94.5	121	97%	Good bias tuning
00A576E	35	418	35	425	70.6	86	10.3	Second harm. type combiner
					35.3	720	86%	Fundamental combining
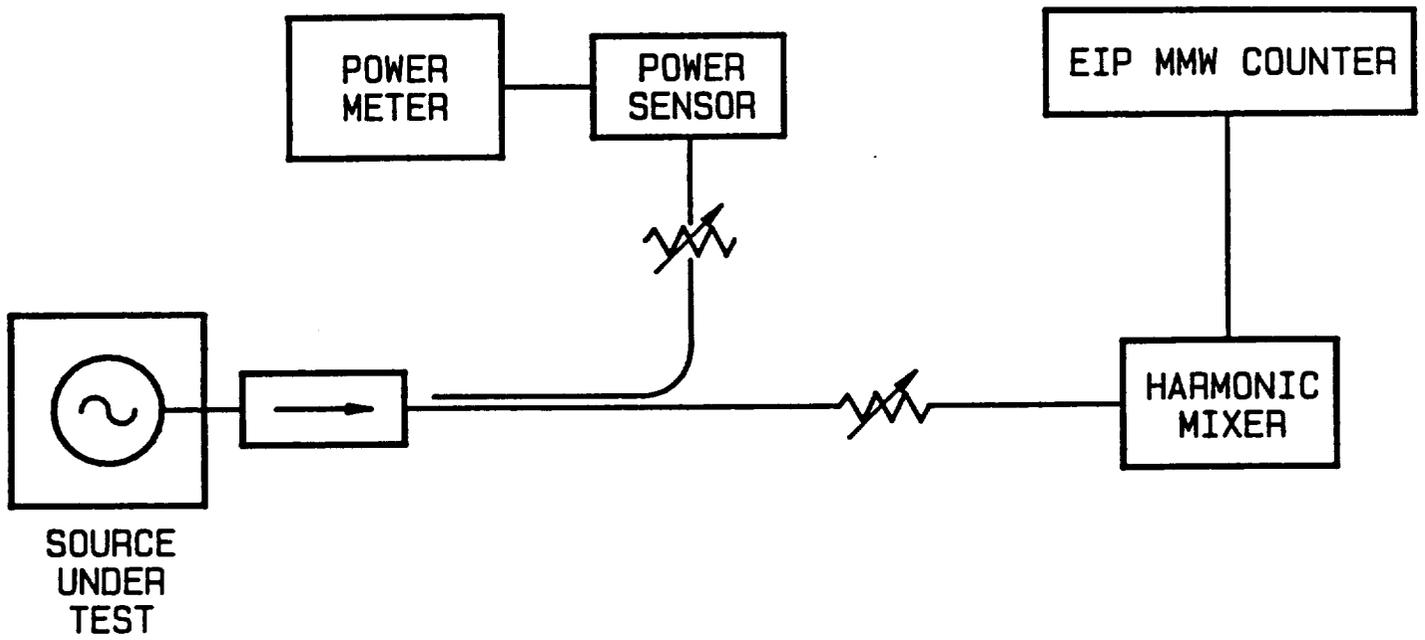
Figure 4.1 Source evaluation test set-up.

4.2.1 Fundamental Power Combining

Prototype units were evaluated at selected operating frequencies over a wide frequency range (34-95 GHz). In most cases, the individual oscillators within the combiner were constructed in a manner very similar to their single-diode versions for that particular frequency region. The results of some of the most significant prototype units are provided in Table 4-1. The following observations and conclusions were made during the course of this phase of combiner evaluation.

1) Individual "sources" within the combiner must operate in a fairly similar manner to achieve optimal results. Broadest mechanically tunable combiner operation was obtained when devices, as well as mechanical structures were virtually identical.

2) The distance between the sources was critical to obtaining made-free and efficient combining. The power output could be peaked by introducing a dielectric tuning rod between the two "oscillators," thereby adjusting their electrical separation.

3) The backshort location played a crucial role in the optimization of the combiner performance.

4) Greater than 100% combiner efficiencies could be achieved in many cases. This is a consequence of improved matching obtained for each individual oscillator in a combiner configuration.

4.2.2 Second-Harmonic Combining

Several prototype units which utilize a second-harmonic power extraction mode were characterized over the 70-95 GHz range. In this effect, individual tuners were incorporated to allow independent frequency adjustment of each oscillator, as well as a path length adjustment for inter-diode distance. Some of the notable observations for this combiner scheme are discussed below.

1) Due to second-harmonic operation of individual oscillators within the combiner, there was only a weak coupling between them, and hence a limited mutual locking (power combining) range. Typical instantaneous combiner bandwidths were less than 0.1% (approximately 100-200 MHz).

2) An advantage of this scheme was the fact that each oscillator could be frequency tuned virtually independently. Hence, prototype units could be readily operated and evaluated over a fairly wide frequency range.

3) The separation between the diodes plays a crucial role in maximizing output power, but has practically no influence on frequency of operation. Thus, an independent optimization of output power was achievable by mechanically adjusting this distance and the backshort location.

In one set of experiments, the individual resonators associated with the two Gunn diodes were independently-tuned mechanically to obtain frequency tuning while still maintaining mutual locking and efficient power combining. By careful adjustment of individual tuners, a minimum of 100 mW output power has achieved over 2 GHz bandwidth at the center frequency of 95 GHz. However, the mechanical adjustment had to be made with considerable care and precision, thereby limiting the usefulness of this source. The difficulty arises due to limited mutual locking bandwidth of a second-harmonic operation ia a WR-10 cavity.

4.2.3   General Observations

The following remarks summarize the conclusions drawn from the test and evaluation of various combiner prototypes.

a)   Greater than 100% power combining efficiencies have been realized as predicted. This implies that the output power from the combiner is typically greater than the sum of the power available from individual devices.

b)   Power combining demands reasonably tight control on operating parameters and geometrical features of the oscillator. In particular, inter-device spacing and resonant dimensions must be accurately controlled to achieve optimal results.

c)   Mode stability and mechanical bandwidths are issues requiring further investigation. Techniques to enhance both were theoretically studied.

d)   Reasonable bias tuning was obtained from these combiners without losing the lock. This makes them attractive for applications requiring a frequency-locked operation.

e)   The sensitivity, stability, and frequency characteristics of power combining are a strong function of the InP Gunn device employed in the oscillator. Higher Q devices (or modes) offer greater stability and superior frequency control in comparison to the low Q device (or structures).

4.3   Doubler Performance Evaluation

The balanced doubler for 166 GHz output frequency was evaluated using the dual-diode InP Gunn combiner oscillators described above. A variable attenuator was employed between the Gunn pump and the doubler to vary the amount of input power, and thus study the conversion efficiency of the doubler as a function of pump power.

This doubler reaches a peak efficiency of 35% with 35 mW input at 79 GHz. Despite the theoretical predictions, the efficiency drops to 32% at the expected optimum drive of 60 mW. This rolloff in efficiency is attributed to heating of the diode junction, which is expected to run at ~50 C above ambient at 30 mW per junction. DC measurements have shown an increase in the diode series resistance as the temperature increases, and thus, a

reduction in the cutoff frequency. It is difficult to quantify the expected increase in R_S with power, since the thermal resistance of the junction is not well known. Despite this effect, reasonable efficiency is maintained at 120 mW input and an output power of 26 mW is produced with the 79 GHz oscillator. An output of 22 mW is obtained with the 83 GHz pump, i.e., output frequency of 166 GHz. The measured output power as a function of input power is shown in Figure 4.2 for the 79 GHz input. The measured efficiency vs. input power is shown in Figure 4.3, as well as the theoretical curve of efficiency. The theoretical curve is generated from a computer program by Siegel and Kerr [3] which was also used to calculate theoretical embedding impedances in this work. Note that the disagreement can not be resolved by any circuit losses, since this would only lower the efficiency at all values and also increase the optimum pump power (for input losses).

The very high efficiency is attributed to a very low loss input structure due to the absence of a filter choke, and to the balancing which suppresses the conversion of power to the third harmonic. Measurements of the output through a high pass filter showed no detectable third harmonic to a level of -35 dBc.

The temperature coefficient may be used to advantage by operating the multiplier at low temperature. By cooling the doubler to 77°K, the peak efficiency increases to 40%, while the maximum output power is 32 mW. This is the highest efficiency and output power reported at this frequency. This mode of operation is practical in some applications where a cooled receiver is involved.

4.4   Tripler Performance Evaluation

The submillimeter wave frequency tripler was characterized using the balanced-doubler source configured as a pump over 158-167 GHz range. This power was directly pumped into the tripler input, while the tripled frequency output was extracted using an integral horn build into this multiplier. The output power was measured using a dry calorimeter, which has a WR-12 waveguide input. The frequency of operation was monitored by sampling a fraction of the pump power of the InP Gunn combiner via a cross-guide coupler into a EIP Millimeter-wave Frequency Counter. Each source component was tuned to achieve optimal performance at the multiplied (X6) frequency.

The maximum output power is 0.7 mW at 474 GHz when driven with the full output of the doubler, while 0.55 mW is obtained at 498 GHz. This is certainly the highest solid state power output generated at this frequency. Powers are probably underestimated, since no mode transition was available from the circular output horn to the WR-12 waveguide of the calorimeter, so these waveguides were simply butted together. An efficiency of ~2% at lower input power is measured at 525 GHz, verifying that operation is over the design band. While designed for fixed tuning, backshorts were optimized at each frequency in these tests. Correcting for connecting guide losses, the best efficiency is 3.0%. Due to the overdriven condition, it is likely that this efficiency would increase at lower input power. The typical tripler bias in these tests was 5-6 V (reverse) with a forward current flow of 0.1 mA, demonstrating that the diode is operating in a true varactor mode. This bias level also implies large reverse breakdown currents since V_b is only 8.5 V.
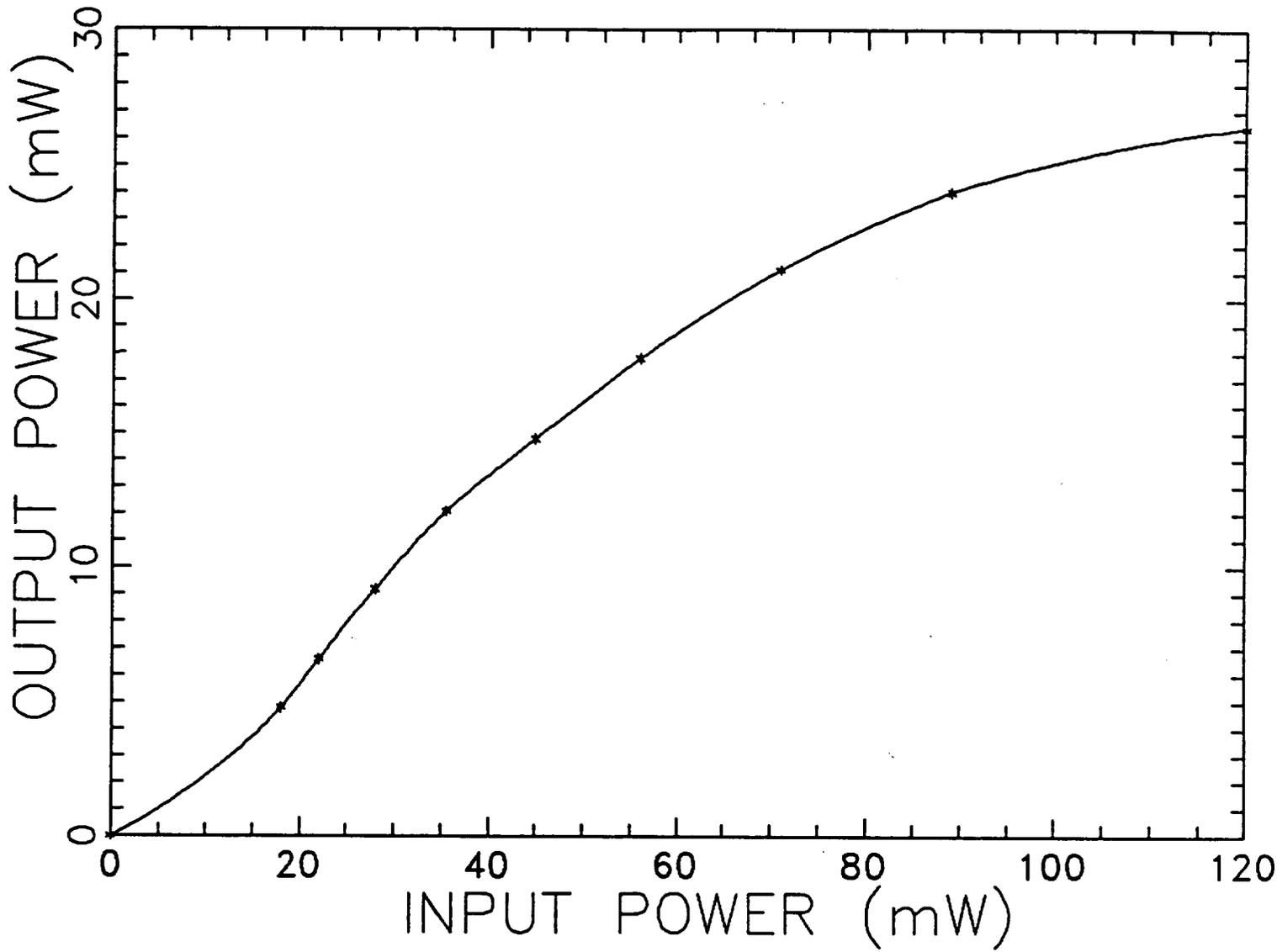
Figure 4.2 Balanced doubler power output as a function of input power.
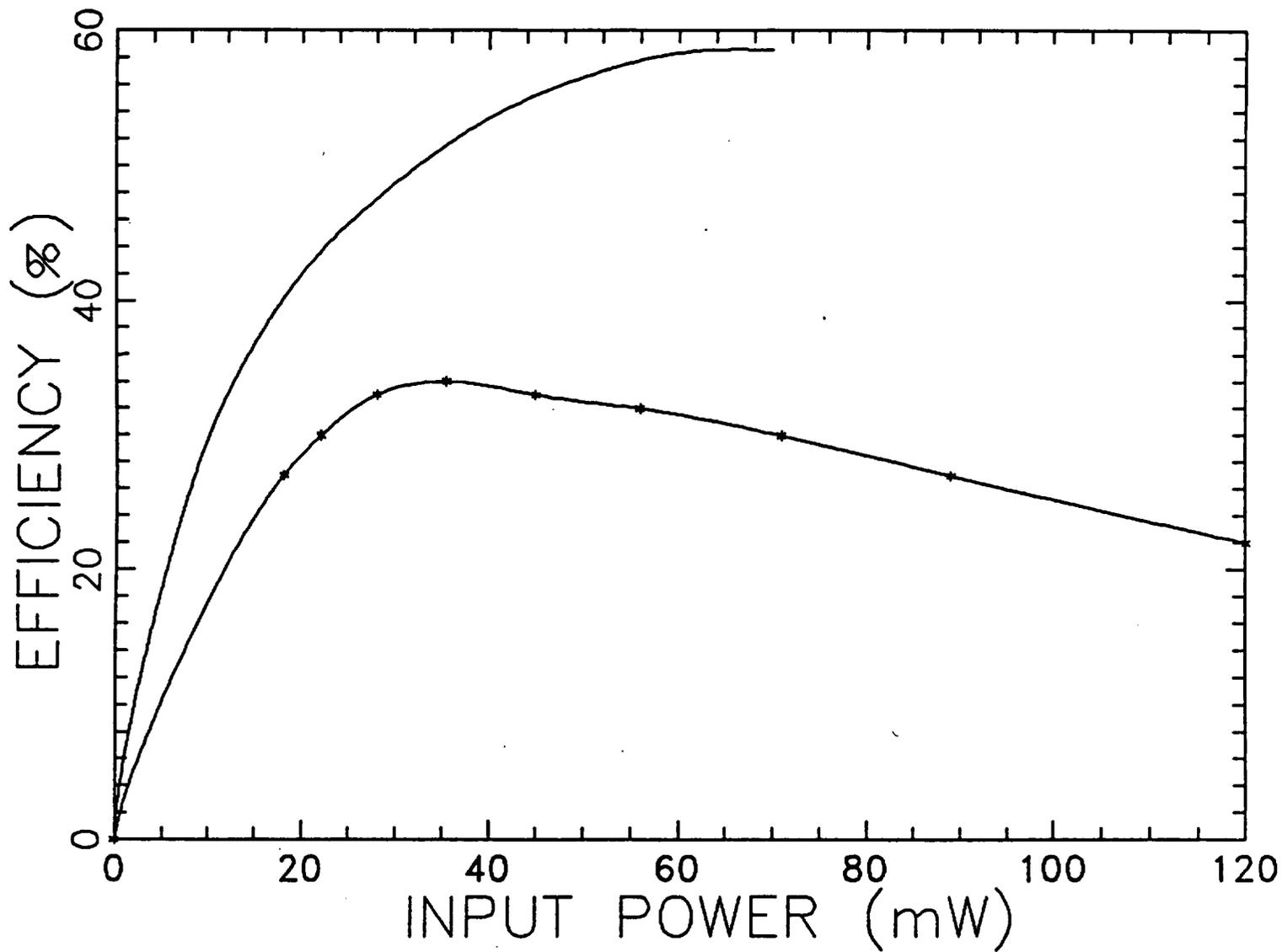
Figure 4.3 Balanced doubler efficiency as a function of input power.

4.5   Gunn Diode Oscillator Development Program

An extensive program aimed at examining the operating characteristics and various modes of operation of Gunn diode oscillators was carried out. In particular, some new phenomena were studied with a view to derive novel source structures for local oscillator applications. Among these are:

1.   Higher-order harmonic generation,

2.   power combining architectures,

3.   subharmonic injection-locking.

In addition, some specific aspects of sources were experimentally studied. The purpose of this was to design and characterize special purpose oscillators such as the ones listed below:

1.   Cavity-stabilized oscillators,

2.   Multi-frequency sources,

3.   Wide-band, mechanically-tuned sources,

4.   High-reliability sources.

Some fundamental studies were also carried out in this program to provide a user-oriented database for Gunn devices. The results of these studies can also be used as design guidelines for a variety of local oscillators in the millimeter-wave range. Some of these investigations were directed toward the following topics:

1.   Device thermal characterization,

2.   Device operating characteristics and harmonic generation,

3.   Cavity design,

4.   Packaging considerations for diodes.

The details of these substudies are presented in the balance of this chapter. Additional results and discussions are included in various Appendices.

4.5.1   Operation Mode of High Power InP Device

One of the key workhorse device for this study is the W-band InP diode which has the following specifications according to the vendor (Varian Associates).

Device Number: VSB9122S13

Operating Frequency: 94 GHz ±2 GHz

Power Output:	60 mW min.
Operating Voltage:	10 V typical
Operating Current:	160-220 mA typical

This device is generally used in a standard coaxial resonator-waveguide cavity with a disk as an essential part of the resonator. A study was directed to unambiguously and conclusively determine the mode of operation (fundamental or harmonic extraction) of this device in the conventional cavity.

Three independent experiments were designed and carried out rigorously using the same Gunn diode in special test oscillators. These experiments, which were aimed at determining the mode of operation of the diode are described next.

1.   Observation of other harmonics: A conventional oscillator was examined for the presence of the "third harmonic" on the assumption that the W-band operation (e.g., 92 GHz) was achieved by second harmonic power extraction of a fundamental frequency of 46 GHz. Using a spectrum analyzer, and a frequency wavemeter independently, the existence of power at 138 GHz (3 X 46 GHz) was verified. This implied that the basic oscillation was indeed at a fundamental frequency of 46 GHz, which is well below cutoff frequency of 59.1 GHz in a W-band waveguide. If the device were operating fundamentally at 92 GHz, no power output at 138 GHz would be observed. Instead, the second harmonic would be at 184 GHz.

2.   Observation of fundamental oscillation: A coaxial probe was inserted into the conventional cavity oscillator similar to the one described above. This probe was located in the immediate vicinity of the device and the resonator. A strong output signal at 47 GHz was extracted via the coaxial probe for the W-band source producing 60 mW output at 94 GHz. This once again confirmed that the 94 GHz operation was a second harmonic type.

3.   Device characterization at half frequency: This InP device was inserted in a standard oscillator cavity for 40-50 GHz range of operation. A very significant power output (>200 mW) in the 40-50 GHz interval was observed. If the device were truly fundamental at 94 GHz, no appreciable output power would have been obtained at the half frequency in the WR-22 cavity.

4.   Injection locking experiments: The locking bandwidth of injection-locking the W-band (94 GHz) source using this device (VSB 9122S13) was measured by injecting a signal at 94 GHz through a circulator into the cavity. A very narrow (virtually non-existent) locking BW was observed at rather low power gains. This narrow locking bandwidth of 15-20 MHz is contrasted with 500-1200 MHz of locking bandwidth measured for a truly fundamental oscillator using a fundamental device VSB 9122S10 and a similar injection scheme.

These experiments conclusively established that the most significant Indium Phosphide device (VSB 9122S13) is not a fundamental device in the W-band, as maintained by the vendor. This knowledge has a major impact on the design and evaluation of all the Gunn oscillators based on this particular diode.

4.5.2 Second Harmonic High Power Frequency Sources

The relative advantages of second harmonic extraction type sources have previously been identified in the Phase I research. During this phase, a concentrated effort was directed toward the development and rigorous characterization of this mode of operation of InP Gunn devices. Some of the experimental work was conducted at lower frequencies (55 to 75 GHz) to model the higher frequency versions. The results of this subtask are summarized in Table 4.2. The construction of these sources is similar to the conventional second harmonic oscillators. Minor modifications to the choke structure, however, were included as part of this study.

TABLE 4.2
HIGH POWER SECOND HARMONIC OPERATION

Oscillator Serial No.	Fundamental Device Characteristics		Second-harmonic Operation Characteristics		Fundamental to Harmonic Power Ratio
	Frequency GHz	Power mW	Frequency GHz	Power mW	
0A827	34.5	275	70	90	3.055
0A565	35.0	303	67	110	2.755
0A828	34.8	285	63	88	3.238
0A495	35.1	255	61	78	3.269
0A441	35.5	285	58	84	3.393
0A441	43.5	250	75	65	3.846

Some of the preliminary conclusions from the study are discussed here:

      a)   Fairly high output power has been obtained at the second harmonic frequency. Figure 4.4 shows the typical output power available from these devices at their fundamental frequencies and in second-harmonic extraction type cavities. The ratio of second harmonic to fundamental power output ranges between 5 and 6 dB.

      b)   Fairly high DC to millimeter wave (second-harmonic) power conversion efficiencies have been achieved. Table 4.3 lists some of these figures together with some representative conversion efficiencies for InP fundamental sources at similar frequencies. Even though the fundamental power extraction is somewhat more efficient, there are other significant advantages of the harmonic extraction mode that make them attractive for local oscillator applications. Some of these will be evident from the following discussion.
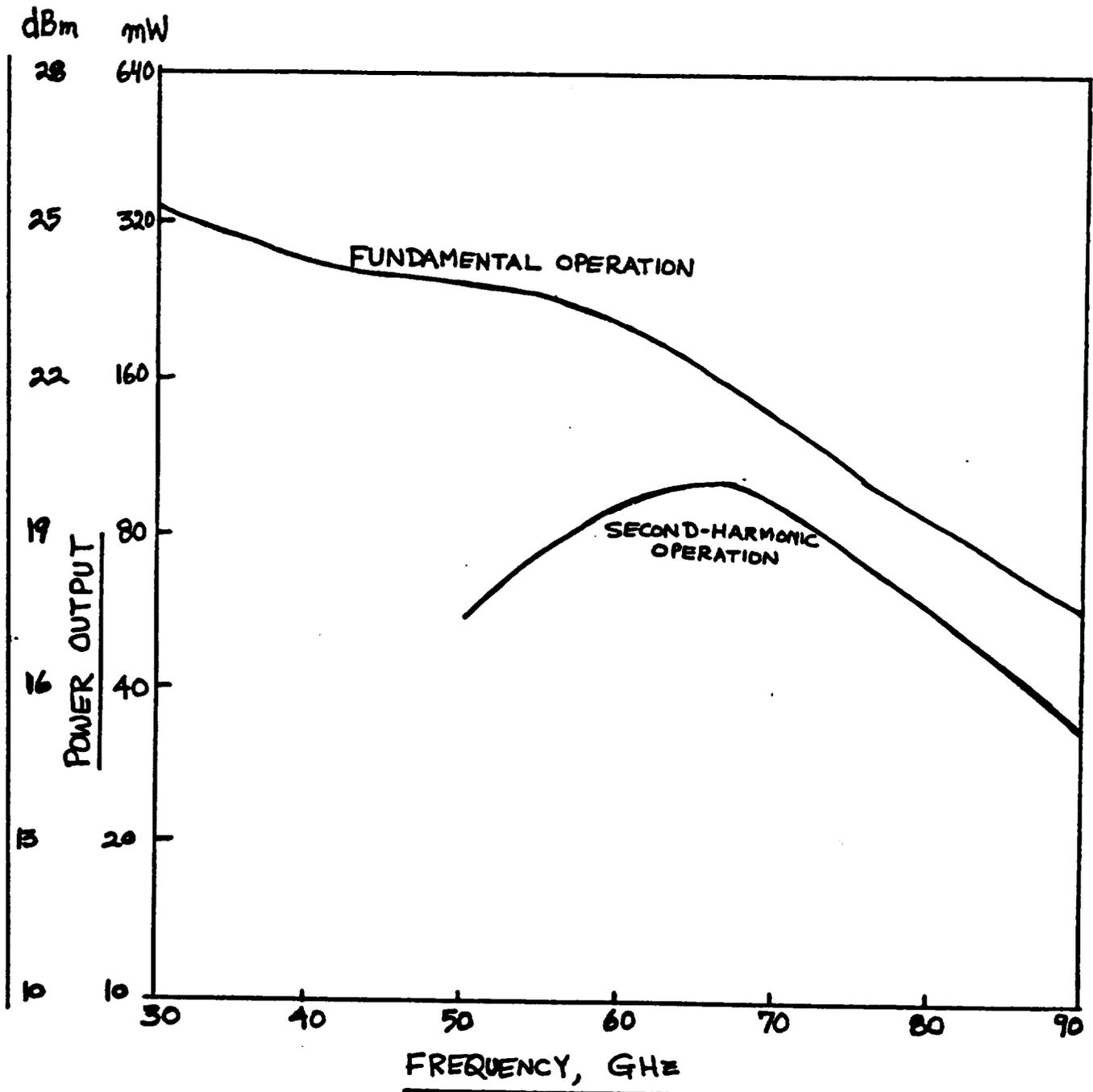
Figure 4.4 (a) Power output potential of various InP Gunn devices for fundamental and second-harmonic operation. Different device types were used in the fundamental and second-harmonic mode at a particular frequency.
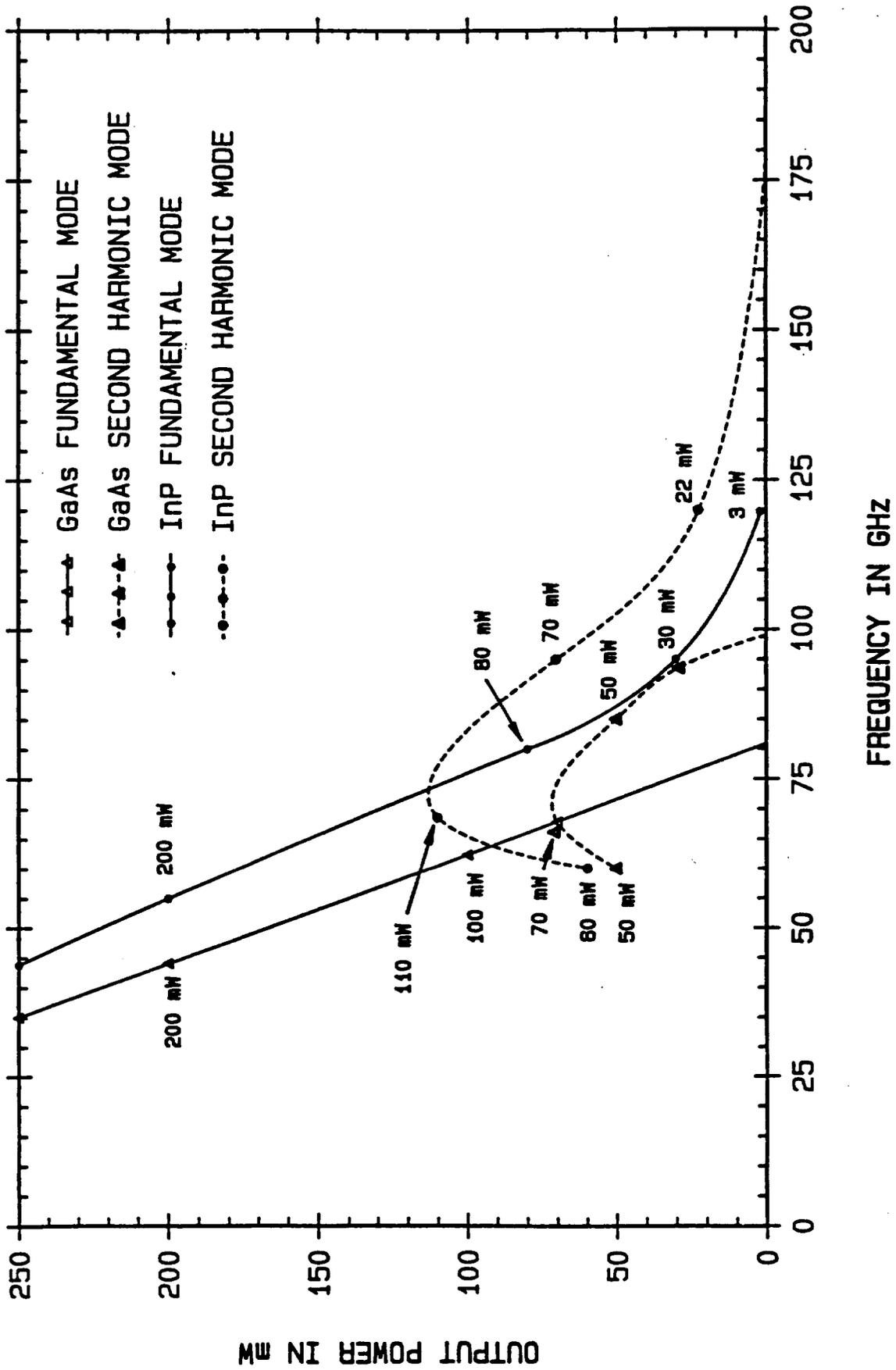
Figure 4.4 (b) Power output vs. frequency for GaAs and InP Gunn diodes operating in both fundamental and second-harmonic mode.

TABLE 4.3
COMPARISON OF FUNDAMENTAL AND SECOND HARMONIC OPERATION
POTENTIAL OF VARIOUS INP GUNN DEVICES

Frequency Range, GHz	Second-Harmonic Operation		Fundamental Operation		Comments and Observations
	Typ. Power Output, mW	Conversion Efficiency*	Typ. Power Output, mW	Conversion Efficiency	
56-62	90	3%	250	11.4%	Harmonic operation non-optimal due to lack of devices below 30 GHz
63-68	110	3.8%	225 to 155	9.3 to 6.4	Fundamental power drops with increase in frequency
69-78	85	2.7%	140 to 100	5.9 to 5.5	Same as for 63-68 GHz range

*Millimeter wave power to DC power ratio

c) The bias tuning characteristics of these sources were well-behaved, monotonic, and fairly predictable. There was a considerable amount of voltage tuning obtainable from these to permit compensation for thermal drift in a frequency stabilized source system, such as a phase-locked oscillator. However, the power versus bias voltage characteristic are noticeably different from unit to unit.

d) These units had low thermal frequency drift coefficients in general. The coefficient is always negative and lies in the range of -0.7 MHz/°C to -4.5 MHz/°C. A fair degree of control has been demonstrated in achieving low drift operation. Further work in reducing drift will be carried out in the near future.

e) The external Q factors of these oscillators are significantly higher than the fundamental units. Typical external Q measurements by the load pull method range from 600 to 1500. Consequently, a fairly load independent operation can be realized. Typically, this eliminates the need for an isolator, thus maximizing the power available to the load.

Further work was conducted in the area of high-performance second-harmonic Gunn diode oscillator. The following results are considered to be very significant, and indicative of the optimal extraction in this mode of operation.

Device Type	Frequency of Operation	Power Output	DC to RF Efficiency
InP, 35-44 GHz	69.6 GHz	114 mW	5%
InP, 44 GHz	75.0 GHz	110 mW	5%
InP, 47 GHz	94.0 GHz	97 mW	5.7%

Considerable amount of developmental work has been performed on the design of a resonator/transformer disc for optimal second-harmonic extraction. A very extensive device/cavity characterization program was also conducted to obtain design curves for sources with any arbitrary frequency-tuning characteristics. Four different devices, listed below, were tested in a WR-10 standard cavity using a wide variety of chokes and resonator structures. The frequency of operation for these oscillators is plotted in Figure 4.5 as a function of geometrical parameters and device types. These curves are useful in understanding the devices' equivalent parameters for the purposes of circuit design.

Varian Device Designation	Frequency	Power
VSA 9110S2	35 GHz	250 mW
VSQ 9119S1	44 GHz	250 mW
VSE 9120S1	56 GHz	150 mW
VSB 9122S13	94 GHz	60 mW
VSB 9122AJ	110 GHz	25 mW

4.5.2   High Frequency Indium Phosphide Oscillators

The object of this aspect of source development was to produce a sequence of Indium Phosphide fundamental and second-harmonic sources in the frequency range of 105 to 180 GHz with the maximum available power output and modest mechanical tuning. In addition, the characteristics of such sources were studied with a view to examining their appropriateness for phase-locked operation and subharmonic pump for mixers.

There are several Indium Phosphide devices which can be used to obtain oscillation in the 105 to 180 GHz range, either in the fundamental mode or as harmonic extraction operation. The following devices have been selected and studied here:

| Device Part Number	Center Frequency, GHz	Power Output, mW
Varian VSE-9120S3	56	250
Varian VSB-9122S4	80	80
Varian VSB-9122S10	94	30
Varian VSB-9122S13	94	60
Varian VSB-9122AJ	110	25
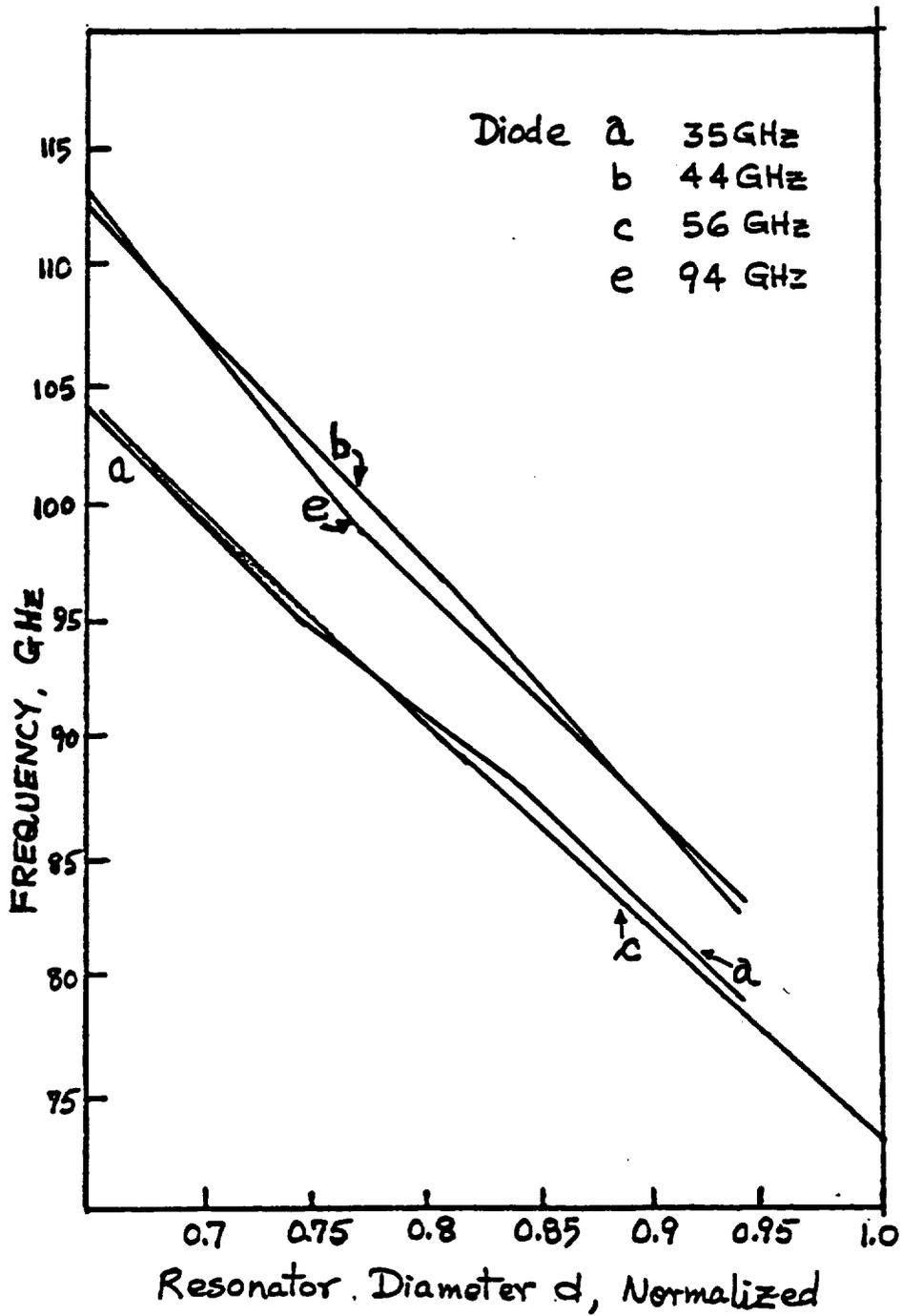
Figure 4.5 (a) Resonance characteristics of various Gunn diodes in cavities with varying parameters.
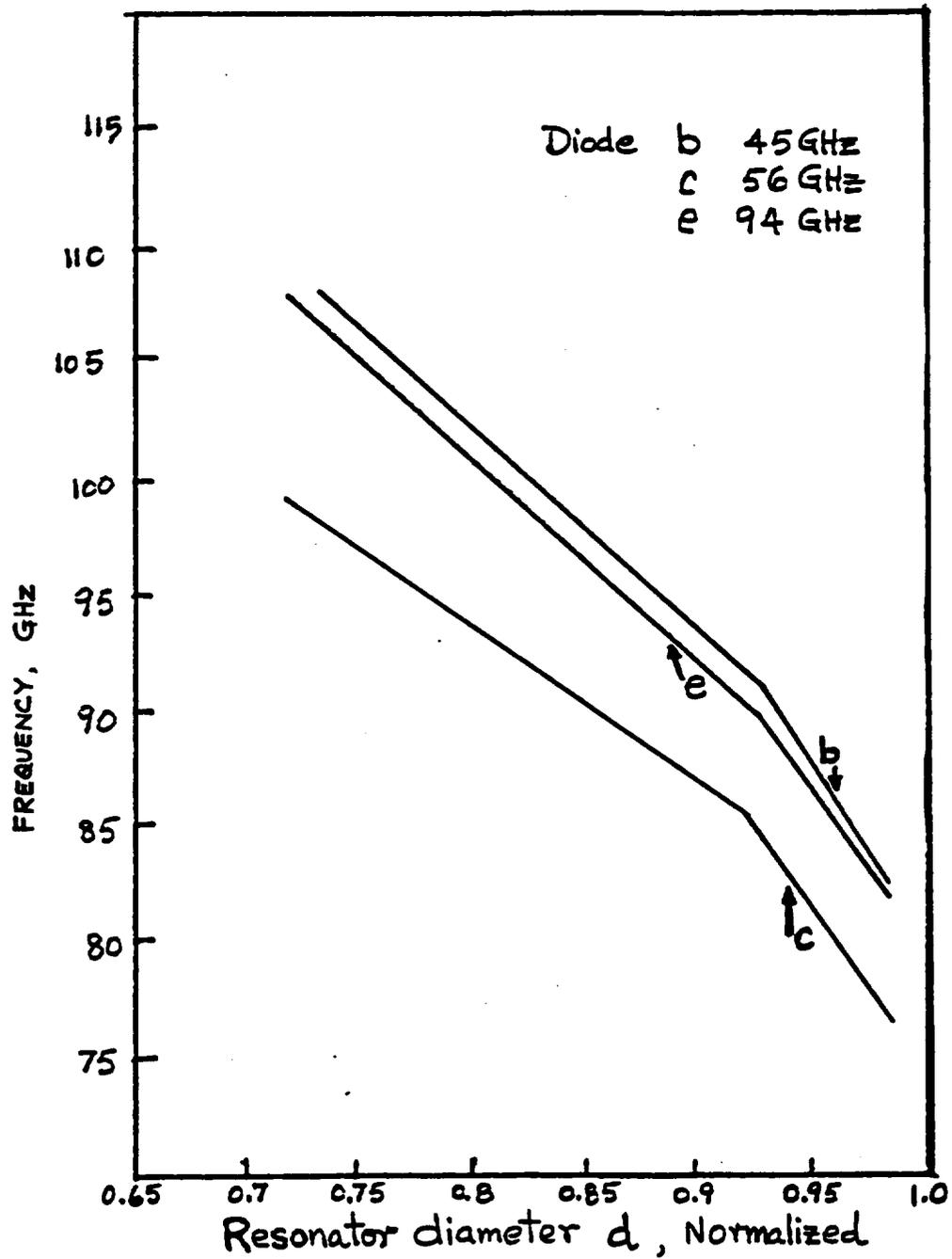
Figure 4.5 (b) Resonance characteristics of various Gunn diodes in cavities with varying geometrical parameters.

These devices have drastically different operating characteristics, such as operating voltages, domain capacitances, etc., stemming primarily from the differences in diode active layer lengths. The majority of the oscillators involved the use of a VSB-9122S13, either in its fundamental mode or as a second harmonic extraction type.

The basic oscillator design is shown in Figure 4.6, and can be described as a resonator coupled, full height oscillator with variable back short location. Minor variations of this general configuration were also studied. The results of several oscillators are summarized in Table 4.4 and Table 4.5 to indicate the status of high frequency source activity. These results are fairly representative in nature and do not indicate limitation of the technique or the devices.

TABLE 4.4
HIGH FREQUENCY OPERATION

Oscillator Serial No.	Waveguide Band	Center Frequency GHz	Power Output mW	Mechanical Tuning GHz	Bias Tuning MHz	Comments Observations
EE-669-40	WR-8	123	23	+/-0.5	400	Rotation sensitive
EE-725-1	WR-8	129	21	+/-0.5	400	Rotation sensitive
EE-669-62	WR-6	140	10	+/-0.2	500	Power drops beyond 135 GHz
EE-726-10	WR-8	119	25	+/-0.5	400	Similar to W-band units

TABLE 4.5
HIGH FREQUENCY SECOND HARMONIC OPERATION

Oscillator Serial No.	Waveguide Band	Center Frequency GHz	Power Output mW	Mechanical Tuning GHz	Bias Tuning MHz	Comments Observations
275a-43	WR-8	119	12	+/-0.5	300	Higher power possible
EE-725-25	WR-6	148	1	+/-0.3	500	Power decreases with frequency
EE-725-13	WR-6	160	1	+/-0.75	600	Mechanically sensitive to structure dim.

Design curves for sources in the range of 105 to 140 GHz have been derived from this segment of the study. Two fundamental limitations of these sources have been identified as far as the high frequency operation of InP Gunn devices is concerned. First, the device package (ceramic ring and metal disk) impose severe performance limitations due to parasitics and resonances. Appendix C deals with the subject of diode packaging. Second, the mechanical dimensions and physical tolerances are highly critical to achieving an optimal performance. In particular, a very significant rotational sensitivity is observed with respect to the Gunn diode and the resonator. The power output is seen to vary by as much as 6 to 7 dB with diode rotation. This can be attributed to imperfections in the diode package and choke, as well as the asymmetry in the chip bonding straps, etc.
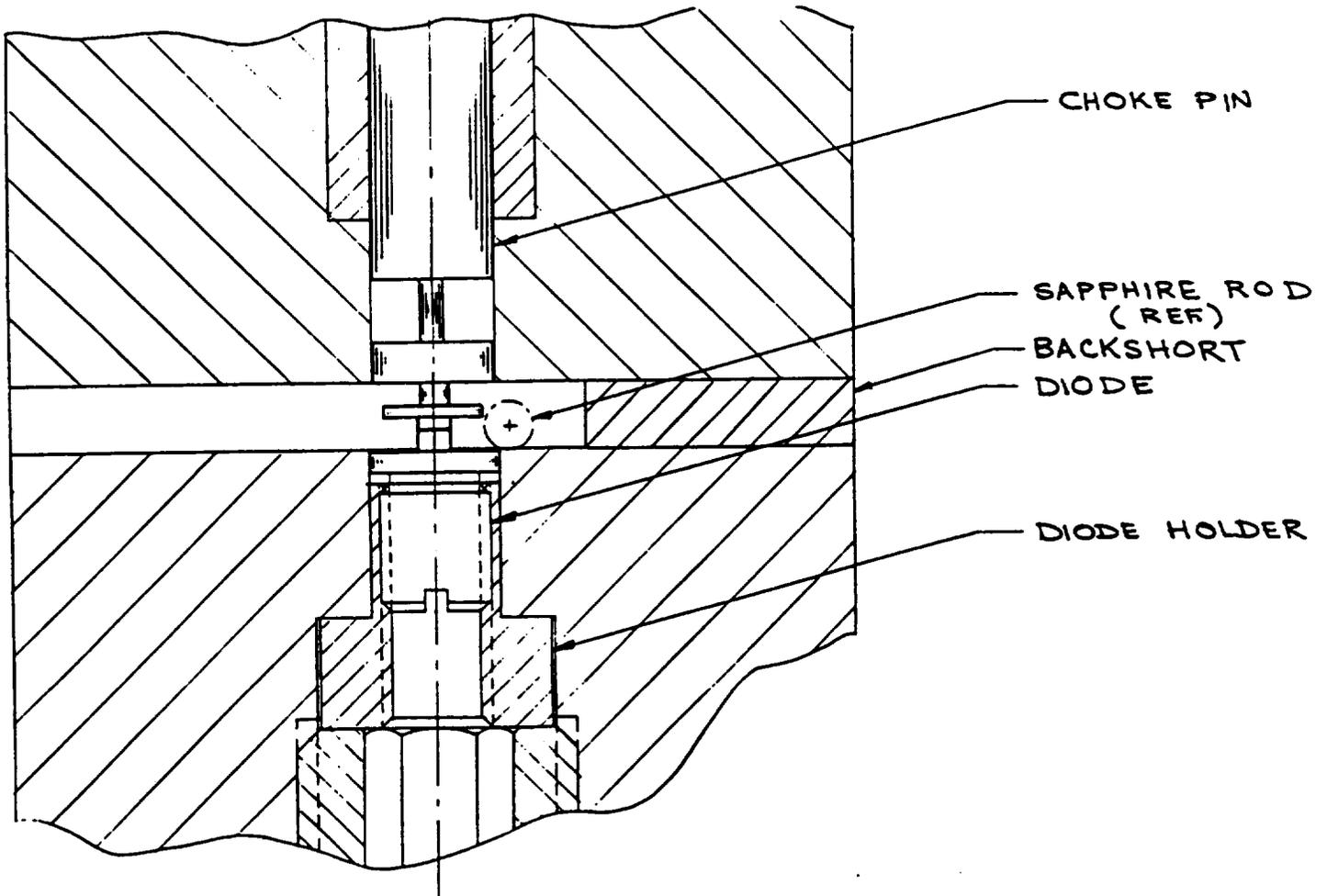
Figure 4.6 Typical high frequency InP Gunn oscillator configuration.

CHOKE PIN

SAPPHIRE ROD
(REF)
BACKSHORT
DIODE

DIODE HOLDER

4.5.4   Wideband Mechanical Tuning

One of the critical objectives of this study was to devise mechanisms and circuit techniques to achieve wideband mechanical tuning characteristics from InP high power Gunn oscillators in the 60 to 110 GHz range. This involved obtaining reliable and reproducible tuning characteristics while maintaining a reasonable constant high power output. Three distinctly different types of tuning mechanisms have been studied thus far:

a)   Movable backshorts,

b)   Dielectric tuners, and

c)   Variable co-axial resonator elements.

Preliminary results of this study are summarized in Table 4.6 to show the relative characteristics and principle features of these three mechanisms.

TABLE 4.6
WIDEBAND MECHANICALLY TUNABLE OSCILLATORS

Type of Mechanical Tuning Arrangement and Mode	Frequency Range of Operation GHz	Power Output Range Min.-Max. Typical
Backshort, Fundamental mode	41.5-61.0	25-90 mW, typ. 80 mW
Backshort, Fundamental mode	65.0-81.0	15-69 mW, typ. 50 mW
Dielectric tuner under the resonator, with backshort for power maximization	81.0-95.0	45-65 mW, typ. 60 mW
Movable coaxial resonator element	69.9-117.0	5-17 mW, typ. 10 mW

A W-band source covering the entire waveguide band was developed on the basis of a design by Carlstrom, et. al., [4]. This oscillator is essentially a coaxial resonator-type, with a mechanically adjustable resonator length. Figure 4.7 shows the construction details of the source. The resonator is formed by the radial disk and the post above it, the length of which is adjustable by means of a mechanical tuner. The tuning mechanism is somewhat complex, and requires considerable care and precision in its implementation, since a positive, stationary contact with the diode must be maintained during tuning.

This oscillator was evaluated using several different Gunn diodes, both GaAs and Indium Phosphide. Very encouraging results were obtained in each case. Figure 4.8 shows the frequency-power characteristics of the oscillator. A power "suck-out" is observed in the vicinity of 78 GHz due to structural resonances. However, as the plot shows, it is possible to extract considerable high power ($\approx$ 45 mW) over a fairly broad frequency range, while

3. Choke hole
4. Choke (outer)
5. Choke (inner)
6. Insulation
7. Bias pin
8. Circuit card
9. Diode
10. Diode holder
11. Locking nut
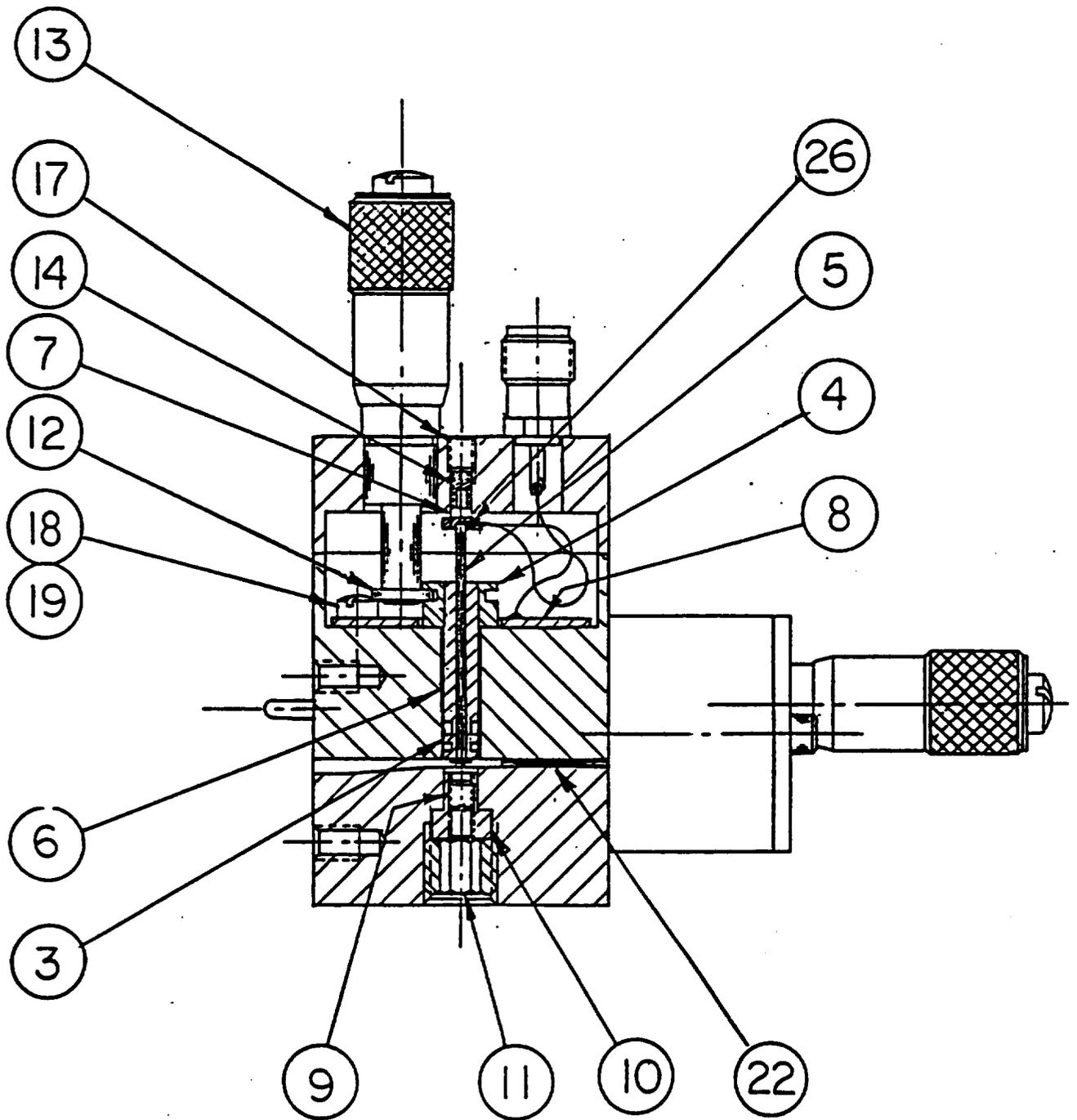
12. Micrometer coupling
13. Micrometer head
14. Choke retainer spring
17. Retainer
18. Screw
19 Dowel pin
22. Backshort
26. Bias ring

Figure 4.7 Sectional view of wideband mechanically-tunable Gunn oscillator.
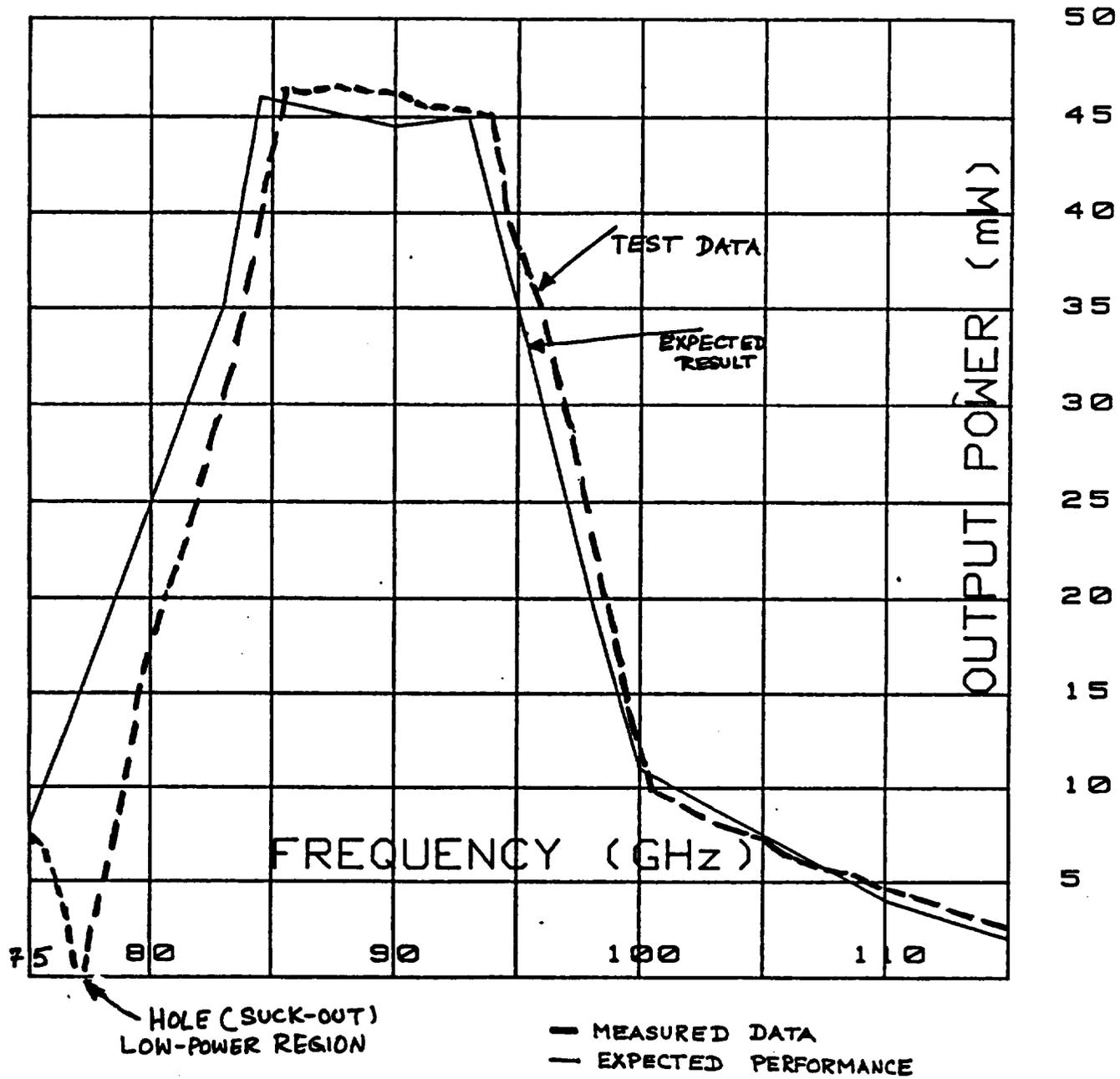
Figure 4.8 Power output vs. frequency for wideband mechnically-tunable Gunn oscillator shown in Figure 4.7.

achieving a nominal 2-10 mW power output from 68-117 GHz. Further work is needed to optimize the performance of the unit over the entire tuning band, and achieve more reliable operation.

4.6   Gunn Diode Characterization for High Reliability Applications

4.6.1   Introduction

Properly designed, assembled and used Gunn Diodes are very rugged and highly reliable. However, it is up to the device manufacturer to ensure that the devices are designed properly for the given application, and manufactured according to established procedures. In common with other semiconductor devices, the devices are prone to early failures due to incorrect assembly and testing. Also, Gunn diodes are power generation devices with relatively low efficiencies. Hence, the maximum temperature of GaAs diode junction under all operating conditions for that application should not exceed 260°C--a number established after an exhaustive reliability study under a U.S. Army Contract No. DAAB07-72-C-0101.

How can a diode user ensure that the diodes have been designed and assembled properly? Are there any independent tests that may be conducted to evaluate the "quality" of the diodes? These and other important questions were examined in this portion of the study.

The active layer temperature of a Gunn diode may be obtained by a measurement of the thermal resistance of the diode using a temperature dependent parameter of the diode as a thermometer. The property of the diode that is sensitive to any mechanical damage that would be encountered during the diode manufacture including epitaxial growth is the diode breakdown voltage. During operation of the diode, Gunn domains form and travel through the material. These domains have very high electric fields exceeding 70 kV/cm. As the operating voltage is increased, the electric mechanical damage of the active layer during diode manufacture will serve to decrease the breakdown electric field. These damages may be caused by excessive ultrasonic power of excessive pressure during die bonding or during wire or strapping operation. The damages may also be caused by excessive handling or the devices or during lapping operation.

The breakdown voltage of the device increases with increasing temperature--a characteristic of avalanche breakdown. The slope of the V_B - T curve depends on several factors, including doping density, doping uniformity, and in some cases, buffer layer characteristics.

A technique for measuring the thermal resistance and the breakdown voltage is described below for Gunn devices.

4.6.2   Thermal Resistance

A convenient way to measure the operating diode temperature is to find a diode parameter which is temperature-dependent and which also could be theoretically related to the operating temperature.

One of the temperature-dependent parameters of the Gunn diode is the current through the diode. The diode current under operating conditions is dependent not only on the device temperature, but also on the operating bias voltage and the load conditions. Hence, it is not easy to relate it theoretically to the operating temperature. The current through the diode below threshold voltage, on the other hand, is not only temperature-dependent, but also is capable of being described theoretically.

In other words, the diode current, I_d, below threshold voltage may be described mathematically as:

$$I_d = q * \mu(T) * E * N_d$$

where

q = 1.6 E -19 coulombs = electronic charge

$\mu(T)$ = Carrier mobility which depends on diode temperature in T (°K)

= $\mu^0 * (T_o/T)^\alpha$

T_0 = reference temperature

T = diode temperature in °K

α = material dependent parameter with a value between -1.5 and +1.5. The limits of ±1.5 is set by the nature of the atomic binding and hence, depends in detail on the carrier concentration, and the method of growth, etc. α may be measured independent of the thermal resistance.

N_d = carrier density of the diode epi layer in No./cc.

The equation may be rewritten for convenience as:

$$I_d = C/T^\alpha$$

where

C = a constant whose value is experimentally determinable.

The equation may be manipulated to arrive at:

$$I_{dH} = I_{dC} * (T_C/T_H)^\alpha$$

Rewriting the equation, we have:

$$T_H = T_C * (I_{dC}/I_{dH})^{(1/\alpha)}$$

where

I_{dH} = diode current at a diode temperature of T_H °K

I_{dC} = diode current at a diode temperature of T_C °K

Or,

$$T_H = T_C * (R_H/R_C)^{(1/\alpha)}$$

where R_H and R_C are the low-field resistance values of the diode at T_H and T_C respectively.

Figure 4.9 shows the typical I-V characteristics of a Gunn diode as a function of temperature. As would be expected, the diode current decreases as the diode temperature increases at a set bias voltage. It is clear from the figure that the operating temperature may be measured by pulsing the diode voltage from the set value to a value below the threshold and measuring the diode low field resistance R_H. R_C may be measured at a diode case temperature of T_C °K.

4.6.3 Breakdown Voltage

The breakdown voltage, V_B, of the diode is conveniently measured by using a pulse of width <1 μs and a duty cycle of 1% or less. The use of a small pulse width minimizes any hearing effect. The applied voltage across the diode is increased until the current saturation is observed. The voltage is increased further until the current starts increasing beyond the saturated value. Nominally, the breakdown voltage is specified at 1.1% of the saturated current value. Typically, a good diode will have a breakdown voltage greater than 8 times the threshold voltage. Typically, at 35 GHz the breakdown voltage of the diode will be 15 V.

4.6.4 Device Characterization and Failure Analysis of InP Devices

The primary objective of this task group is to study the reliability and operational characteristics of the Indium Phosphide devices for use in ground and space-based radiometers. A number of critical evaluation subtasks and tests have been carried out with support from the vendors of Indium Phosphide Gunn devices.

The first subtask was to devise and implement a measurement system for the junction temperature of Gunn diodes. This set-up is shown in Figure 4.10. The test results from the measurements on a few devices (GaAs and InP) are documented in Figure 4.11. In addition, the thermal and I-V characteristics of devices undergoing burn-in or suspected of having degraded were measured for analysis. Typical maximum junction temperature of 160°C has been determined to be acceptable for 10^6 hours of operation with less than 2% probability of failure. The thermal impedance of the device is approximately 45°C/W, with a typical of 2 Watts of input dc power. Hence, the maximum allowable baseplate temperature of 70°C is prescribed for these InP diodes. These results are based upon the following failure criterion. The dc bias current of an InP Gunn device is measured at a standard baseplate temperature. When the dc bias current exceeds the nominal value by 10%, a permanent damage (device failure) is assumed to have taken place.

The second subtask was to determine any failure modes of performance anomalies of significance. These tests have been made on a broad scale, utilizing all different types of InP devices over a considerably wide range of operating conditions and environmental
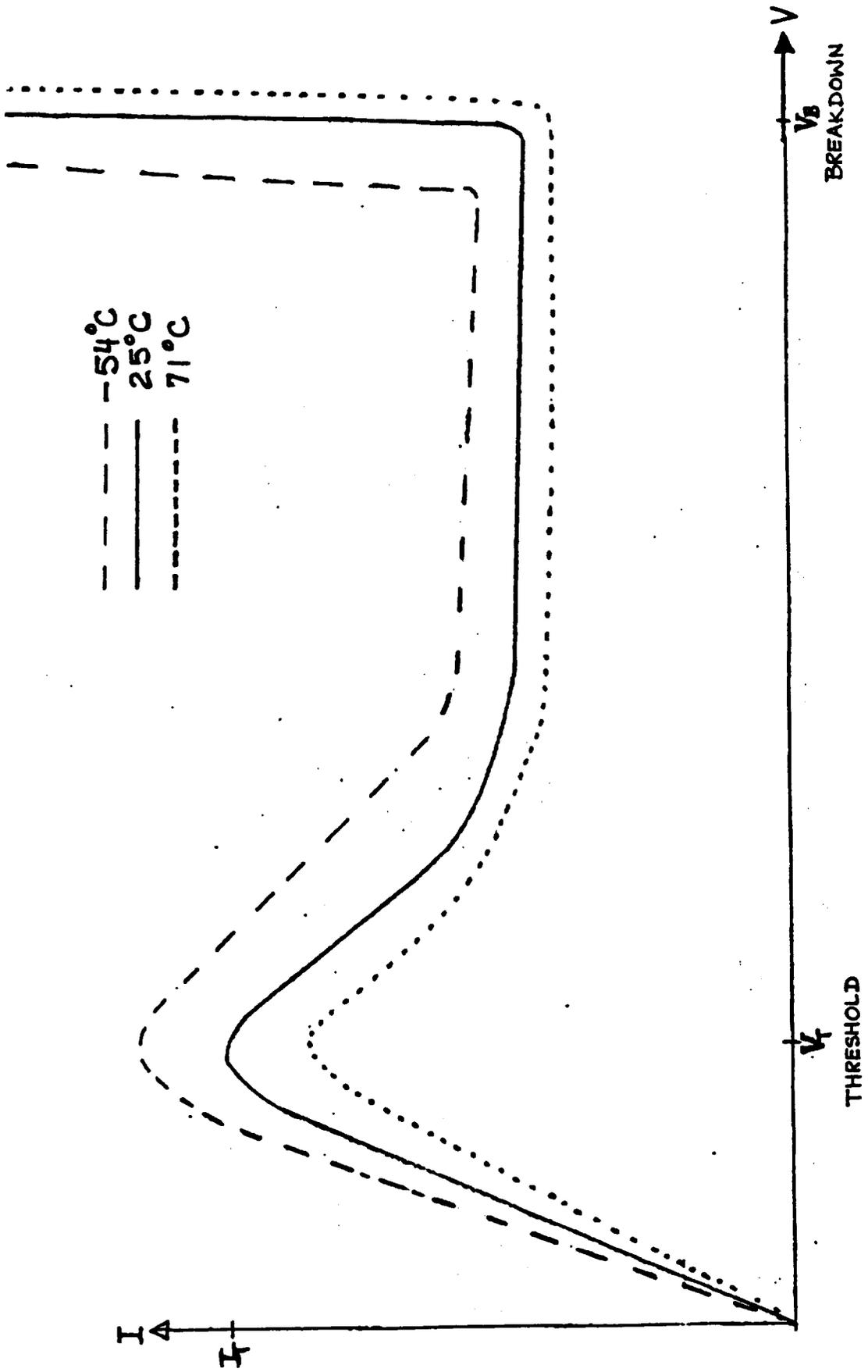
Figure 4.9 Gunn diode I-V characteristics for several different case temperatures.
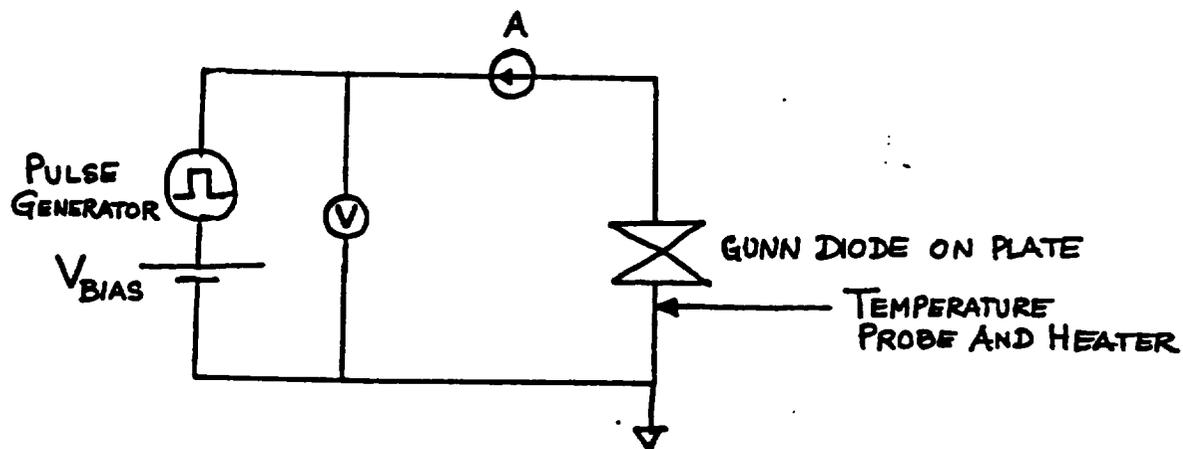
Figure 4.10 Experimental measurement system for thermal characterization of Gunn devices.
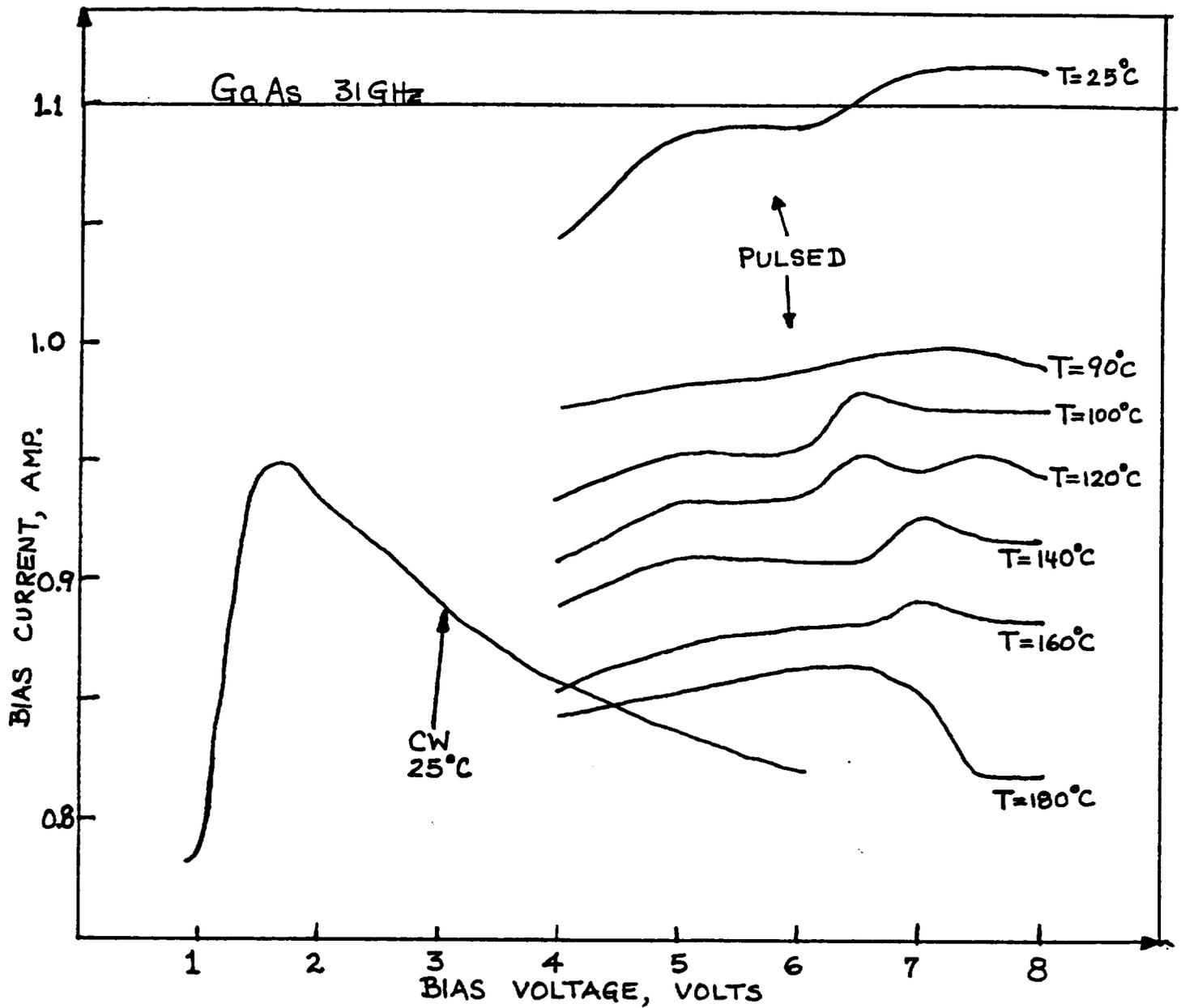
Figure 4.11 Experimentally measured I-V characteristics of 31 GHz GaAs Gunn diode for various baseplate temperatures.
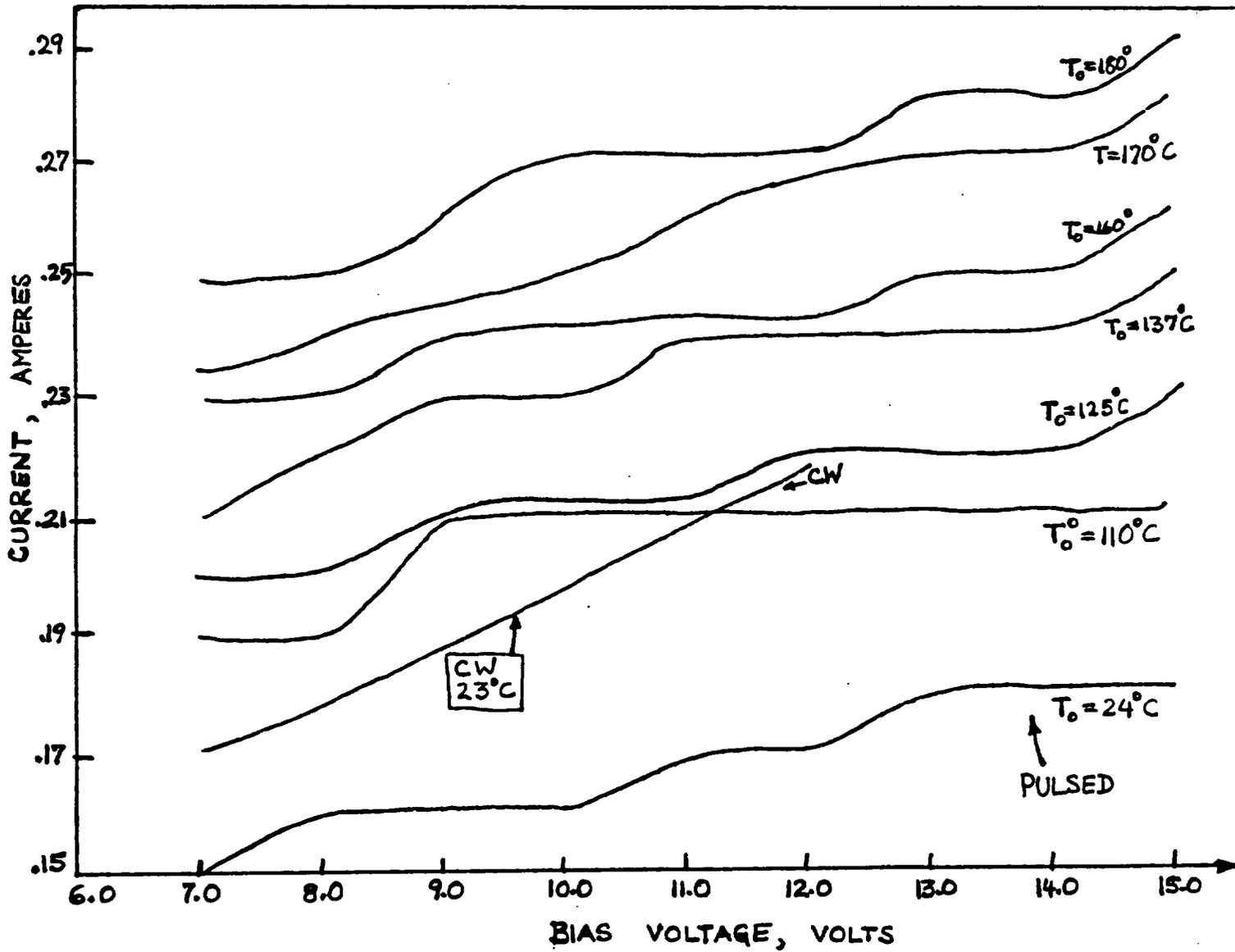
Figure 4.12 Experimentally measured I-V curves for 44 GHz InP diode for different baseplate temperatures.

factors in various applications. An extensive data base has been generated as a result. Some of the preliminary conclusions of this scrutiny are summarized below:

1.   The devices' physical dimensions are somewhat incompatible with the standard microwave diode package. The InP Gunn chip is extremely thin and small in area. The bond wires used in a standard package (Varian N34) are very long, and form a catinary that is located fairly close to the base (ground). Excessive mechanical stress on the diode package lid or thermal effects are potentially capable to elongating the bond leads sufficiently to cause a short circuit, and hence a device failure. In essence, the package is much too large physically for the InP high frequency devices. It adversely impacts both the integrity and electrical performance of the devices. The need for a new, "millimeter-wave appropriate" package is critical to further progress in the oscillator area.

2.   The InP device contains a current-limiting contact in its construction. This contact is central to the performance of the device. However, it poses some problems in practice, mostly in regard to biasing. The device cannot tolerate a rapid negative-polarity transient, or a negative bias. For example, a short circuit across a fully-biased device can result in a catastrophic failure.

3.   Concerns have been raised with respect to long-term drifts in InP diode-based oscillators. These are based on a very limited observations and not from any systematic study. To date, there is no conclusive data or information base to either support or negate these observations. Millitech has produced a very large number of InP device oscillators, which were mechanically tunable. Therefore, it has not been possible to gather information on any fine grain frequency or power drift in these units. An accelerated test is currently being configured to examine these characteristics of InP device-based sources.

4.   Acceleration Test: Several W-band (nominally 94 GHz) Indium Phosphide diode-based Gunn Oscillators were tested for shock and high acceleration survivability. In a pyrotechnic shock test, these units were subjected to accelerations in excess of 24000 g (10 kHz). All the oscillators successfully survived this shock level.

Several InP devices which had failed during this development program were analyzed in a very systematic fashion following the standard industry procedures. These detailed results of these analyses are included in Appendix B, together with actual test reports.

5.0 SOURCE SUBSYSTEM PERFORMANCE AND NOVEL DEVELOPMENTS

5.1 Source Subsystem Performance Summary

The 500 GHz Submillimeter-wave local-oscillator source was configured and tested as a completed subsystem. The pump (driven) oscillators at 79 and 83 GHz were individually optimized to extract the best stable operation achievable using fixed power supplies. The balanced doubler was also tuned for the output frequency range of interest. Under the conditions of maximum input pump power, the tripler operation was optimized.

The results of the entire subsystem performance are summarized below:

Parameters and Units		Case 1	Case 2
Input Frequency, f_o GHz		79	83
Input DC Power, W_{in} Watts		3.6	3.6
Input Power, P_{in} mW		120	110
Output Frequency, $6f_o$ GHz		474	498
Output Power, P_{out} mW		0.7	.55
Multiplier Chain Efficiency	$\left(\dfrac{P_{out}}{P_{in}}\right)X100\%$	0.6	0.5
DC to submillimeter-wave output efficiency	$\dfrac{P_{out}}{W_{in}}X100\%$	0.020	0.16

This output power produced by the source subsystem at 500 GHz is well in excess of reported performance of submillimeter-wave multiplier chains to date. Also, this power level (~1 mW) is expected to be sufficient to drive either a quasi-optical frequency doubler or a SIS-device to provide sufficient local oscillator pump power in the 1000 GHz frequency regime.

The complete source assembly is relatively easy to operate and produces highly repeatable performance on subsequent operation. No critical adjustments or alignments are necessary to achieve proper operation. The source is environmentally stable, and reasonably rugged for radiometry applications.

5.2   Novel Developments in Related Areas

In conjunction with this present 500 GHz source development program, a number of other peripheral components were developed to enhance the usefulness of the source development effort. The noteworthy among these innovative components are:

a)   Carity-stabilized local oscillator sources

b)   Injection Locked Millimeter-Wave Sources

c)   Quasi-optical Ferrite Isolators.

In addition, theoretical work was conducted on a new multiplier device for high-power generation in the millimeter-wave range of 40 to 140 GHz. A summary of these development studies follows.

5.3   Cavity-Stabilized Local Oscillator Sources

Our goal was to design and build a cavity stabilized Gunn diode oscillator at 91 GHz. A cavity stabilized oscillator is desirable, since its frequency stability is essentially that of the resonant cavity. Thus, if the cavity is made of some low thermal expansion material, such as INVAR, the frequency of the oscillator will be very stable over wide temperature ranges.

In Figure 5.1 is shown a diagram of a cavity stabilized Gunn diode oscillator. The oscillator is designed to run at a fundamental frequency (i.e., 45.5 GHz) and to extract the second-harmonic power (i.e., 91.0 GHz). The fundamental frequency is set approximately with the post resonator and the distance between the post and the output waveguide. The oscillator cavity is made wide enough to allow propagation of the fundamental frequency. The WR-10 output waveguide acts as a high pass filter, due to its cuttoff frequency (59 GHz) and only allows the second-harmonic to pass.

The mode chart for the cavity is shown in Figure 5.2, including the actual data for the oscillator shown in Figure 5.1. The data has a frequency dependence of -14.7 MHz for each 0.001" of back short motion at $f_o \simeq 46$ GHz. The theoretical slope for the TE_{221} mode is -15.0 MHz/.001" leading to the conclusion that the cavity is operating in this mode for the data shown. The displacement of the data and theoretical curve is probably due to the loading effect that is probably due to the loading effect that the oscillator has on the cavity. The theoretical unloaded Q of the cavity in the TE_{221} mode is calculated to be 19,600 at 46 GHz.

In this mode the oscillator has a measured loaded Q of greater than 12,500 and the voltage pushing is reduced to less than 2 MHz/volt, compared to 20-30 MHz/volt without a stabilizing cavity.

WR-10 OUTPUT WAVEGUIDE
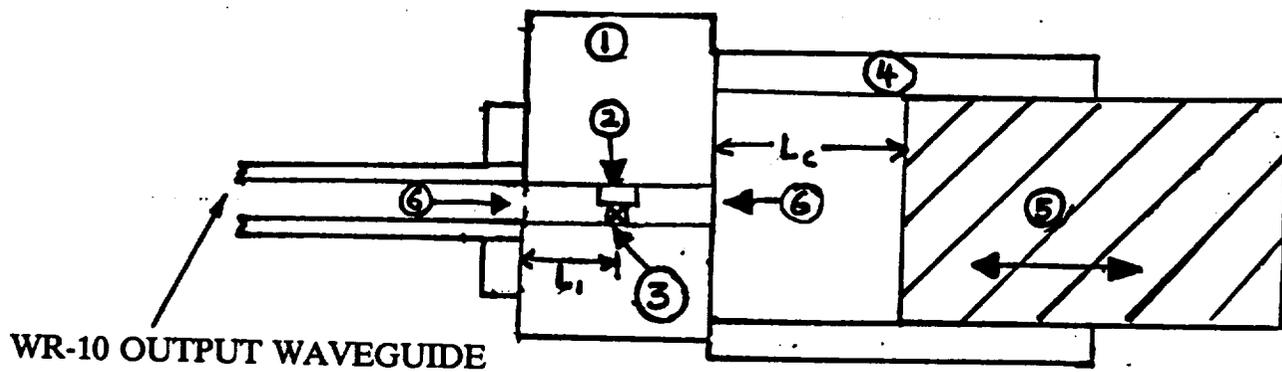
1. GUNN DIODE OSCILLATOR
2. POST RESONATOR
3. GUNN DIODE
4. RESONANT CAVITY 0.585 IN. DIAMETER
5. RESONANT CAVITY BACKSHORT
6. COUPLING IRIS

Figure 5.1 (a) Cavity-stabilized Gunn diode oscillator sectional view.
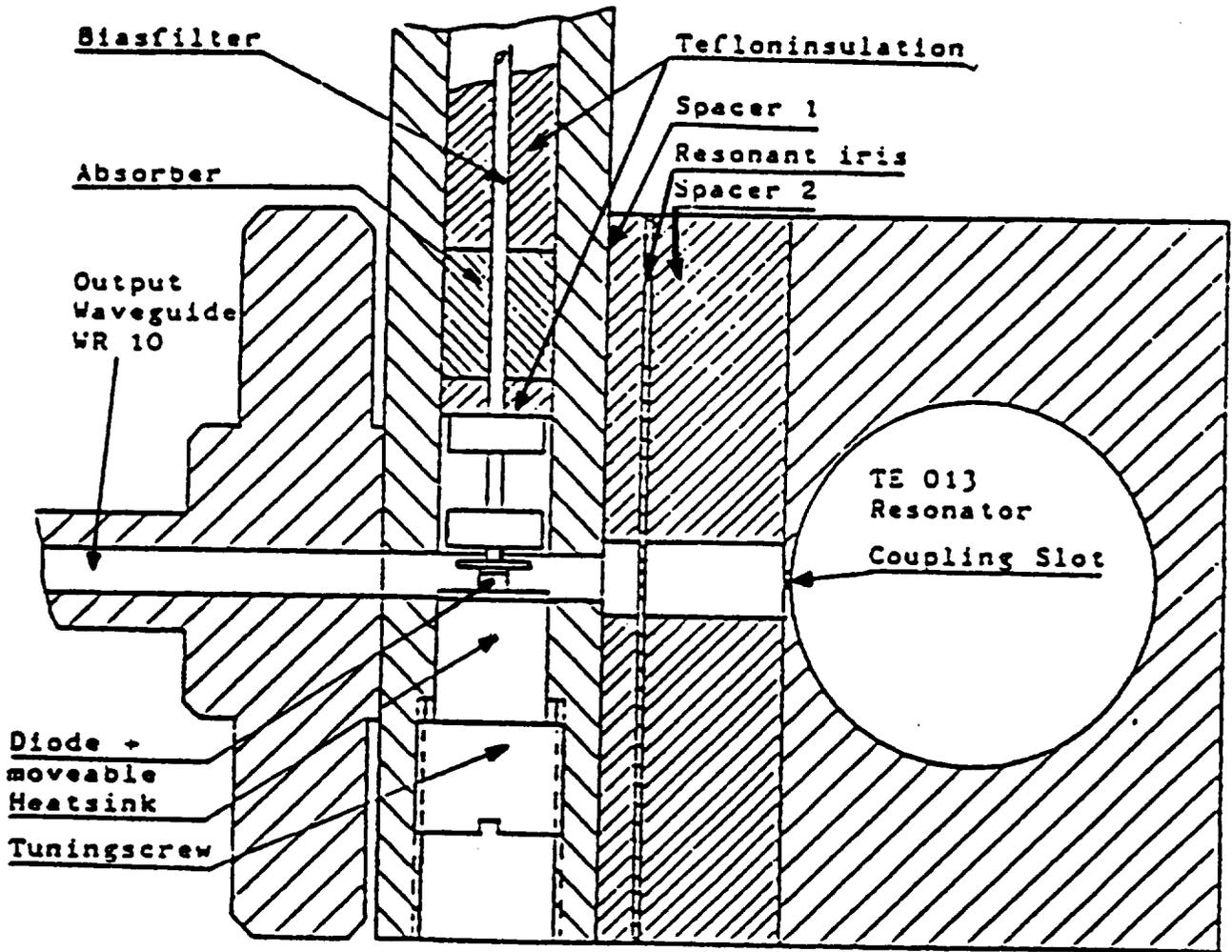
Figure 5.1 (b) Cavity-stabilized Gunn oscillator sectional view for second harmonic operation (Ref. Barth, in 1986 MTT Symposium Digest)
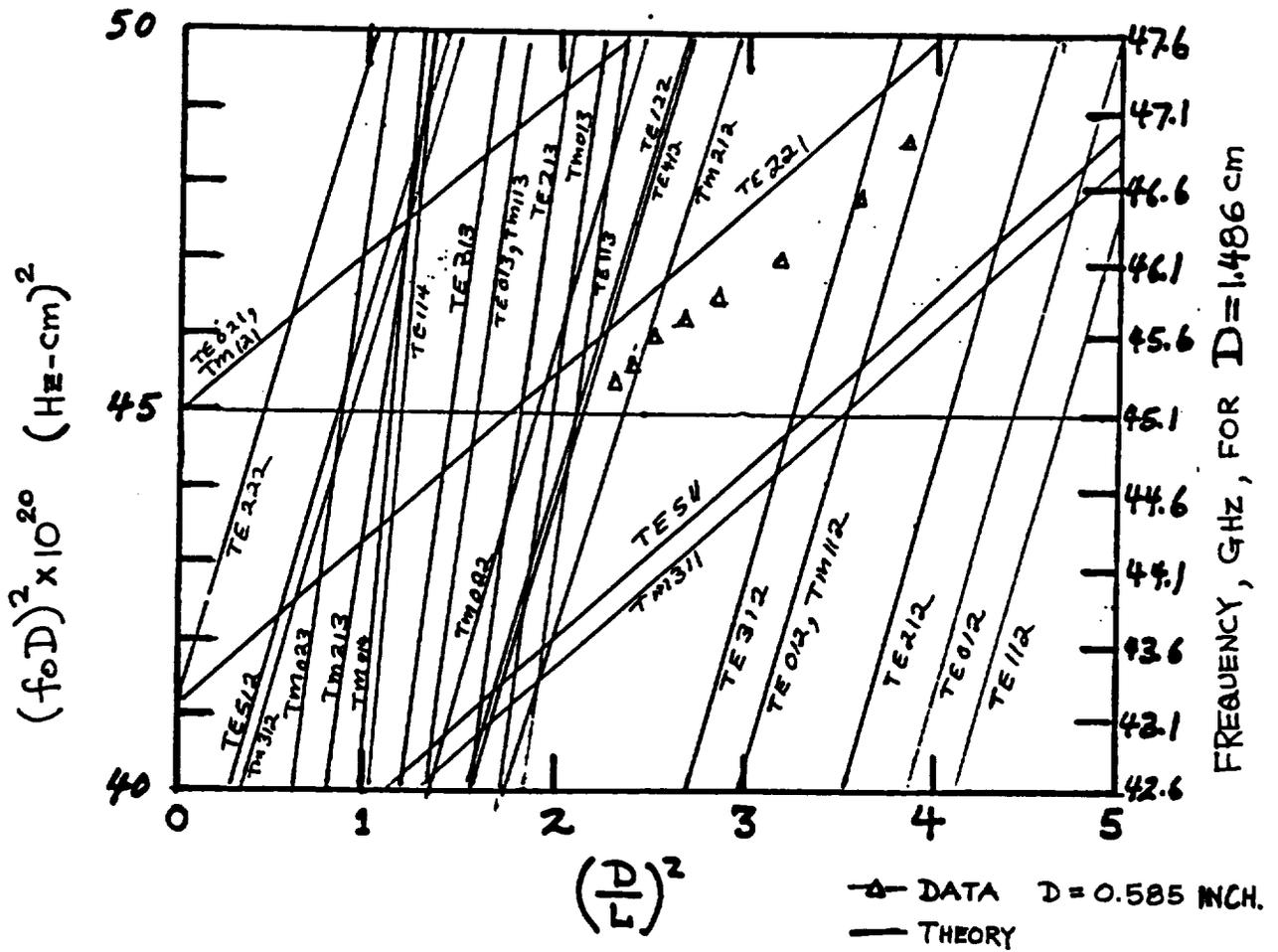
Figure 5.2 Mode chart for resonances of a cylindrical resonator cavity.

With an all brass cavity the temperature dependance of the frequency was measured to be -2 MHz/°C at 91 GHz. The theoretical value is given by:

$$\frac{df}{dT} = \frac{\partial f}{\partial L} \cdot \frac{dL}{L} \cdot \frac{L}{dT} + \frac{\partial f}{\partial D} \cdot \frac{dD}{D} \cdot \frac{D}{dT}$$

for the TE_{221} mode:

$$\left.\frac{\partial f}{\partial L}\right|_{46GHZ} = \frac{15MHz}{.001''}$$

$$\left.\frac{\partial f}{\partial D}\right|_{46GHZ} = \frac{-69MHz}{.001''}$$

and for brass

$$\frac{dL}{LdT} = \frac{dD}{DdT} = 19 \times 10^{-6}/°C$$

For the present case at 45.5 GHz with L = .370" and D = .585"

$$\frac{df}{dT} = -0.88MHz/°C$$

The second harmonic frequency will then change as fast as the fundamental frequency giving a predicted value of -1.8 MHz/°C, which agrees well with the observed value of -2 MHz/°C. This implies that the cavity is indeed controlling the drift of the oscillator. Noting that INVAR has a temperature stability of $1.6 \times 10^{-6}/°C$, a cavity of this material would lead to a drift of -0.74 MHz/°C at 91.0 GHz. If greater stability is required, an INVAR cavity with a brass backshort may be used. This allows the dissimilar expansion rates of the two metals to compensate each other: the brass for $\partial L/\partial T$ and the INVAR for $\partial D/\partial T$.

5.4   Hexagonal Ferrite Quasioptical Isolators

Quasioptical isolators are gaining acceptance for use in millimeter wave systems. The purpose of this research effort was to develop a quasioptical isolator using a ferrite with internal magnetization, and thus, requiring no external magnets. This could pave the way

for very large aperture isolators to be used in radiometer systems. The material used in this work was Ba-type hexagonal ferrite.

The magnetized bar was cut into 2 small rectangular samples and the magnetic field of each piece was measured. The thick sample "A" had a field of 1150 Gauss perpendicular to its 2.1 X 1.5 cm face and 86 Gauss perpendicular to the 2.1 X 1.0 cm face.

The return loss of the unmatched samples were measured to determine the dielectric constant by treating the sample like a Fabry-Perot resonator. The dielectric constant was in the range of 20-25. Fused silica disks of thickness of 0.015" were used for antireflection.

The Rotation Measure (RM) of both samples was measured. The thin sample apparently didn't have any. It is difficult to determine the RM of the thick sample because the maxima were broad.

A 94 GHz halfwave plate was mounted in series with the hexagonal ferrite sample. The combination behaved like an isolator, giving an isolation of ~20 dB and an insertion loss of ~3-5 dB. There is large uncertainty in the insertion loss because much of the contribution stems from the fixtures. The geometry of the fixtures does not conform well to the geometry of the sample. When isolating, the device rotates the input polarization 90°, like Millitech's other quasi-optical isolators. RM and isolation were tested with 200 Gauss of external bias from 2 ring magnets. The isolation and insertion loss results did not change much. The minima broadend during the RM tests.

A promising technique for realizing a practical quasi-optical isolator has been demonstrated. Further work is necessary to improve the performance of these components to acceptable levels. Also, additional development effort in the area of hexagonal ferrite materials is needed to facilitate components at any specific center frequency.

6.0 CONCLUSIONS

6.1 Summary

This development program addressed many diverse aspects of millimeter wave and submillimeter wave local oscillator sources. The studies conducted under this technical effort examined several different techniques of realizing sources in the 60-100 GHz range, and rigorously characterized the basic Gunn diode oscillators that are the prime drivers for the submillimeter wave local oscillators. Figure 6.1 is a composite which shows the power generation capability of sources developed in this program from 75 to 600 GHz. The following are the highlights of the main developments in this Phase II program.

6.1.1 Submillimeter-wave 500 GHz Source Assembly

A 500 GHz source assembly was developed using high-power InP Gunn oscillator-combiner driving a cascaded times six multiplier chain. The salient characteristics of this prototype unit are:

Center Frequency	500 GHz	474 GHz
Power Output	0.55 mW	0.7 mW
Multiplying (X6) Efficiency	0.5%	10.6%

The performance of this assembly met the objectives of the program. The design of this unit can be modified for other center frequencies in the submillimeter-wave region. Reasonable tunable operating bandwidth was obtained.

6.1.2 High Performance Multiplier Development

A balanced-doubler design capable of handling significantly high input powers was developed for virtually any center frequency of operation. Very high conversion efficiencies were achieved even at high output frequencies (166 GHz and higher). This doubler performance makes cascading multipliers attractive for submillimeter wave power generation. The design is relatively easy to implement, and broadband enough for most radiometry applications. Typical efficiencies expected from this type of multipliers range from 30 to 45%.

A high frequency tripler with reasonably good conversion efficiency was also developed during the course of this research program. This tripler design is an extension of standard tripler configuration with some necessary fabrication-related modifications. It is usable to frequencies well beyond 600 GHz by appropriate scaling and device selection. Figure 6.1 depicts the performance characteristics of this class of multiplier.
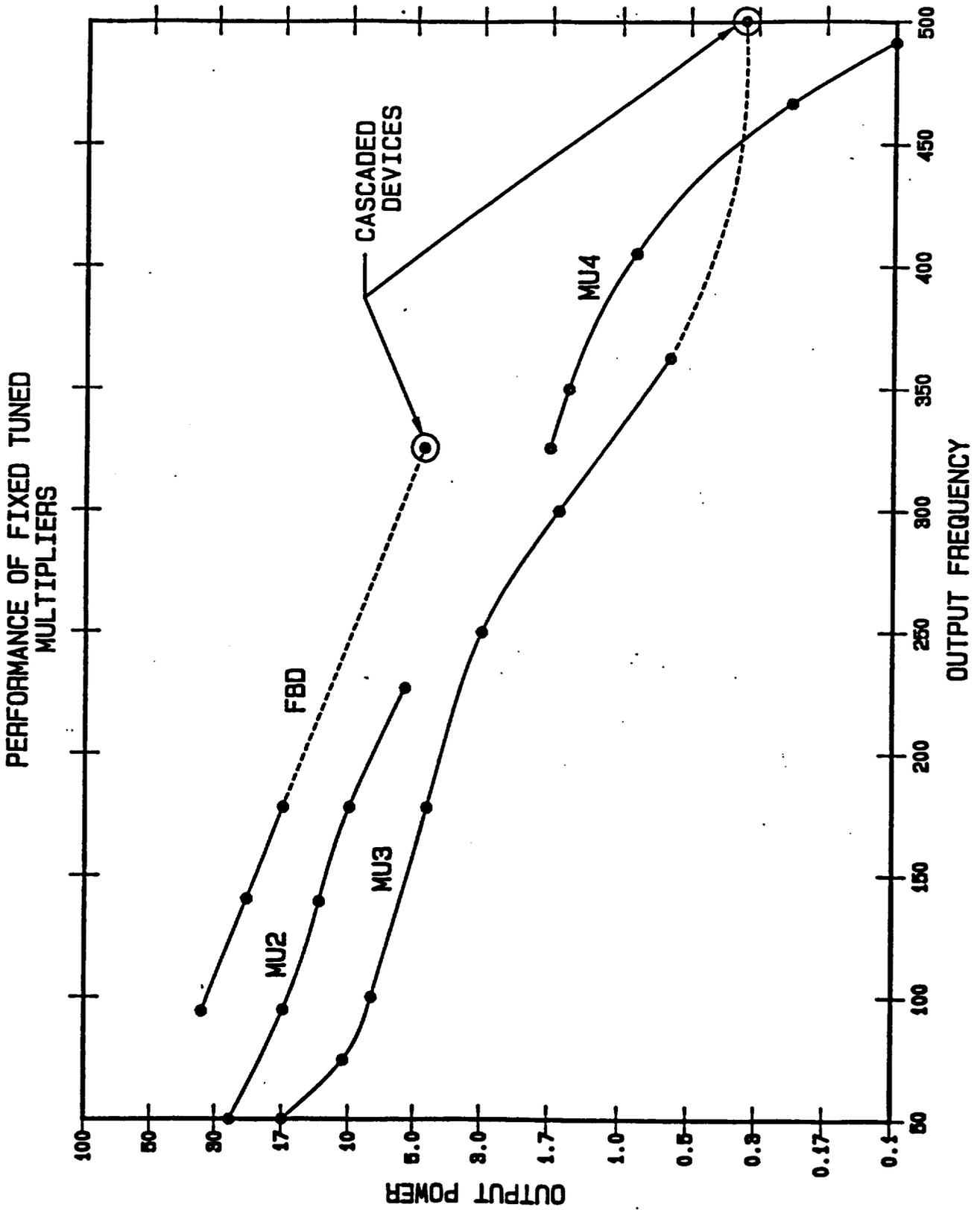
Figure 6.1 Composite performance characteristics of varactor multipliers for high frequency applications.

6.1.3   Gunn Diode Oscillator Development

Virtually all possible capabilities and features of Gunn diode oscillators were extended to their limit in this research effort. Also, a very systematic characterization of the operating parameters of InP Gunn devices was carried out. Cavity designs were analyzed and experimentally evaluated. Higher power, broadband tuning and higher operating frequencies were achieved than previously available as a direct consequence of this program. Design databases were established to aid the production of virtually any type of oscillator in the 60-150 GHz range. Stability and other related features of local oscillators were investigated in great detail.

6.1.4   Source Reliability Study

Indium Phosphide devices were analyzed for their reliability and thermal characteristics with a view to provide confidence in their use for spaceborne and other critical applications. The recently developed Indium Phosphide Gunn devices were determined to be highly reliable for reasonable baseplate temperatures. The diode package was analyzed in view of the performance degradation caused by it at upper millimeter-wave frequencies. Device failures were examined using an industrial procedure.

6.2   Conclusion

The chief conclusions and technical observations resulting from this research and development program are summarized next:

1.   Usable local oscillator power can be obtained from cascaded multiplier chains for frequencies somewhat beyond 600 GHz. The architecture os using a doubler followed by a high-frequency tripler appears to be optimal.

2.   Sufficiently high input pump power can be obtained from Indium Phosphide Gunn diode combiners. Such combiners can be configured at virtually any millimeter wave frequency to generate practically any desired output power, the only limitations being cost and size. The operating bandwidth of most combiners are somewhat limited.

3.   Indium Phosphide Gunn devices can be employed to generate fairly high output power over 30 - 160 GHz range in various modes of operation. A wide variety of devices are currently available for use in many different types of oscillator types to achieve practically any combination of operating characteristics.

4.   Indium Phosphide devices offer a highly-reliable operation comparable to their Gallium Arsenide counterparts in terms of failure rates and hours of operation. The performance of InP devices is generally superior to the GaAs diodes, in the dc to rf conversion efficiency and output power.

5.   Alternate devices and circuit techniques are currently emerging in the millimeter wave region for generating pump power. Gallium Arsenide FET and other new

devices, combined with epitaxially-stacked varactors could conceivably become the prime drivers for future submillimeter wave sources.

6.3   Recommendations for Future Work

Several areas of research and development in this Phase II effort are worthy of additional work. Significant potential has been demonstrated in this study for generating submillimeter wave power using the scheme adopted here. However, further development efforts are needed to perfect the techniques and ideas produced here. In particular, considerable work in area of device package design is needed to meet the future challenges. Appendix C describes the possible solutions for this performance limiting factor. Also, continuation of the work in cavity stabilization of Gunn oscillators is recommended for future applications of this technology.

In the area of varactor multipliers, the bandwidth enhancement of high frequency multipliers is considered to be worthwhile. The epitaxially stacked varactor multipliers for lower millimeter wave frequencies require intensive development to achieve the necessary pump power levels. However, these devices have already demonstrated the potential for meeting the needs of high power balanced double pump requirements. Appendix A describes these devices and their performance projections for millimeter wave sources.

REFERENCES

[1]   K. Chang and C. Sun, "Millimeter-wave Power-combining Techniques," *Trans. Microwave Theory Tech., vol.* MTT-31, pp. 91-107, February, 1983.

[2]   N.R. Erickson, "A high efficiency frequency tripler for 230 GHz," in PRoceeding 12th European Microwave Conf. (Helsinki), pp. 288-292, 1982.

[3]   P.H. Seigel, A.R. Kerr, and W. Hwang, "Topics in the optimization of millimeter-wve mixers," NASA Technical Paper 2287, 1984.

[4]   Carlstrom, J.E., et. all, "A Continuously tunable 65-115 GHz Gunn Oscillator," *Trans. Microwave Theory Tech.,* Vol. MTT-33, pp. 610-619, July 1985.

APPENDIX A

EPITAXIALLY GROWN STACKED VARACTOR MULTIPLIER DEVICES

Introduction

Frequency multipliers have been used for power generation since 1958. These multipliers depend on the non-linear reactance or resistance characteristics of semiconductor diodes. In general, there are three types of multiplier diodes:

- Step Recovery Diodes

- Variable resistance multiplier diodes

- Variable capacitance multiplier diodes

Step recovery diodes (SRD) depend on the charge stored in the diode during the forward excursion of the applied rf (please see Fig. 1(a)). During the forward swing, charges are injected into the active layer. When the rf swing takes the diode into the reverse bias region, the injected charge begins to decay. If the carrier life time is larger than the rf period, and if the voltage swing is large enough, the reverse current suddenly drops to zero. This rapid drop in the current results in efficient harmonic generation. Silicon SRD diodes are prime examples of this mode of operation. Applications include higher order multipliers and comb generators. In GaAs, however, the carrier life time is very short - of the order of a few nanoseconds. Hence, efficient SRDs cannot be fabricated using GaAs.

The second type of multipliers depends on the rectification property of the diode with the applied bias voltage (please see Fig. 1(b)). Under forward bias condition, there is a current flow. When the diode is reverse biased, there is no current flow. By Fourier analysis of the current wave form, it is apparent that higher order harmonics may be generated. This class of multipliers has a low efficiency because of the dc resistive losses (there can be no multiplication with the resistive multiplier unless there is a dc loss).

The third type of multipliers depends on the non linear capacitance of a semiconductor diode with the applied bias. With this class of multipliers, there can also be sub-harmonic generation (also called frequency dividers). This class is generally used for low order multiplication - typically ≤ 4.

The fundamental power, P_{in}, into the diode is given by:

$$P_{in} = \Gamma_3 \cdot P_N \cdot (f_o/f_c)$$

where P_N = Normalized power = $(V_b + \phi)^2 / R_T$

V_b = Breakdown voltage of the diode

ϕ = Built-in potential of the diode

= 1.2 Volts for GaAs P^+ N diode

R_T = Series resistance of the diode

f_o = Input frequency to the multiplier

f_c = Cut-Off frequency of the diode

= $1/(2 \cdot \pi \cdot C_m \cdot R_T)$

C_m = Minimum capacitance of the diode

Γ_3 = A constant which depends on the order of multiplication

= .0277 for a doubler

= .0241 for a tripler

= .0201 for a quadrupler

This equation is valid for:

f_o/f_c ≤ 0.5% for doublers and triplers

≤ 0.1% for quadruplers

The efficiency of the multiplier is given by:

$$\eta = e^{-\alpha \cdot (f_{op}/f_c)}$$

Again, α is a constant which depends on the order of multiplication.

α = 9.95 for a doubler

= 11.7 for a tripler

= 16.55 for a quadrupler

f_{op} = output frequency of the multiplier

It is useful to observe that the efficiency increases as the cut-off frequency increases for a given input frequency.

The output power, P_o, is then : $P_o \quad = \quad P_{in} * \eta$

Thus, the output power is proportional to the square of the breakdown voltage.

The output power may be increased for a given order of multiplication by increasing the breakdown voltage. However, the loss associated with the diode also increases with increasing V_b. Consequently, there is a limit to obtaining increased power by increasing V_b.

The cut-off frequency, f_{cm}, at a voltage corresponding to C_m of the diode is given by:

$$f_{cm} \quad = \quad 1/(2*\pi*C_m*R_T)$$

where $\quad R_T \quad = \quad$ Total resistance of the diode

$$= \quad R_s + R_m + R_{m1} + R_d + 0.1$$

$R_s \quad = \quad$ Substrate resistance including skin effect

$$= \quad \mathcal{S}_s/(4*\pi*\delta))*\{1+(4*T/D)\}$$

$R_{m1} \quad = \quad$ Skin resistance of the Plated Heat sink

$$= \quad \mathcal{S}_m/(4*\pi*\delta_m))*\{1+2*\ln(D_1/D) + (4*h/D_1)\}$$

$R_m \quad = \quad$ Resistance due to contact layers and ohmic metallization

$$= \quad (\mathcal{S}_N *L_N + \mathcal{S}_P *L_P) + \mathcal{S}_C)/A$$

$R_d \quad = \quad$ Diode resistance due to time averaged undepleted epi layer thickness - usually the resistance of half the total epitaxial layer.

$$= \quad L_A /(2*q*\mu*N_D *A)$$

$0.1 \quad = \quad$ Resistance of connecting gold straps

The power input, P_{in}, may be written as:

$$P_{in} \quad = \quad \Gamma_3 *(V_b + \phi)^2 * (f/f_{cm}) /R_T$$

As may be seen, the power input decreases when the diode resistance increases.

One way out of this dilemma is to stack the diodes physically as shown in Fig. 2. By such

stacking, the breakdown voltage may be increased without significantly compromising the total resistance. For an N diode stacked device, the breakdown voltage, V_{bN} , is given by:

$$V_{bN} = N * V_b$$

Consequently the power input and the power output increase by N^2 for a fixed C_m. The area of the individual diodes of the stacked device also increases by N.

Physical stacking,however, also increases the electrical resistance due to bonds between diodes. More importantly, though, the thermal resistance of the stacked device is substantially higher than that of a single diode. This is mainly because of the substrate thickness of the individual diodes and the bonds between the diodes. The increased electrical and thermal resistances may be circumvented by stacking the diodes epitaxially as shown in Fig. 3.

The stacking by epitaxial growth has been named "Integrated Series Impatt Structure" or ISIS for short. Originally, the structure was used with Impatt profiles to develop a high power device. Hence the name.

ISIS DIODE

DC Characteristics

a. Forward Characteristics

Fig. 4 shows the I-V characteristics of a 2 stacked ISIS diode. The forward conduction does not begin till almost 7 volts. The reason for this high a forward drop may be understood by examining
Fig. 3. A 2 stacked forward biased ISIS diode consists of 2 forward biased P^+ N junctions and a reverse biased N^+ P^+ junction. When a small voltage is applied,the diode cannot conduct because the reverse biased junction will not permit conduction. Hence, for the diode to start conducting, the reverse biased junction has to breakdown. Since both the N^+ and the P^+ regions are very heavily doped, the breakdown voltage is about 5 to 6 volts. Once the junction breaksdown, additional voltage has to be applied to overcome the potential barrier of the forward biased P^+ N junctions. Thus, the forward drop for reasonable conduction to take place, the applied voltage has to exceed about 7 to 8 volts. In general, then, the forward drop of a N- stacked ISIS diode will be (assuming that the diodes of the stack are identical):

$$V_F = N \times 1.2 + (N-1) \times V_{BR}$$

Where:
$\quad V_{BR}$ = Breakdown voltage of the reverse biased N^+ - P^+ junctions

The forward conduction current is basically controlled by the space charge resistance of the reverse biased junctions.

b. Reverse Characteristics

Under reverse biased conditions, a 2 stacked ISIS diode has two reverse biased P^+ N junctions and one forward biased N^+ - P^+ junction. If there is no current flow, the applied voltage across the forward biased junction is zero. Hence, the applied reverse voltage splits evenly between the 2 junctions. Thus, in general the applied voltage across a reverse biased N- stacked ISIS diode will split evenly among the N reverse biased junctions.

If the diodes of the stack have a capacitance of C_1 pF at 0 bias, the capacitance, C_{JNVR} of the N stakced ISIS diode at a reverse voltage V_R will be given by:

$$C_{JNVR} = (C_1 \times C_2)/[C_1 + C_2 \{1 + (V_R/N\phi)\}^r]$$

where:

ϕ = built-in voltage of the P^+ N junction

= 1.2 volts for GaAs

C_2 = zero bias capacitance of the forward biased N^+ - P^+ junctions

V_R = applied reverse bias voltage across the ISIS diode

The tuning ratio, T_R , is given by:

$$T_R = C_{JN0}/C_{JNVB}$$

$$= [C_1 + C_2 \{1 + (V_B/N\phi)\}^r]/(C_1 + C_2)$$

The tuning ratio of an N - stacked ISIS diode is lower than the tuning ratio of N diodes connected in series due to the presence of the parasitic junctions. Incidentally, the tuning ratio of N diodes connected in series is the same as that of a single diode.

From a multiplier view point, the minimum elastance $S_{min} = 1/C_{max}$ is obtained when the forward voltage is large enough to cause avalanche breakdown of the parasitic junctions. The maximum elastance $S_{max} = 1/C_{min}$ is, of course, obtained at reverse breakdown.

Electrical considerations

The theory behind the operation of an N stacked ISIS diode is identical to that of a single diode multiplier except the breakdown voltage is N times that of a single diode. The cut-off frequency of the diode, f_{cNV} , at a reverse bias voltage V is given by:

$$f_{cNV} = (2 * \pi * C_{JNV} * R_{TNV})^{-1}$$

This equation is identical to the earlier one. The subscript N identifies the N stacked ISIS diode.

$$C_{jNV} = \quad C_{jv}/N \text{ and}$$

$$R_{TNV} = \quad \text{Resistance of the N stacked ISIS diode}$$

$$= \quad R_s + R_{n1} + N * (R_n + R_d) + 0.1$$

The optimum output resistance of a multiplier for maximum power output is given by :

Where

$$R_o \approx \quad r_1/(N_1 * 2 * \pi * f_o * C_{jNVB})$$

$$f_o = \quad \text{input frequency and assumed to be} << f_{cNVB}$$

	r_1	N_1
Doubler	.271	2
Tripler	.168	3
Quadrupler	.136	4

The calculated cut-off frequency of 2 and 3 stacked varactors as a function of the breakdown voltage of the stacked device is shown in Fig. 5 at output frequencies of 44 and 94 GHz with the output resistance of the ISIS diode as a parameter. The calculations were made under the following assumptions:

1. The active layers of the individual diodes are identical and have a flat doping profile.

2. The active layer thickness equals the depletion layer thickness at breakdown.

3. The N$^+$ buffer layer of each diode is 1 μm thick and has a resistivity of 0.002 ohm-cm.

4. The P$^+$ layer of each diode is 0.75 μm thick and has a resistivity of 0.008 ohm-cm.

5. The substrate has a resistivity of 0.002 ohm-cm and a thickness of 15 μm.

6. The specific contact resistivity of the top ohmic contact is $5 * 10^{-6}$ ohm-cm^2 and other metal connections have a resistance of 0.1 ohm.

These assumptions are very realistic and in particular these parameters match those of the ISIS diodes that are fabricated by MDT.

The figures show that the cutoff frequencies have a broad maximum as a function of the breakdown voltage of the ISIS diode. At low breakdown voltages, the carrier concentration of the individual diode of the stack is high. Consequently, the capacitance per Sq. cm of

the diode is large. Hence, the diode area is very small for a fixed capacitance. The reduced diameter results in increased parasitic spreading resistance. The cutoff frequency, thus, decreases with decreasing breakdown voltage.

At the other end, when the breakdown voltage is large, the carrier concentration is small. For a fixed capacitance, the diode area is larger. The substrate resistance increases with increasing diameter. Hence, the cutoff frequncy decreases with increasing breakdown voltage.

To get an idea of the magnitude of the quantities, let us consider a 2- stacked ISIS diode to be used as a doubler at 94 GHz with an output resistance of 10 ohms. From Fig.4c we see that the maximum cutoff frequency of 1580 GHz occurs at a breakdown voltage of about 80 volts. The output resistance of 10 ohms is equivalent to a capacitance at breakdown of 0.046 pF. The diode diameter is about 42 μm. For this capacitance and the breakdown voltage of 80 volts, the series resistance is about 2.2 ohms.

Thermal considerations

The difference between the input power at the fundamental frequency and the output power at the harmonic is essentially dissipated in the stacked device. Assuming that the power dissipation is evenly divided among the N diodes, we may calculate the temperature rise of the N stacked device as a function of the breakdown voltage.The temperature of the diode obviously depends on the thermal conductivity of GaAs. The thermal conductivity of GaAs is dependent on temperature as given by :

$$K = C/T$$

$$C = 150 \text{ Watt/cm for N type GaAs}$$

$$= 120 \text{ Watt/cm for N}^+ \text{ GaAs}$$

$$T = \text{Temperature of GaAs in } °K$$

Using these relations, it may be shown that the temperature of the N th diode of the N-stacked ISIS device is given by :

$$T_N = ((P_d*N*0_1)+T_H) * \exp((P_d/(2*C*A))*N_2* L_d)$$

Where
P_d = Power dissipation in the individual diode of

the stack and assumed to be $= P_{Md}/N$

$$0_1 = ((4*h/(\pi*K_1*D)) + (2/(\pi*K_2)))/d_1$$

K_1 = thermal conductivity of plated heat sink material

K_2 = thermal conductivity of heat sink material

A = diode area = $\pi * D^2 / 4$

h = plated heat sink thickness

d_1 = D + (2*h)

L_d = thickness of each diode of the stack

T_H = heat sink temperature in °C

Figure 6 shows the calculated thermal resistance of 2 and 3 stacked devices as a function of breakdown voltage V_{bN} under the same conditions enumerated above with the plated heat sink gold thickness of 50 μm (at output frequencies of 44 and 94 Ghz)

The thermal conductivity of GaAs depends on temperature. Hence, the thermal resistance is a derived function from the temperature calculations. Caution is to be exercised in interpreting the temperature raise obtained by multiplying the thermal resistance by the power dissipation. In general, the power dissipation per diode was assumed to be about 0.75 watts per diode of the stack for these calculations. Conservative temperatures will be obtained when the actual power dissipation is lower than the number used in the calculation.

Again, to get an idea of the magnitude of the quantities, let us calculate the temperature rise of a 2- stacked ISIS multiplier diode to be used as a doubler at an output frequency of 94 GHZ with an output resistance of 10 ohms. The optimum breakdown voltage for this diode (from Fig.5c) is 80 volts. The thermal resistance of such a diode (from Fig. 6c) is 72° C/W. Hence, the temperature rise above the heat sink temperature is: 2 times 0.75 W times 72° C/W. Or,

$$T = 112° C$$

Frequency Considerations

For a fixed load impedance, it is clear that the diode capacitance will decrease as the frequency is increased. This means that for a fixed number of stacks, the diode diameter will have to decrease. Figure 7 shows the cutoff frequency dependence on the diode diameter for a fixed capacitance. It is clear that there is an optimum diameter to obtain the highest cutoff frequency.

With ISIS diodes, there is another degree of freedom available. we can increase the number of stacks to increase the diameter of the diode. However,the electrical resistance due to additional P^+ and N^+ layers will also increase. Hence, the cutoff frequency will be a slowly increasing function of the number of stacks. Figure 8 shows the cutoff frequency

dependence on the number of stacks, N for a fixed breakdown voltage of individual diode of the stack. In other words, the breakdown voltage of the ISIS varactor, V_{BN}, is N times the fixed breakdown voltage of the individual diode. In this case, the fixed breakdown is 40 Volts.

Increasing the number of stacks, however, increases the thermal resistance of the diode. Hence, there may not be any advantage to increasing the number of stacks.

Power output Consideration

The output power of the ISIS diode, P_o, is given by:

$$P_o = \eta * N^2 * (V_B + \phi)^2 * 2 * \pi * f_o * C_{jNVB} * r_3$$

It is clear that the output power will increase as the square of the number of stacks even for a fixed capacitance value. The power dissipation , P_{Nd}, also increases. The power dissipation is given by

$$P_{Nd} = P_{In} *(1- \eta)$$

It is evident that the output power is limited by the maximum temperature of the N th diode of the stack.

Figure 9 shows the **power output at 44 and 94 Ghz** as a function of the number of stacks with output resistance and the type of multiplier as parameters under the assumption that the junction temperature is 200°C.

The optimum number of stacks to get the highest power of about 9 watts at a doubler output frequency of 44 GHz is 4 when the diode output resistance is 5 ohms. When the diode output resistance is 10 ohms, the optimum number of stacks is 5 for an output power of about 8.2 watts.

The reason for change in the optimum number of stacks when the output resistance changes is because of the imposed condition limiting the maximum temperature to 200 +/- 3 °C. When the output resistance is lower, the diode diameter will be larger resulting in higher power handling capability of the diode. The temperature rise will be lower. Thus, the number of stacks to realize a fixed maximum temperature will decrease as the output resistance decreases. On the other hand, when the output resistance is large the diode diameter will be small. The power handling capability of the individual diode will decrease resulting in higher temperature rise. Thus, the number of stacks increases for a fixed temperature rise.

At 94 GHz, the maximum power of about 1.9 watts is obtained for a 2- stacked ISIS diode with an output resistance of 5 ohms. For an output resistance of 10 ohms, the maximum power is about 1.45 watts.

Equivalent Circuit

a. Packaged ISIS Diode

Figure 10 shows the equivalent circuit of an ISIS multiplier diode in MDT package style M 23 (Fig. 11). The equivalent circuit consists of the diode capacitance in series with the diode resistance. The bond wire inductance of about 0.2 nH is in series with the diode impedence. The package capacitance of about 0.13 pF is in shunt with the rest of the circuit elements.

b. ISIS Diode with Quartz Stand-Off (MDT case Style M29)

The packaged diode may be used at lower mm wave frequencies without significant performance degradation. However, at higher frequencies the junction capacitance will be comparable or even less than the package parasitic capacitance. In this case, an unpackaged ISIS diode is preferable. Fig. 12 shows an ISIS chip connected to a quartz stand-off (MDT case style M29). The nominal dimensions of the quartz stand-off are 0.008" x 0.008" x 0.005" resulting in a parasitic capacitance of less than 10 fF. Fig. 13 shows the equivalent circuit of the quartz stand-off. The maximum distance between the quartz stand-off and the chip is 0.005". A nominal 0.0005"x 0.003" gold ribbon is used to connect the chip to the stand-off. The maximum length of the gold ribbon is about 0.016" resulting in a maximum lead inductance of about 0.3 nH. Many diodes in this package style have been made with a zero bias capacitance in the range 250 to 300 fF. At breakdown, the capacitance is about 80 to 100 fF.

SUMMARY

The ISIS multiplier diodes are very useful in generating high powers at mm wave frequencies reliably. The epitaxial technology is known and has been used for growth of a variety of devices. The processing technology is also known quite well and has been in use for a number of years. The operating junction temperature can be well below 200°C even at a case temperature of 75°C.

The attractiveness of ISIS multiplier diodes stems from the high conversion efficiencies and the relatively low voltages needed for their operation. Also, the circuit technology is a proven one. Hence, the risks are minimal.

Figure 1(a). Priniciple of Operation of a SRD Diode
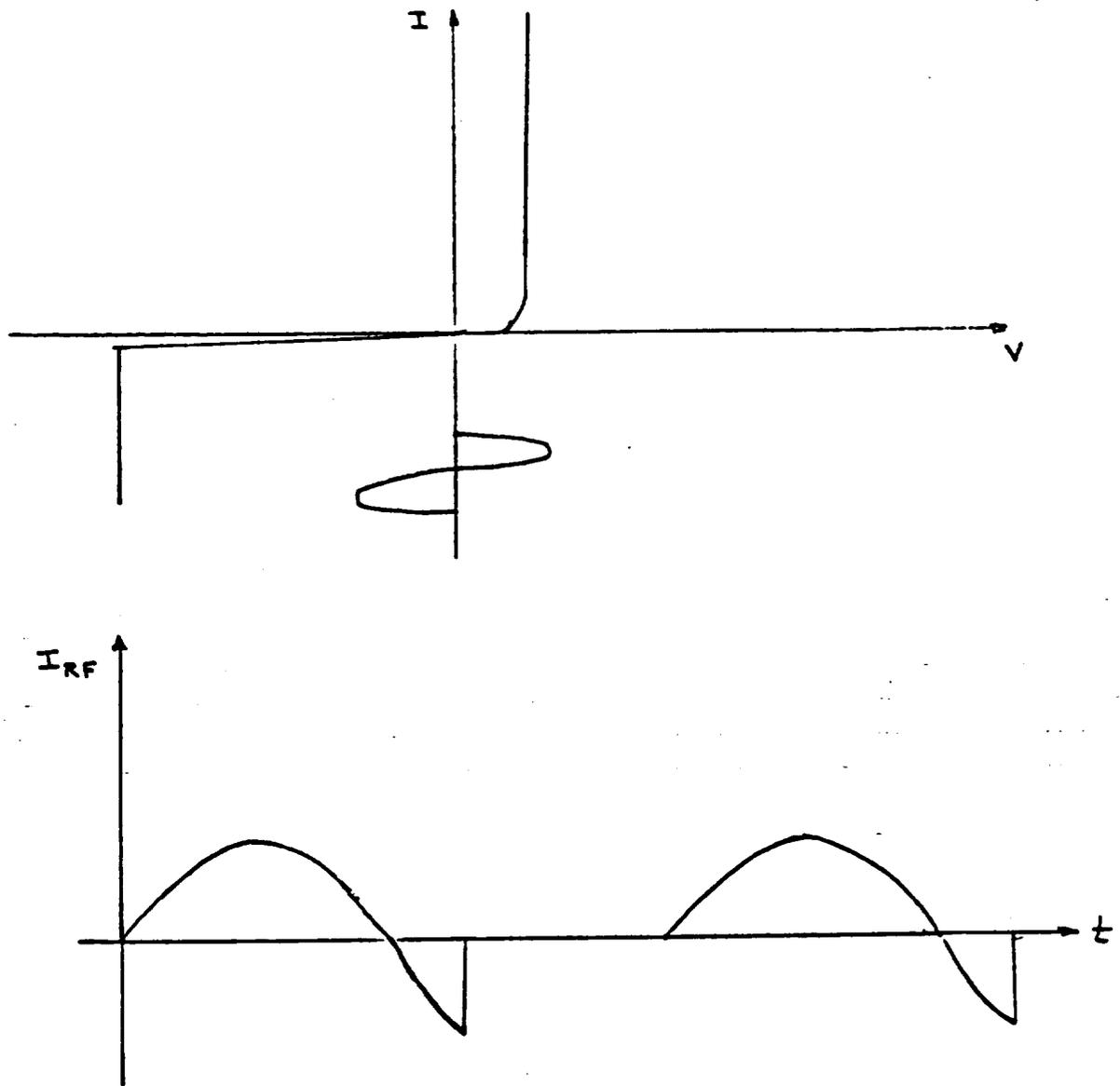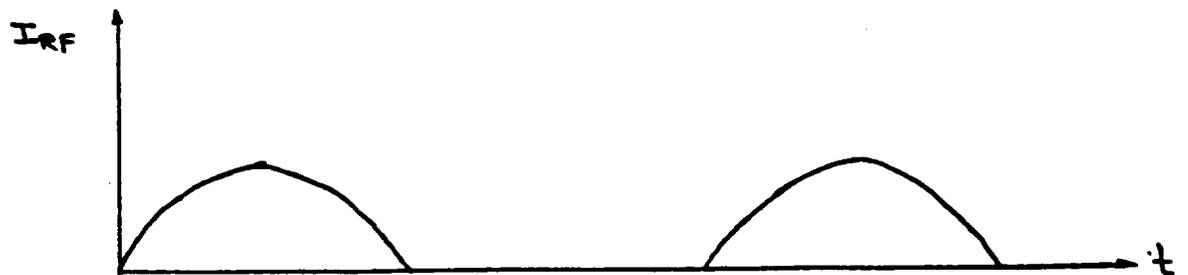
Figure 1(b). Principle of Operation of a Rectification Diode
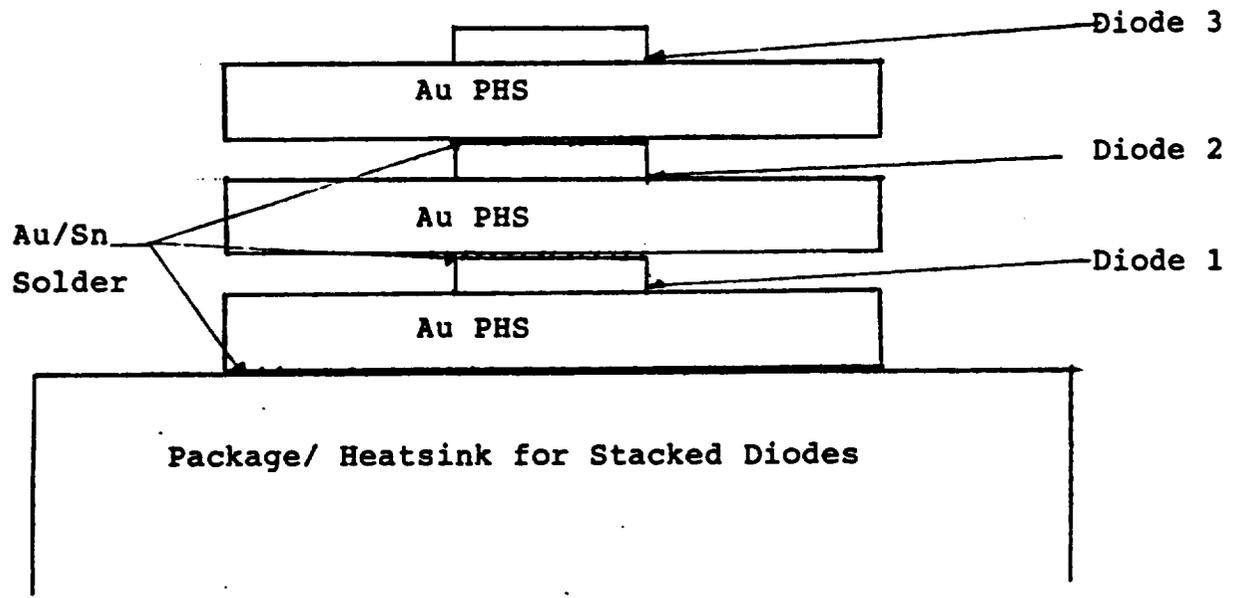
Figure A-2   Physical Stacking of Single Multiplier Diode Chips.

Contact metal

n$^+$ Substrate

ISIS ACTIVE REGION

Gold PHS
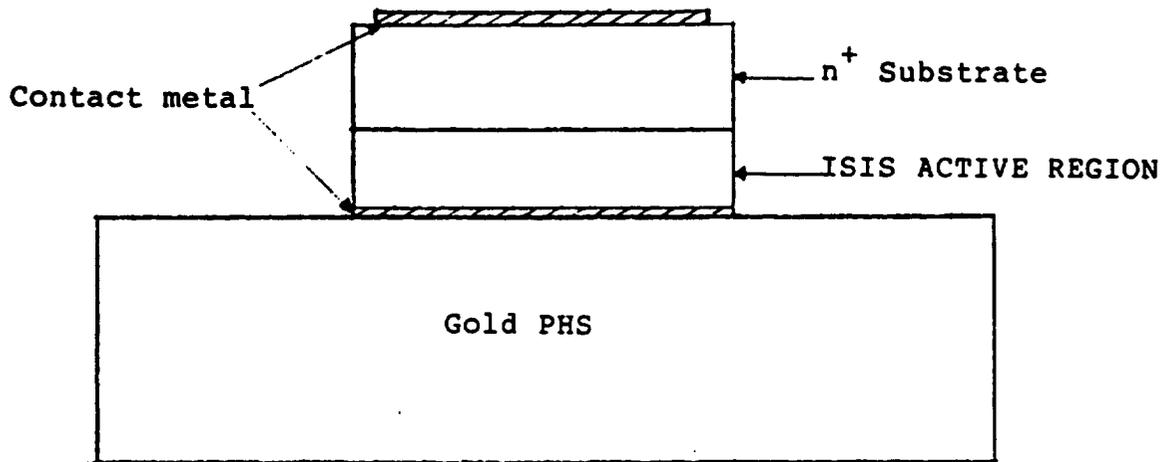
a. A Schematic of ISIS Diode Chip

Substrate

n$^+$

Junction N

n active

p$^+$

Junction 2

n$^+$

n active

p$^+$

n$^+$

Junction 1

n active

p$^+$
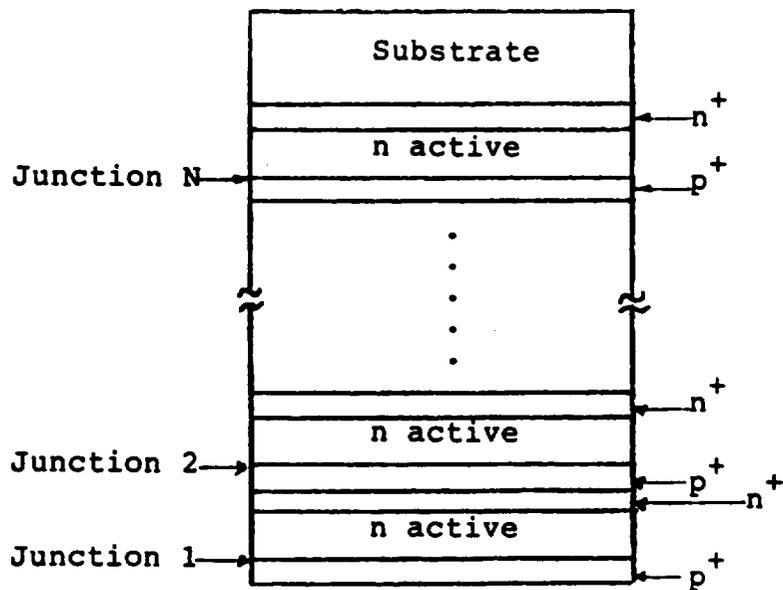
b. Detail of ISIS Active Region

Figure A-3 ISIS diode configuration.
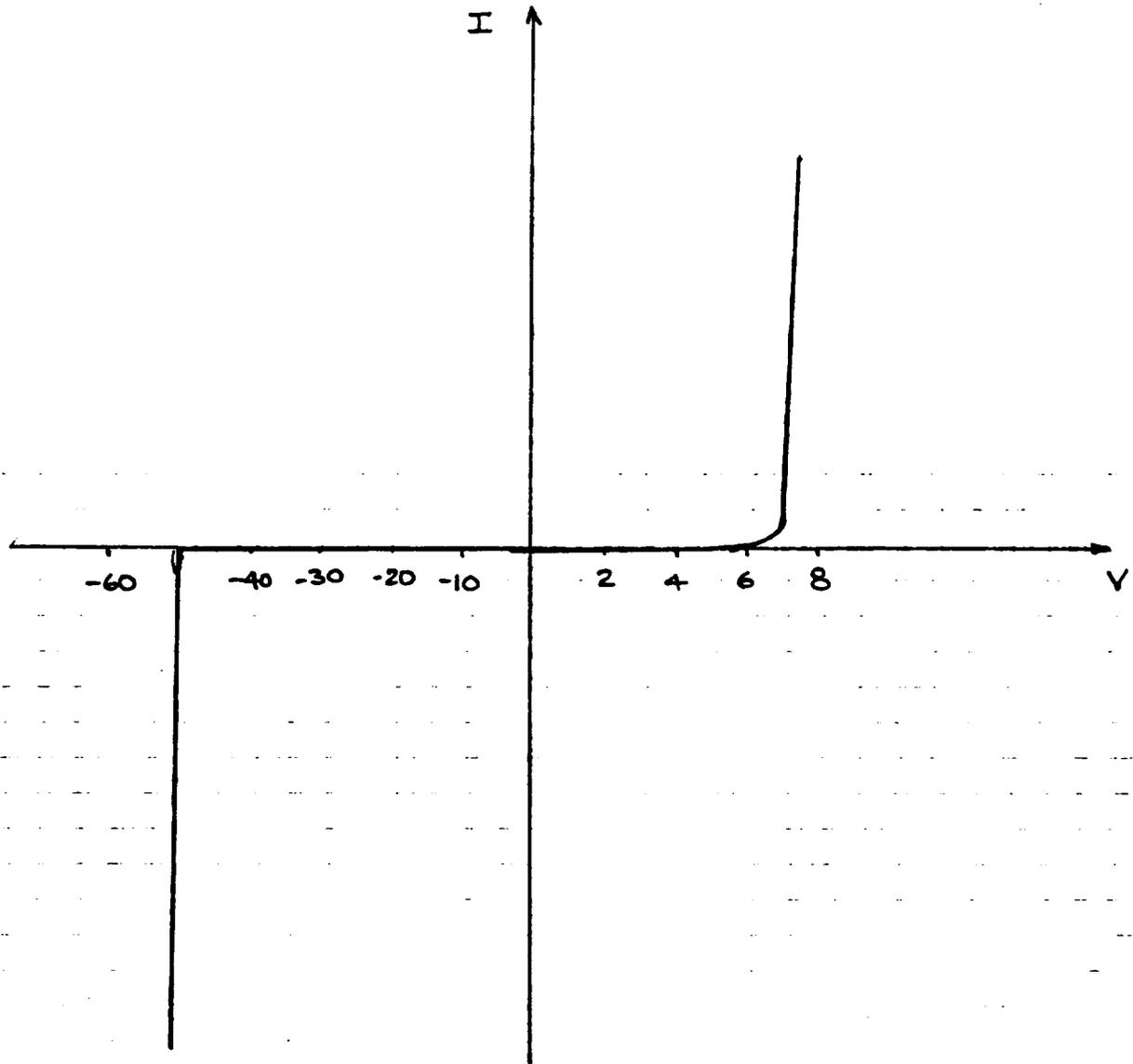
Fig. A-4 I-V Characteristics of a 2-Stack ISIS Multiplier Diode

(Note: Change of scales between the forward and reverse Characteristics)

BREAKDOWN VOLTAGE, V_B, VS. V_B
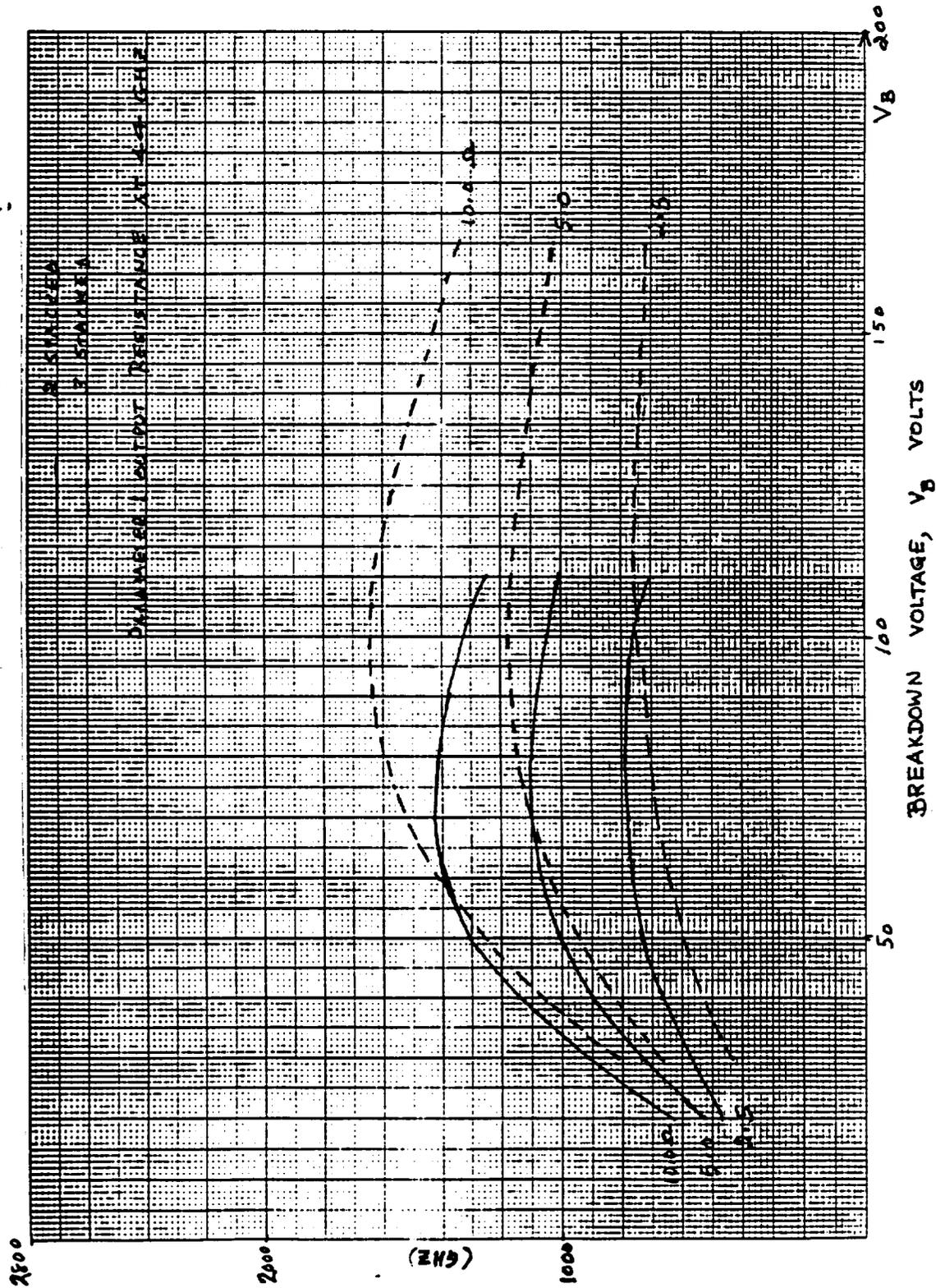
Figure A-5a: Cutoff frequency at V_B, VS. V_B for 44 GHz output ISIS doubler
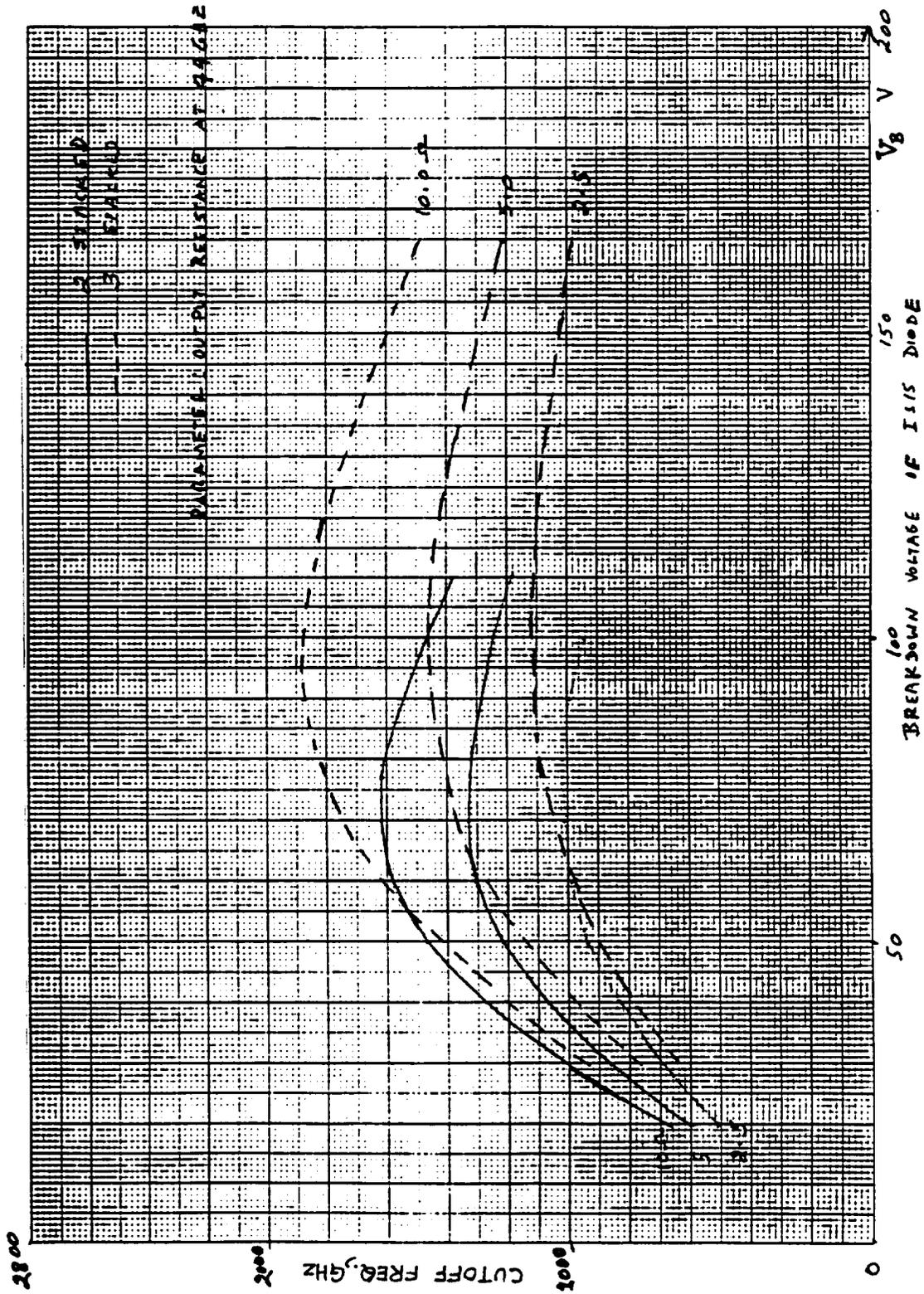
Figure A-5b: Cutoff frequency at V_B vs. V_B for 44 GHz tripler using ISIS.

Figure A-5c: Cutoff frequency at V_B vs. V_B for 94 GHz output ISIS doubler.
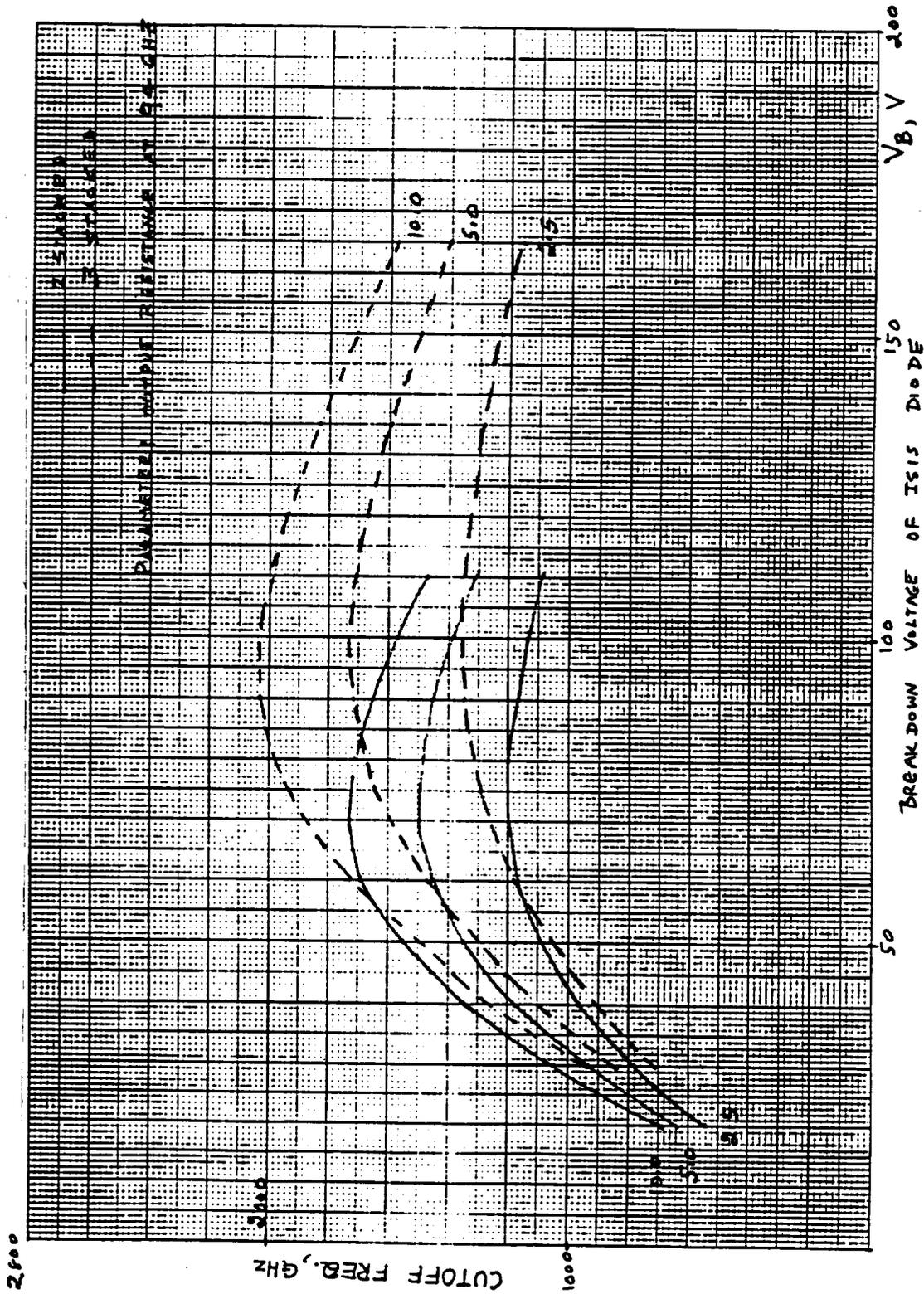
Figure A-5d: Cutoff frequency at V_B vs. V_B for 94 GHz output ISIS tripler.
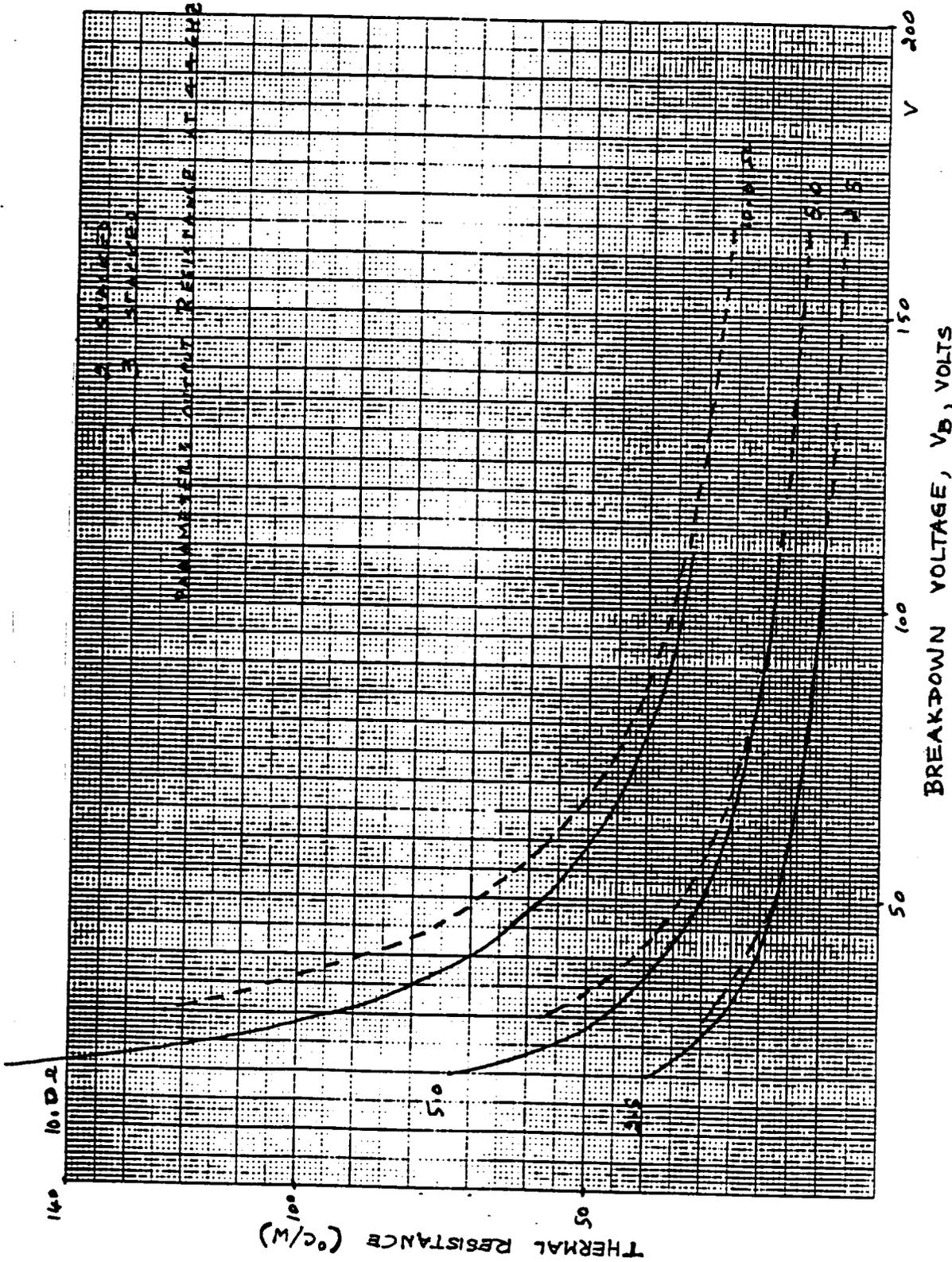
Figure A-6a: Thermal resistance vs. breakdown voltage for 44 GHz output ISIS doubler.
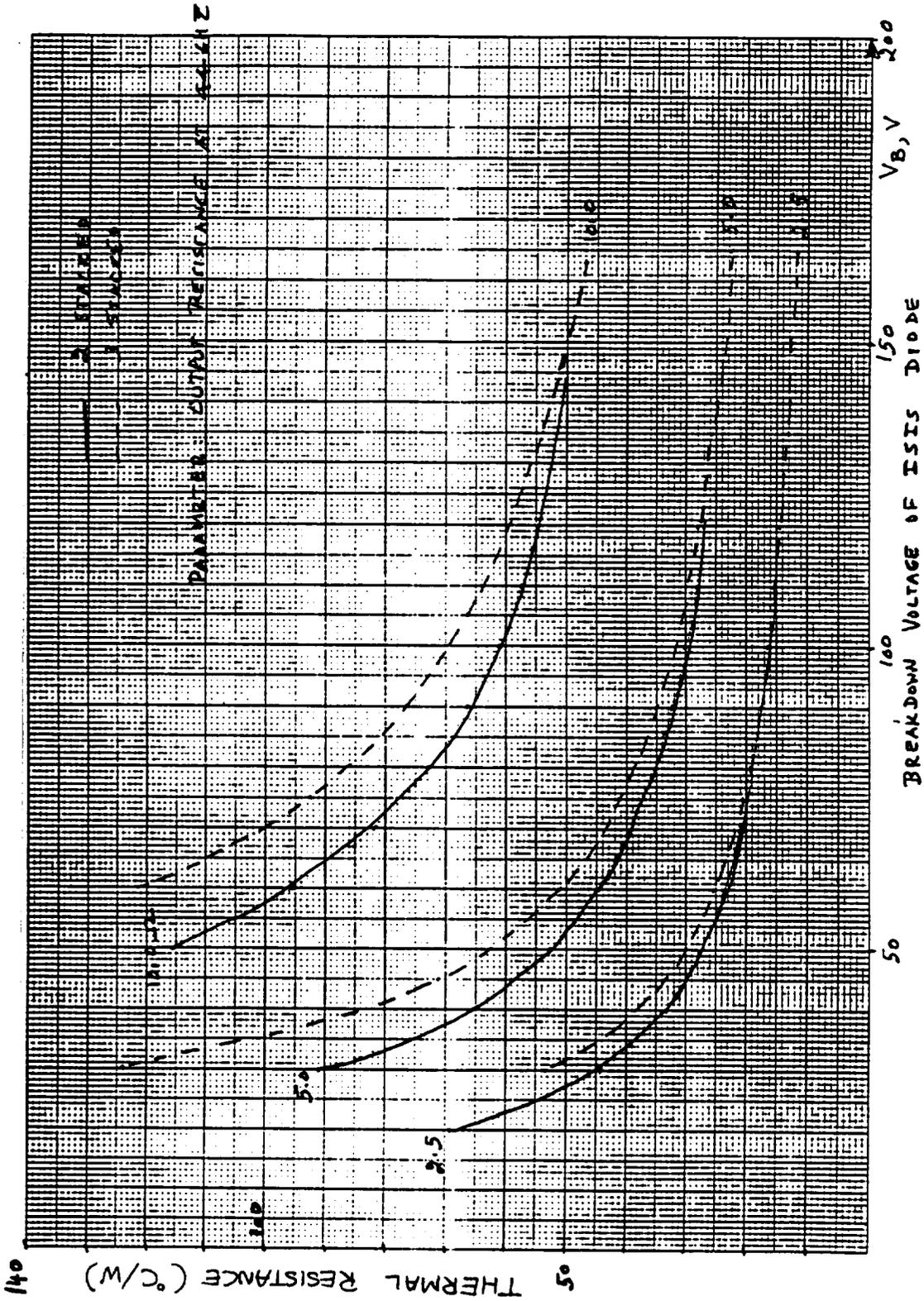
Figure A-6b: Thermal resistance vs. breakdown voltage for 44 GHz output ISIS tripler.
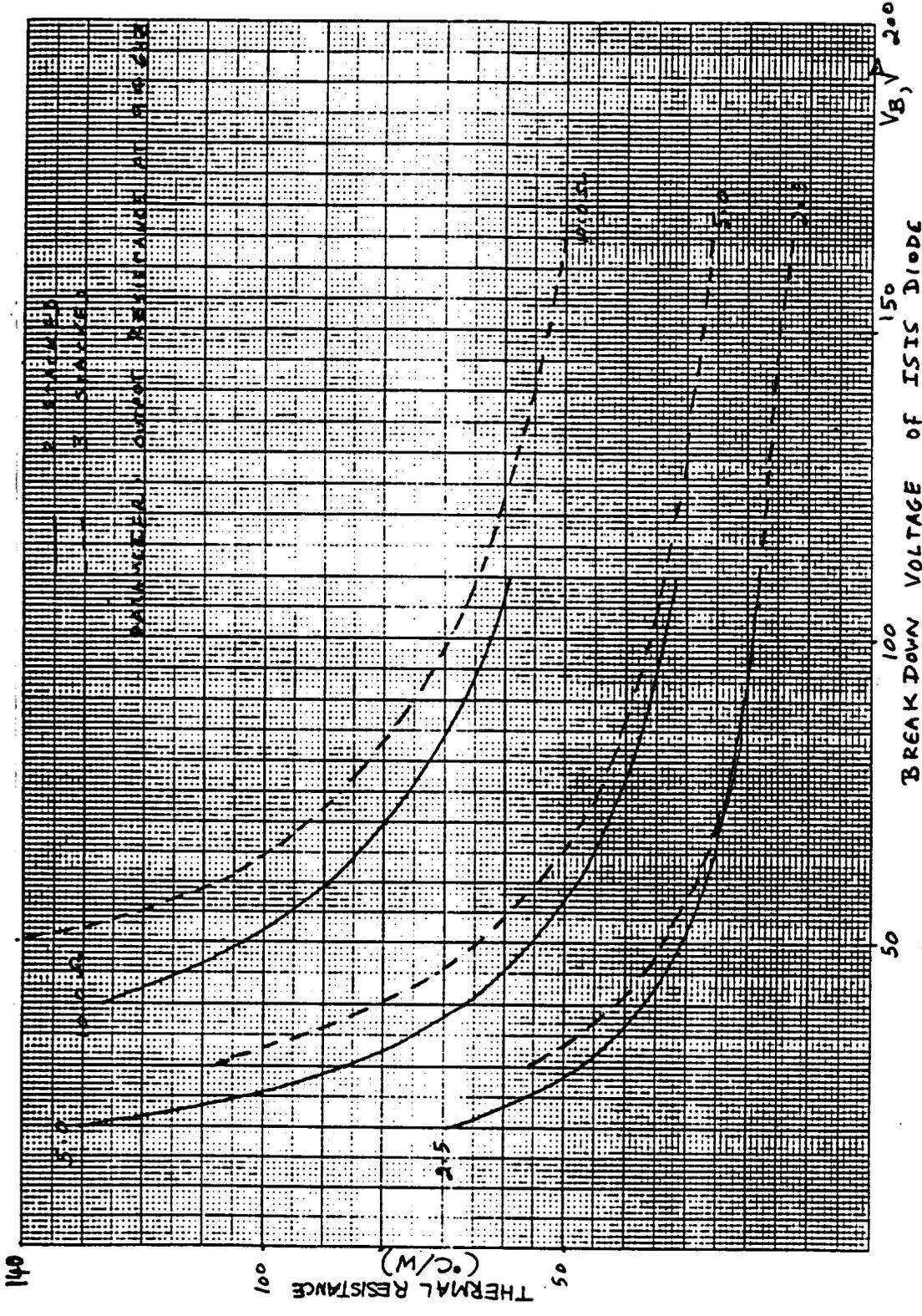
Figure A-6c: Thermal resistance vs. breakdown voltage for 94 GHz output ISIS doubler.
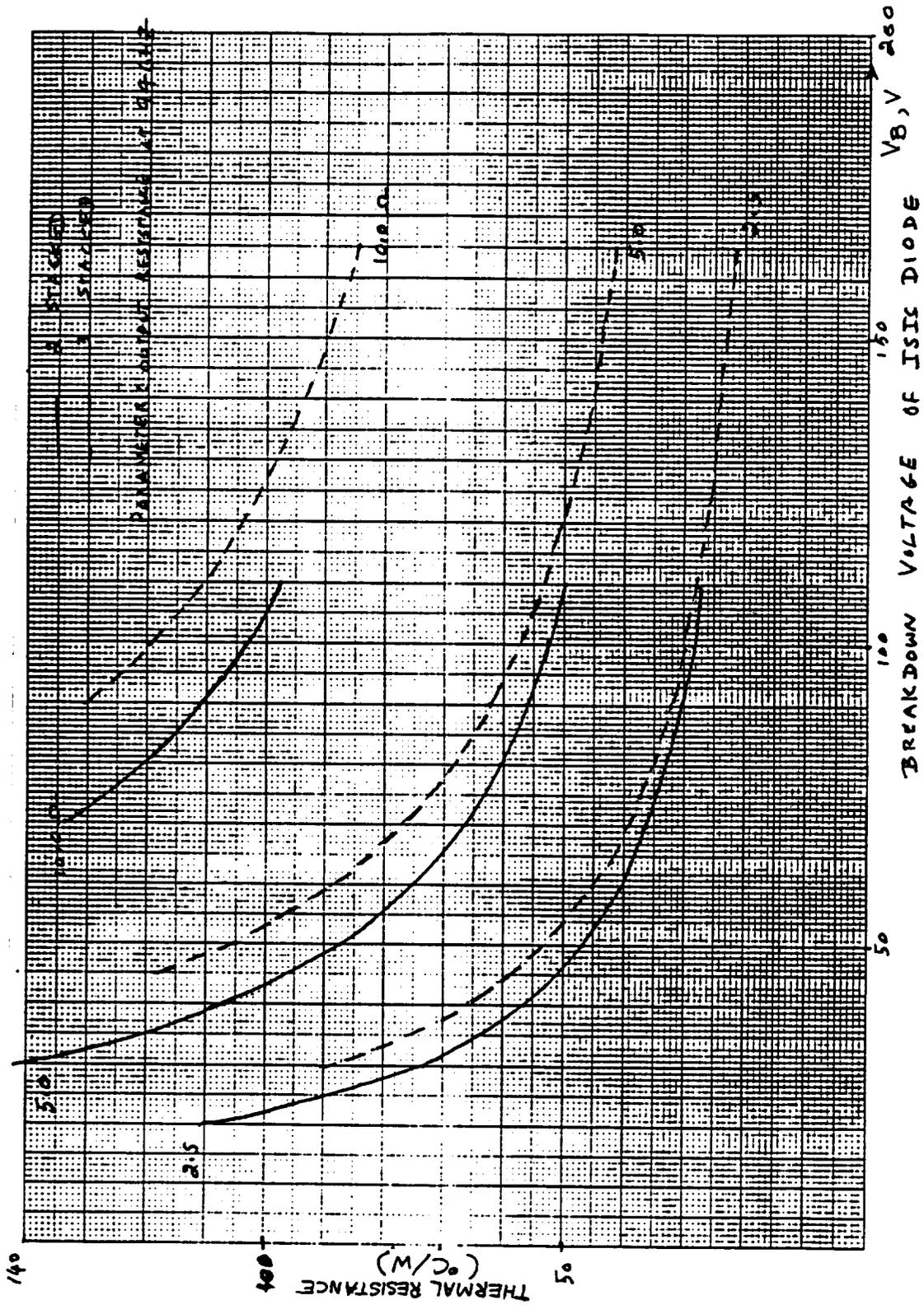
Figure A-6d: Thermal resistance vs. breakdown voltage for 94 GHz output ISIS tripler.
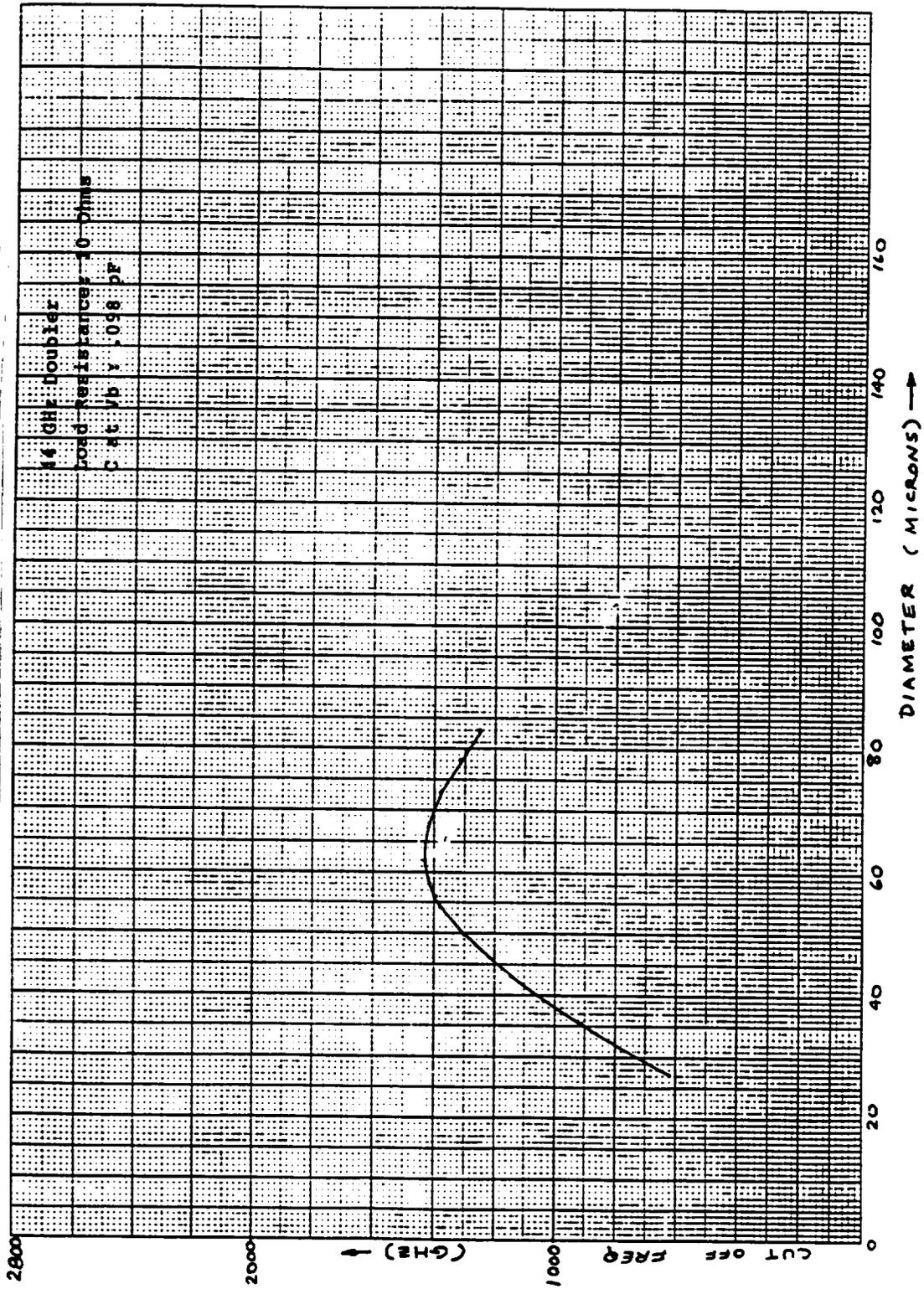
Figure A-7: Cutoff frequency at V_B vs. diode diameter for a fixed capacitance.
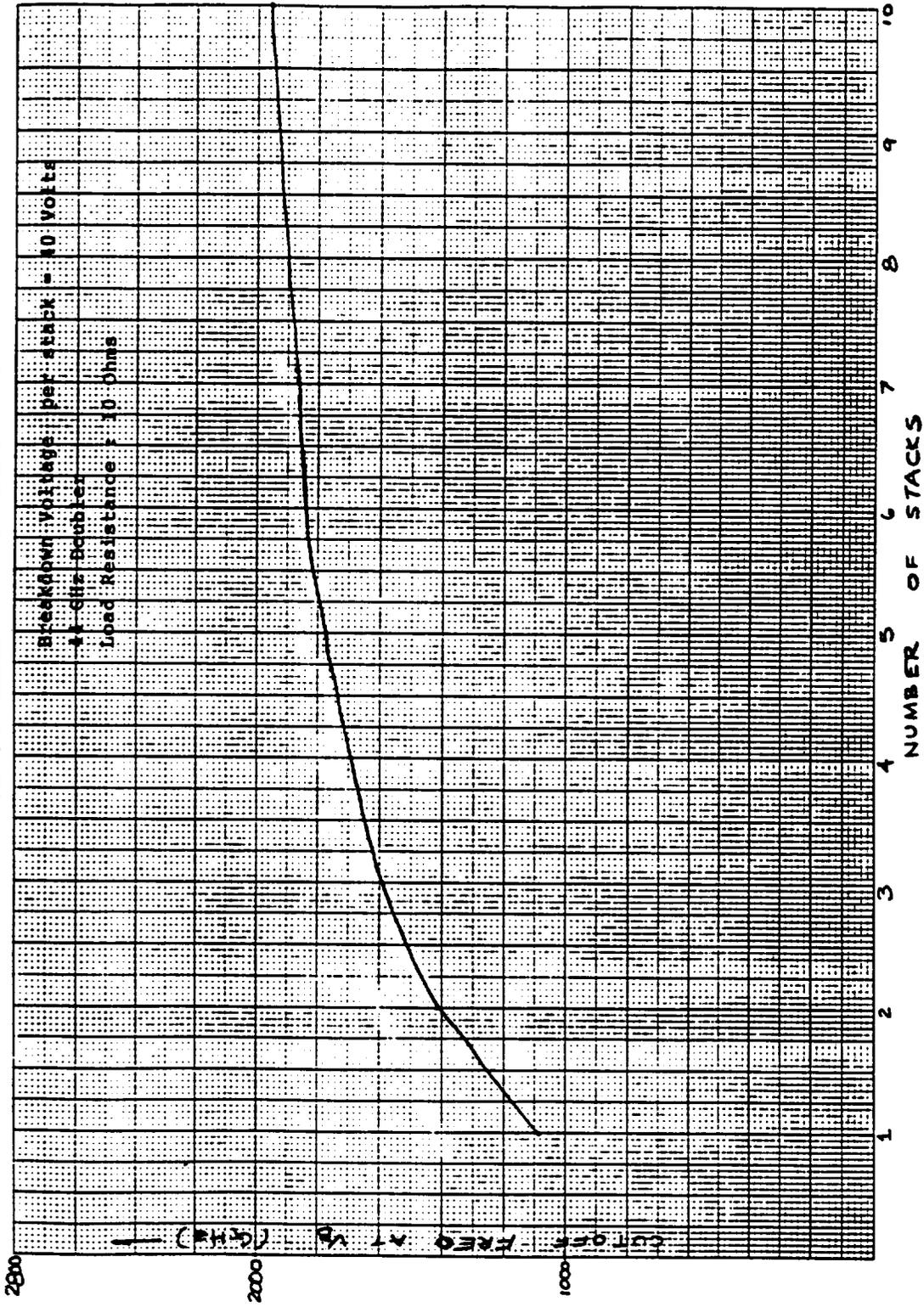
Figure A-8: Cutoff frequency at V_B vs. number of stacked devices.
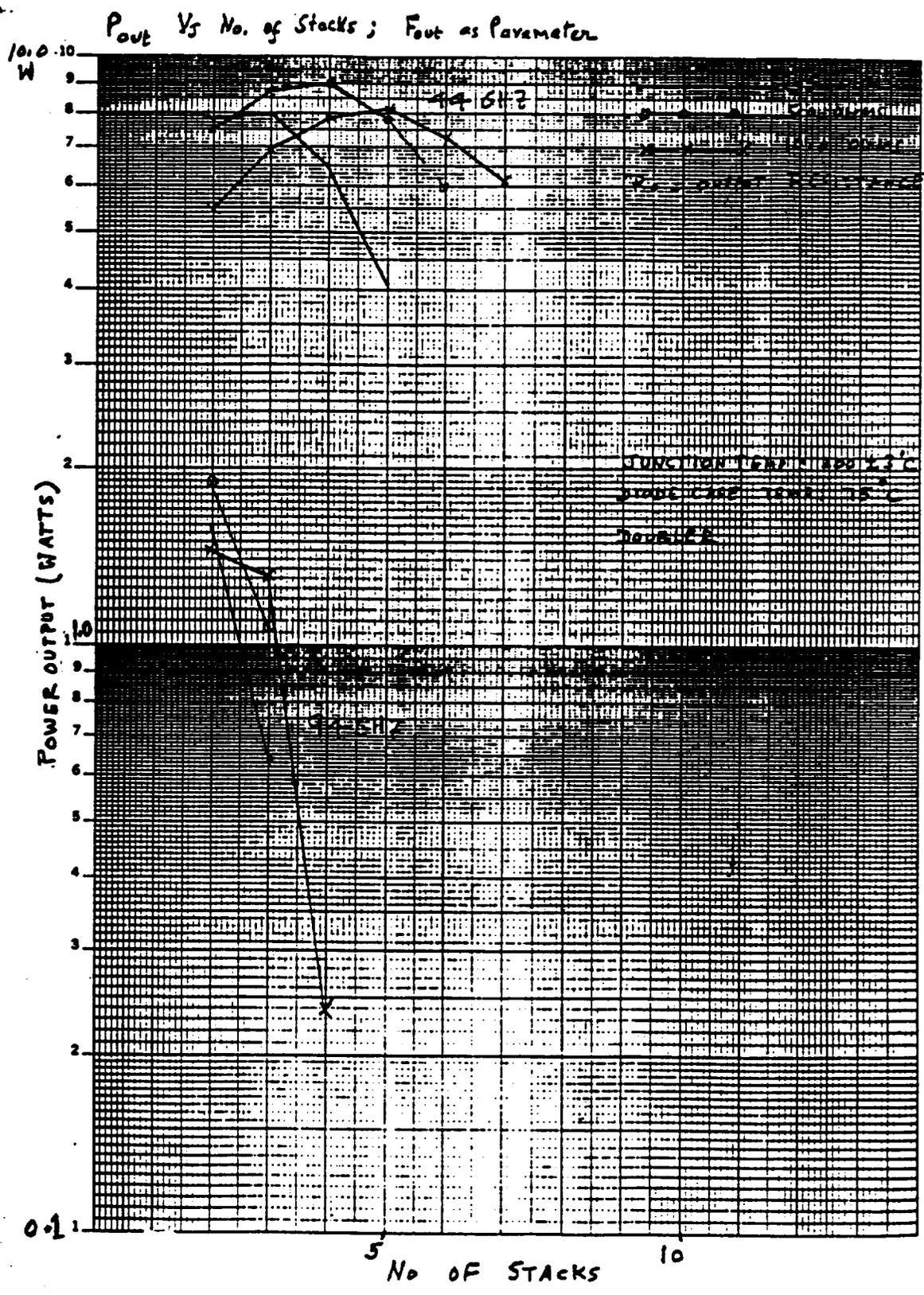
Figure A-9a: Power output of ISIS doublers at 44 and 94 GHz as a function of number of devices in a stack.
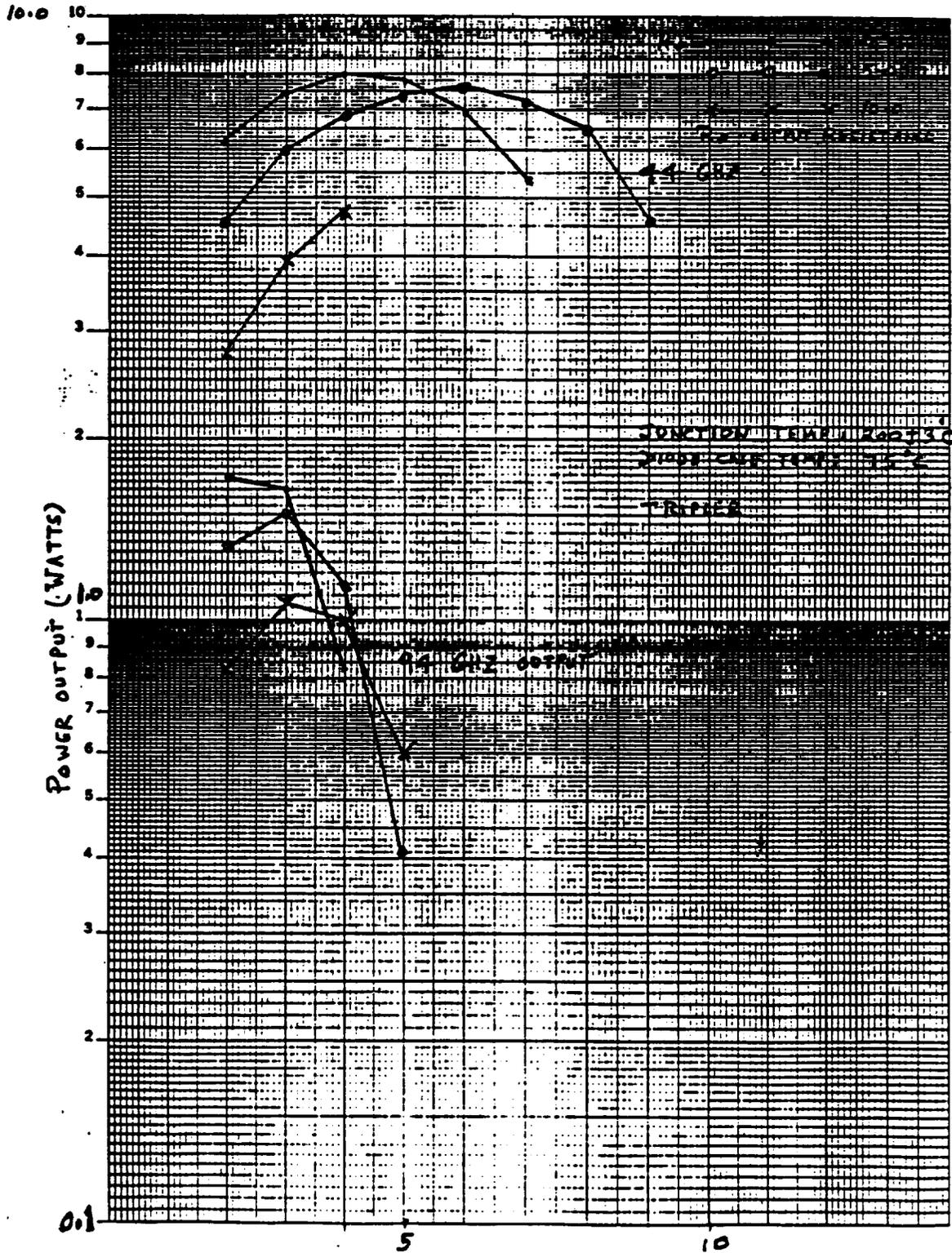
Figure A-9b: Output power at 94GHz and 44 GHz as a function of number of devices in stack as a tripler.
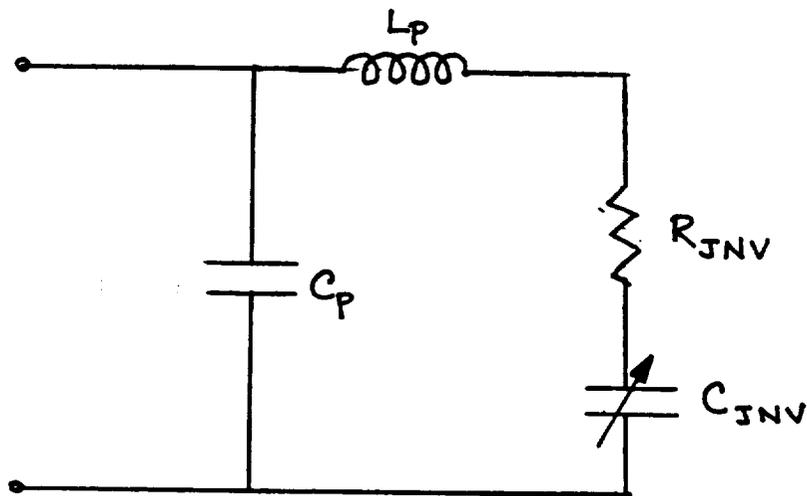
$$C_p \approx 0.13 \text{ pF}$$

$$L_p \approx 0.2 \text{ nH}$$

$$R_{JNV} = \text{Total Series Resistance of N- Stacked Diode}$$

$$C_{JNV} = \text{Junction Capacitance of N- Stacked Diode}$$

Figure A-10 Equivalent circuit of ISIS Multiplier Diode in M 23 Package

M23

A DIA

B

C

D DIA
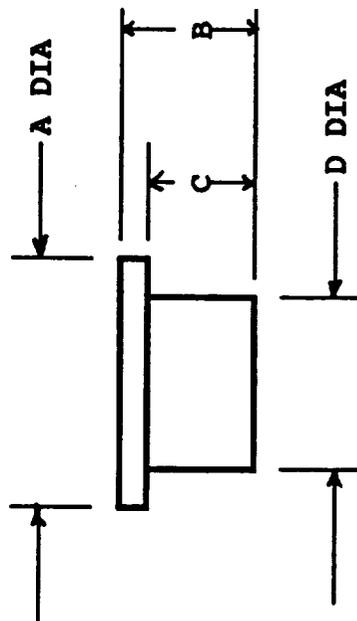
M23

DIM	INCHES		MM	
	MIN	MAX	MIN	MAX
A	0.043	0.047	1.09	1.19
B	0.024	0.033	0.61	0.84
C	0.014	0.019	0.36	0.48
D	0.029	0.033	0.74	0.84

Figure A-11 Schematic of M23 Package.

GOLD PHS
ISIS DIODE CHIP

QUARTZ
STANDOFF

.007" x .007"
x .005" (HT)

A

B

3-48
UNC

C

E

D
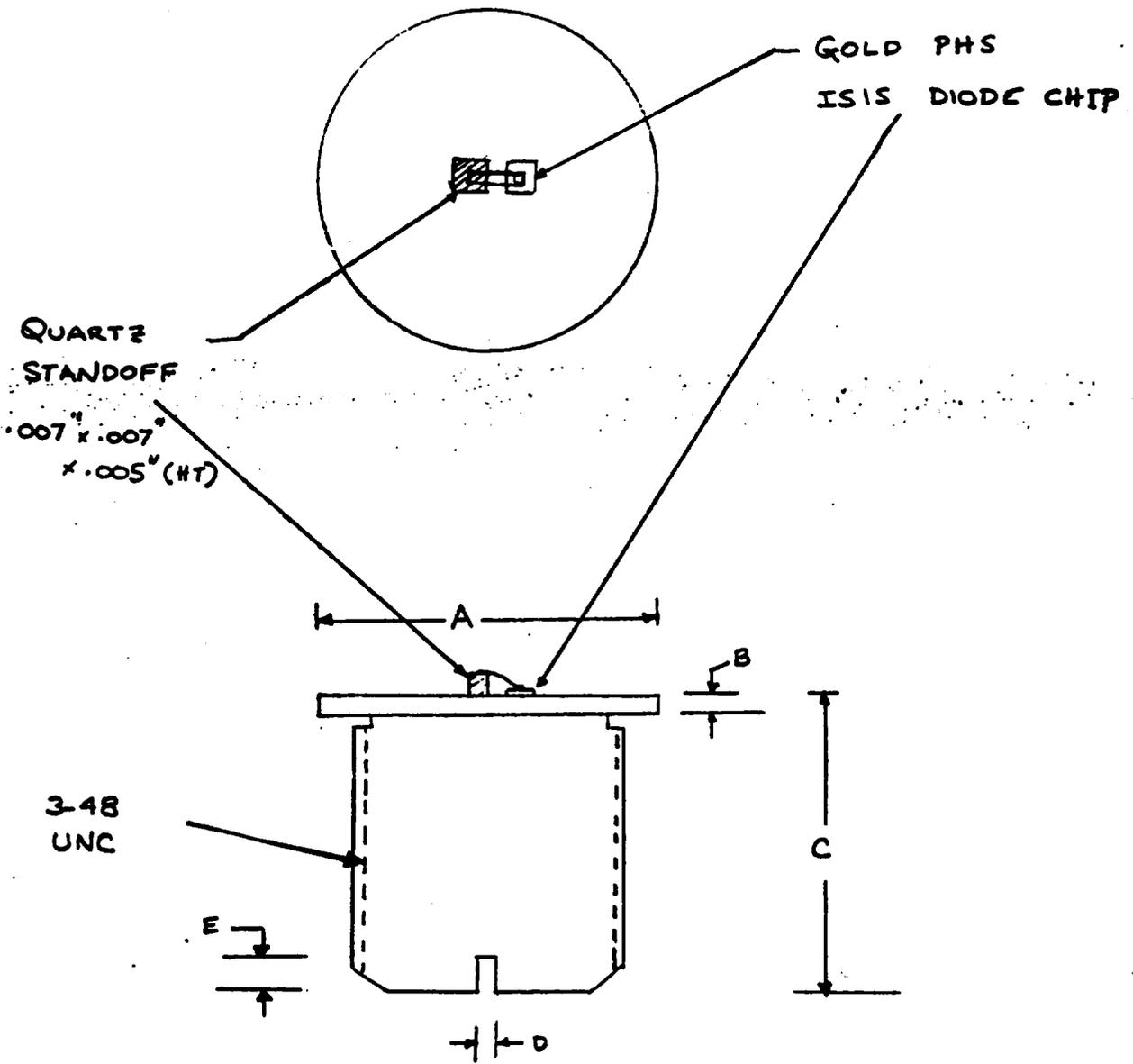
M29

DIM	INCHES		MM	
	MIN	MAX	MIN	MAX
A	0.113	0.118	2.87	3.00
B	0.018	0.022	0.46	0.56
C	0.128	0.138	3.25	3.51
D	0.015	0.025	0.38	0.64
E	0.035	0.045	0.89	1.14

NOTE: USE ONLY COMPRESSIVE FORCE ON TOP OF THE QUARTZ.

Figure A-12 M29 Quartz Standoff Package
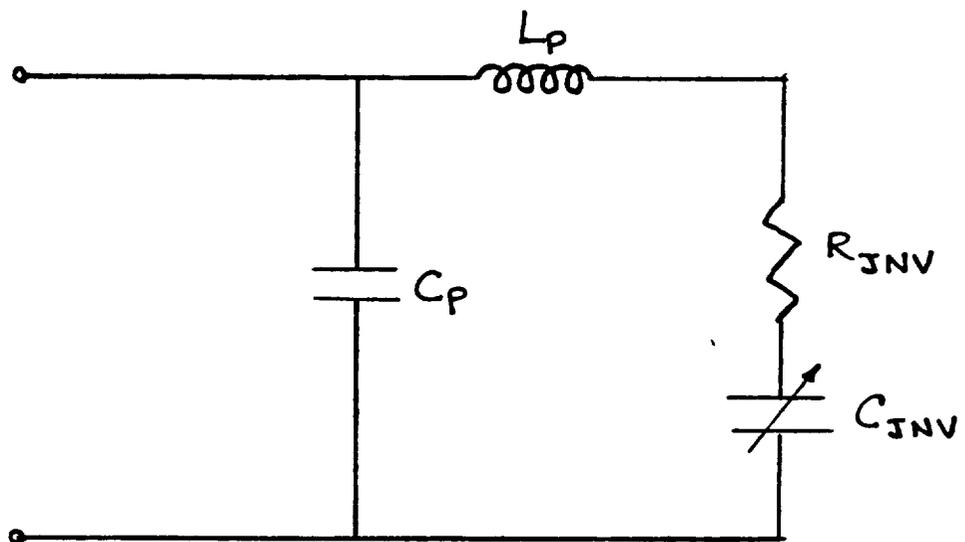
$$C_p \approx 11 \text{ fF}$$

$$L_p \approx 0.3 \text{ nH}$$

R_{JNV} = Total Series Resistance of N- Stacked Diode

C_{JNV} = Junction Capacitance of N- Stacked Diode

Figure A-13:   Equivalent Circuit of M 29 Package (Quartz Standoff)

APPENDIX B

FAILURE ANALYSIS OF INDIUM PHOSPHIDE GUNN DIODES

FAILURE ANALYSIS REPORT

A) **Diode 1**   InP Gunn   Varian

Model Number   VSB-9122510
S/N   EE 558-601
4.8V, .167A, 34 mW @ 94.4 GHz

a) External Examination:

Mechanical inspection revealed that the diode flange is bent indicating excessive torque was used while the diode was threaded into the cavity. When excessive torque is used, heatsinking to the cavity is reduced, thus increasing the active layer temperature. This sometimes can lead to the device failure.

Electrical examination indicated that the diode was open.

b) Internal Examination:

After the cap was removed, the diode was examined under the high power (x1000) optical microscope. Most of the InP diode was burned out, only leaving fragments of InP material on the chip. The diode was processed into a gold plated heatsink structure. The thickness of the gold plated heatsink is approximately 12-14 μms. The chip is of hexogonal shape with an InP circular mesa in the center.

There was no evidence of the diode being bonded to gold plated copper heatsink using Au/Su solder. Hence we can conclude that the diode was thermo-compression bonded to the package, thus achieving lowest possible thermal resistance.

B) **Diode 2**   GaAs Gunn   Varian

VSA 921053
Lot 5450, S/N 28 N34 Pkg.
5.0 V, 578 mA, 114 mW @ 35 GHz

C-2

All the GaAs material is splattered around on the heatsink. The diode is complete-
ly burned out. There is evidence that the chip is square and the side is approxi-
mately 80 μm.

External examination before cap is removed:

The diode is open electrically.
The threads are completely damaged.

C) **Diode 3**   InP Gunn   Varian

   VSB 9122513
   S/N EE 860-041
   198A, 63 mW @ 92.6 GHz

External Examination

The diode was open electrically.
The threads and the heatsink and the package were mechanically intact.

Internal Examination:

The diode is a circular chip. There is no evidence of solder and therefore, the
diode is thermo-compression bonded for lowering thermal resistance. A circular
tool was used for TCB bonding and this is evidenced by a small ring on Au PHS
chip at the edges. The diode has a circular Au PHS structure. The total height of
the chip is $\approx$ 20 μm. Since these diodes were completely burned out, cross-sectional
examination would not yield any additional information.
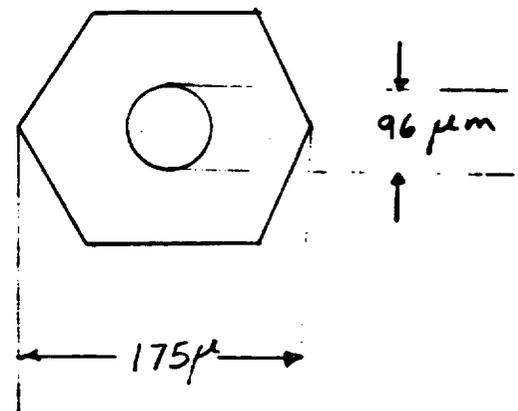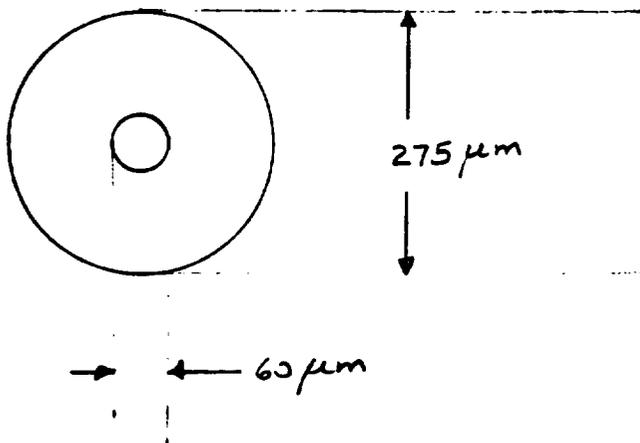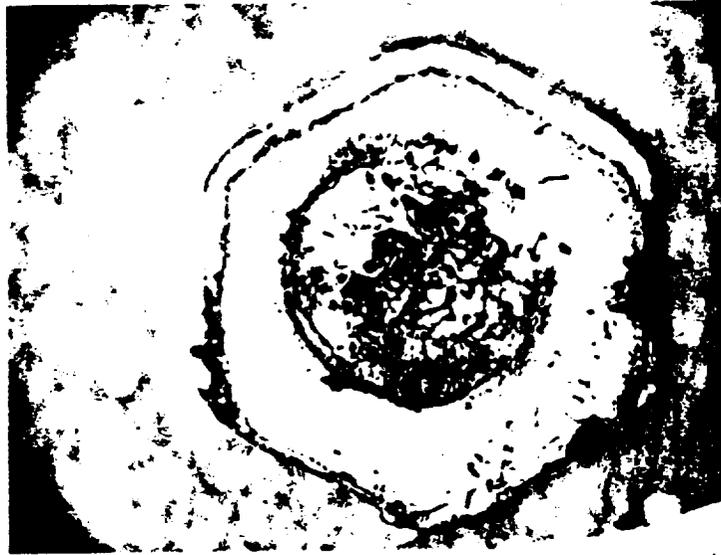
275 μm

60 μm

96 μm

175 μ

#1

200X   VSB 9122S10

#1

400X   . VSB 9122S10

200X   VSA 921 0S3

400X   VSA 921 0S3

#3
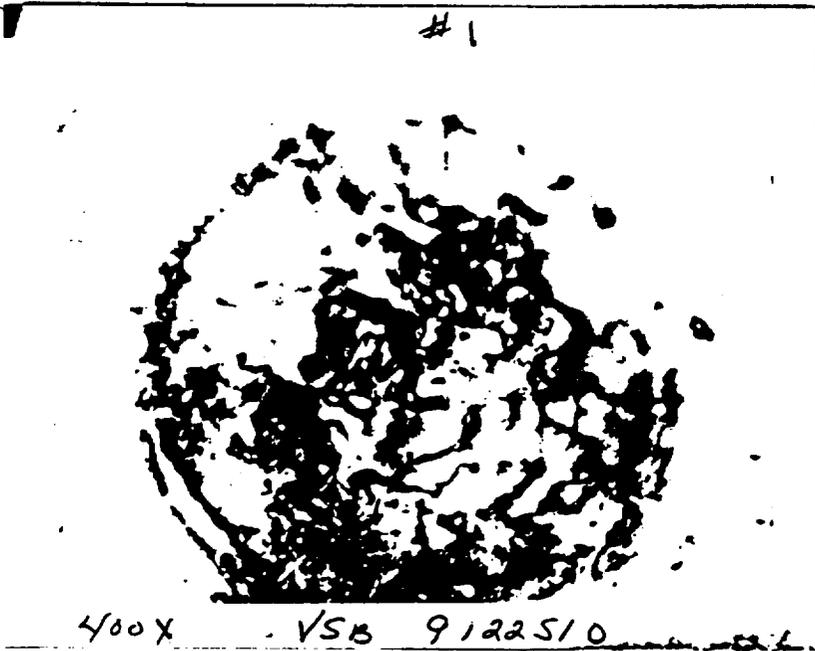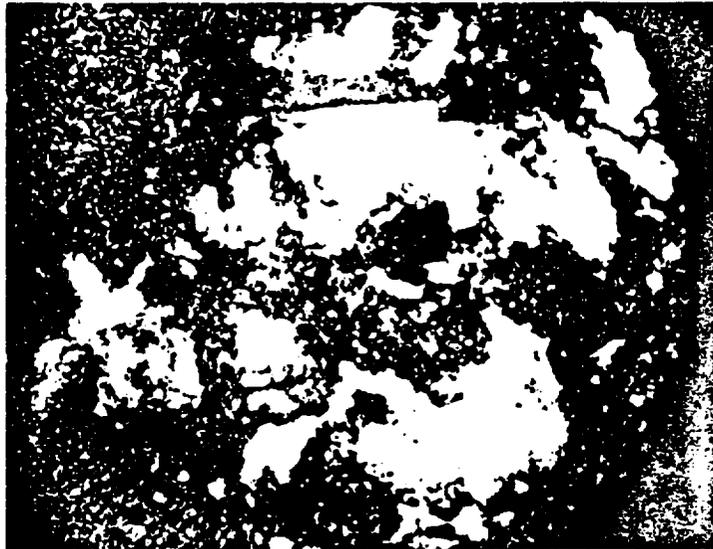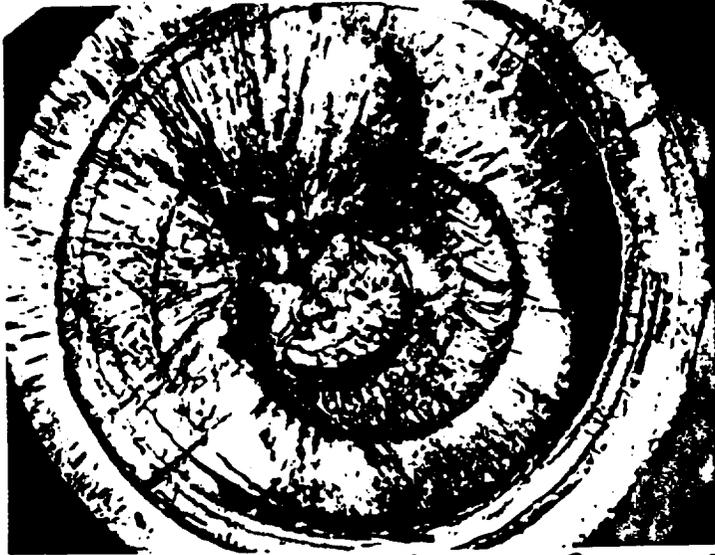
200X   INP   VSB   9122513

#3

400X   INP   VSB   9122513

Appendix C

GUNN DIODE PACKAGING CONSIDERATION FOR PERFORMANCE ENHANCEMENT

Performance of a Gunn diode depends on many factors including the circuit topography, doping profile, active layer thickness in relation to the transit time thickness, the nature of the cathode contact, the efficiency, and in the case of a packaged device, the thermal resistance and the package parasitics. When the circuit topology is known and chip diodes are to be used, then the Gunn diode design may be optimized to obtain the required performance. However, when chip diodes cannot be used, then the package design must be considered as a part of the Gunn diode design.

Ideally, the package must have zero parasitics and infinite thermal conductivity. In practice, packages tend to have finite thermal conductivity and non-trivial parasitics - especially at mm wave frequencies.

One of the most important design considerations for a Gunn diode is the thermal resistance. The thermal resistance of a packaged diode consists of two components:

- Intrinsic Thermal Resistance due to the chip and
- Extrinsic Thermal Resistance due to the package

The thermal resistance, θ_T, of a chip shown in Figure C-1 is given by:

$$\theta_T = \theta_N + \theta_C + \theta_S$$

where θ_N, θ_C, and θ_S are the thermal resistances of the active layer, the contact layer and the spreading thermal resistance into the infinite heat sink of the package respectively. It may be shown that θ_N, θ_C, and θ_S are given by:

$$\theta_N = (T_2/P_D) * \{\exp(\alpha_2) - 1\}$$

$$\theta_C = (T_1/P_D) * \{\exp(\alpha_1) - 1\}$$

$$\theta_S = (2/(\pi * K_1 * d_1))$$

where

$$\alpha_1 = (P_D * l_2/A * C)$$

$$\alpha_2 = (P_D * l_1/2 * A * C)$$

l_1, l_2 = active and contact layer thickness respectively

A = area of the diode = $\pi * d_1^2/4$

d_1 =   diameter of the chip

C   =   a constant = 150 W/cm for GaAs

T_1 =   temperature of contact layer -Pkg interface in °K

T_2 =   temperature of contact layer -active layer interface

Of these terms, the thermal resistance of the chip due to the contact and the active layers are area dependent while the spreading thermal resistance is diameter dependent. Because of the diameter dependence, there is a possibility to reduce the thermal resistance by spreading the area over many mesas or even by an annular ring.

Figures C-2 and C-3 show the reduction in thermal resistance due to multi mesas and due to the annular ring geometry respectively. To achieve a 40% reduction in thermal resistance with 4 mesas, the mesas have to be spread apart by about 6-8 time the radius of the diode. As an example, a realistic number for a single chip mesa diameter is 100 μm. To get an equivalent area with 4 mesas , the individual mesa diameter has to be 50 μm. Then, the separation between the mesas has to be about 175 μm. Thus, the chip size will be about 350 μm x 350 μm. Strapping the chips to fabricate a diode will result in rather a large lead inductance. In addition, the mesas have to be linked together which will also add to the inductance.

Similarly, to achieve a 40% reduction in thermal resistance using an annular geometry we need to have an aspect ratio of 2.5. With this aspect ratio, the width of the annual ring is about 24 μm when we consider the 100 μm diameter diode as example as in the earlier section. The diameter of the annular ring is 103 μm.

Thermal resistance reduction for the total diode may be realized by using high thermal conductivity heat sinks rather than by using multi-mesas or using annular ring geometries.

Figure C-4 shows the thermal conductivity of natural diamond IIa and synthetic diamond Ib as a function of temperature. As may be readily seen, the thermal conductivity is about 3 times larger than that of copper. Naturally, this will lead to a large reduction in the thermal resistance but more importantly to a reduction of the diode junction temperature.

The thermal resistance due to spreading, θ_S, into the heat sink is:

$$\theta_S \quad = \quad 2/(\pi * K_1 * d_1)$$

where

K_1 =   thermal conductivity of the heat sink
d_1 =   diode diameter

Now, the total thermal resistance, θ_T, for a diode diameter of 100 μm, active layer thickness of 2.50 μm, a contact layer thickness of 0.5 μm with a power dissipation of 5 Watts is :

$$\theta_T \quad = \quad 22.9 \text{ °C/W} \quad \text{for copper as heat sink}$$

$$= \quad 11.5 \text{ °C/W} \quad \text{for diamond IIa or Ib as the heat sink}$$

RF Equivalent Circuit of the Package

Figure C-5 shows the equivalent circuit of the package. Essentially, it consists of a capacitance of about 0.14 pf due to the alumina ceramic of outer diameter of .032", a wall thickness of 0.008" and a height of .010". The inductance is due to the strap and is of the order of 0.1 nH.

If the ceramic of the package is replaced by quartz with a dielectric constant of 3, the parasitic capacitance will be reduced to about 0.05 pF. The replacement of alumina with quartz will allow the diode to operate at a higher frequency.
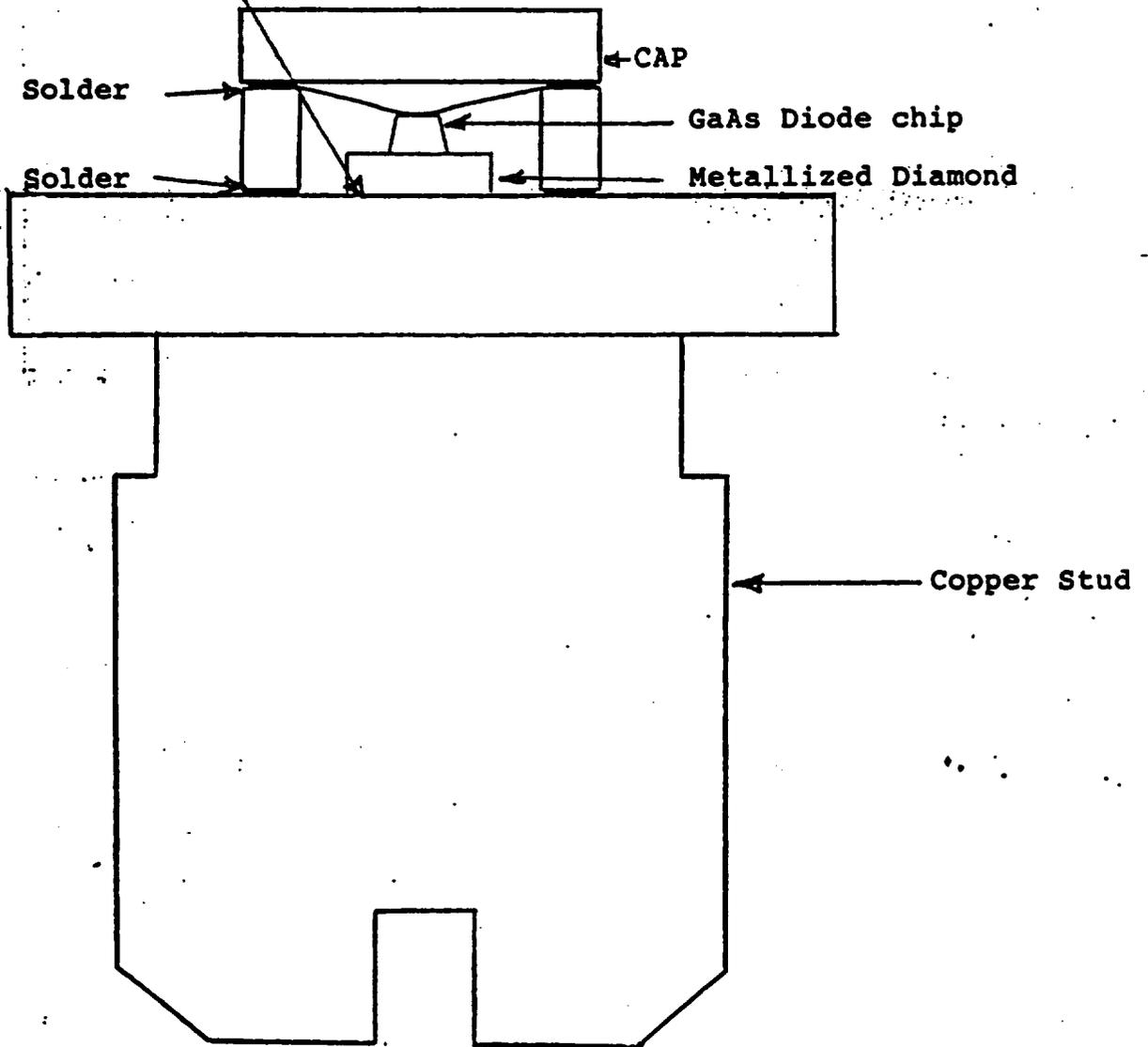
Figure C-1   Hermetically Sealable Diamond Heat Sink Package
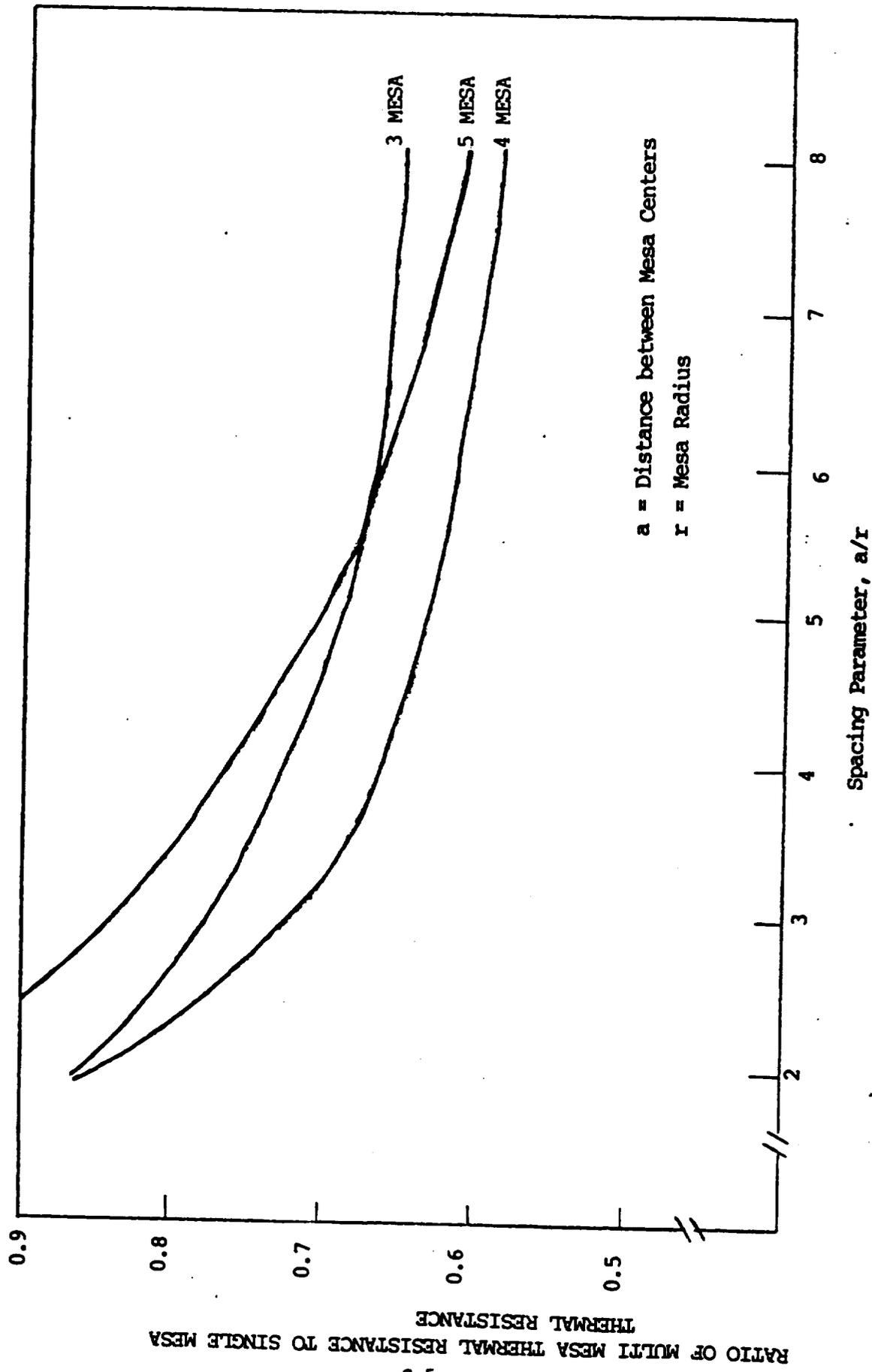
Figure C-2   Thermal Resistance Ratio of Multi Mesa Structure to Single Mesa with same Total Area Vs. Spacing Parameter.

Figure C-3   Thermal Resistance Ratio of Annular Mesa Structure to Single Mesa
with same Area Vs. Annulus Aspect Ratio

The chart plots "Ratio of Annulus Thermal Resistance To Single Mesa Thermal Resistance" (0.4 to 0.8) versus "Annulus Aspect Ratio, $R_1 / (R_2 - R_1)$" (2 to 6).
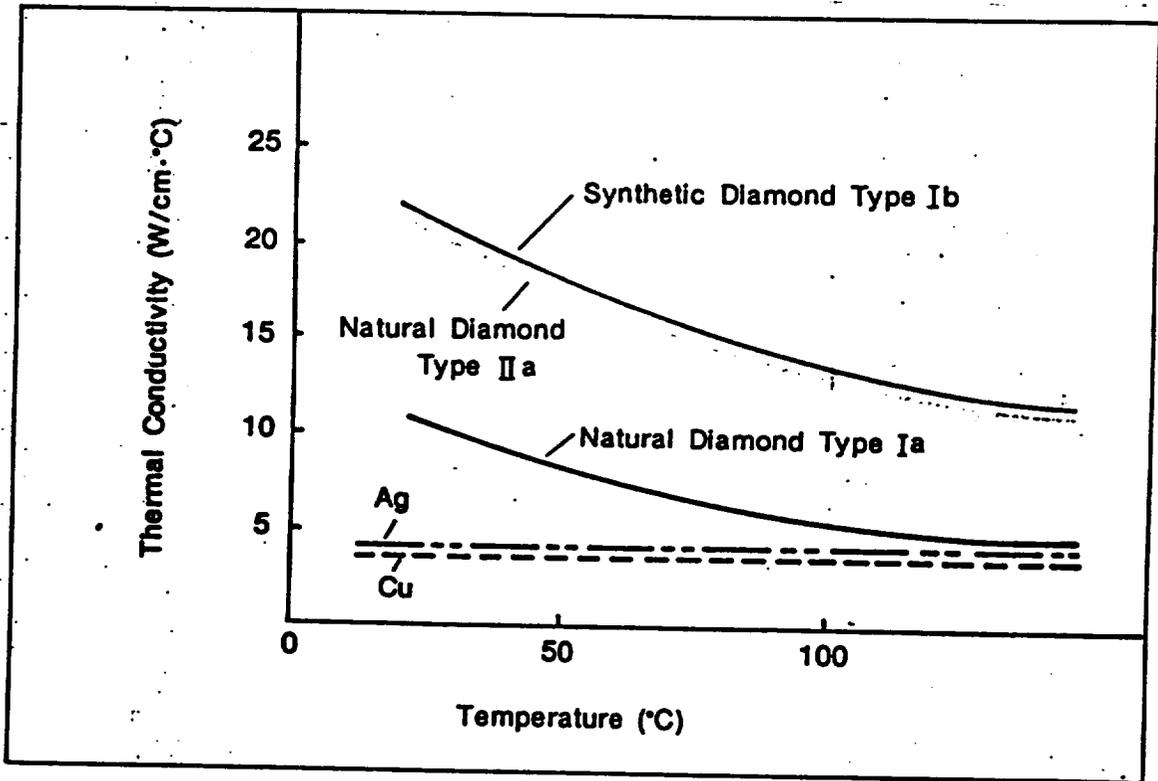
Figure C-4 Thermal Conductivity of Various Heat Sink Materials as a function of Temperature
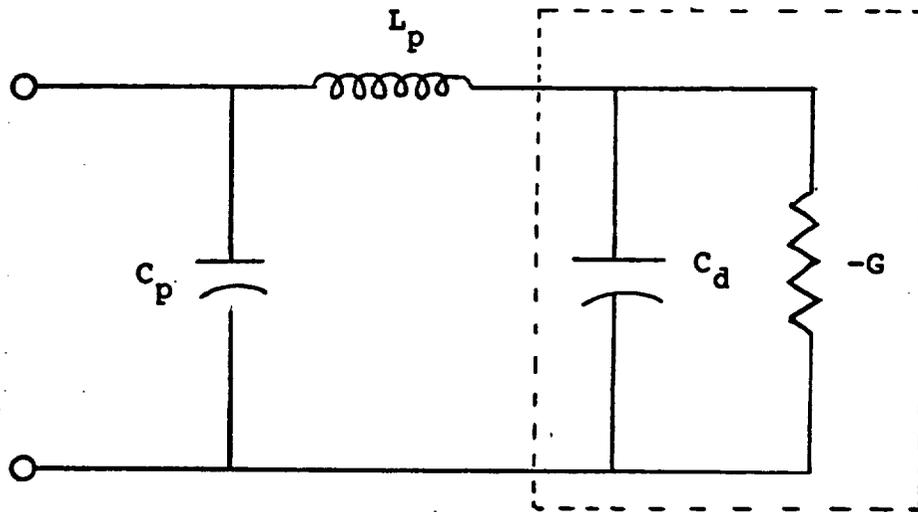
Figure C-5   Equivalent Circuit of Gunn Diode

NASA

National Aeronautics and Space Administration

Report Documentation Page

1. Report No.	2. Government Accession No.	3. Recipient's Catalog No.

4. Title and Subtitle	5. Report Date
SUBMILLIMETER SOURCES FOR RADIOMETRY USING HIGH POWER INDIUM PHOSPHIDE GUNN OSCILLATORS	February 1990
	6. Performing Organization Code

7. Author(s)	8. Performing Organization Report No.
NARESH C. DEO	A565 TR 1990
	10. Work Unit No.

9. Performing Organization Name and Address	11. Contract or Grant No.
MILLITECH CORPORATION P.O. BOX 109 SOUTH DEERFIELD, MA 01373	NAS7-996
	13. Type of Report and Period Covered

12. Sponsoring Agency Name and Address	Final Report Apr. 1987-Dec. 1989
National Aeronautics and Space Administration, Washington, D.C. 20546-0001 NASA Resident Office - Jet Propulsion Lab	14. Sponsoring Agency Code

15. Supplementary Notes

16. Abstract

Study aimed at developing high frequency millimeter wave and submillimeter wave local oscillator sources in the 60-600 GHz range was conducted. Sources involved both fundamental and harmonic-extraction type Indium Phosphide Gunn diode oscillators as well as varactor multipliers. In particular, a high power balanced-doubler using varactor diodes was developed for 166 GHz. It is capable of handling 100 mW input power, and typically produced 25 mW output power. A high frequency tripler operating at 500 GHz output frequency was also developed, and cascaded with the balanced-doubler. A dual-diode InP Gunn diode combiner was used to pump this cascaded multiplier to produce on the order of 0.5 mW at 500 GHz.

In addition, considerable development and characterization work on InP Gunn diode oscillators was carried out. Design data and operating characteristics were documented for a very wide range of oscillators. The reliability of InP devices was examined, and packaging techniques to enhance the performance were analyzed. A theoretical study of a new class of high power multipliers was conducted for future applications. The sources developed here find many commercial applications for radio astronomy and remote sensing.

17. Key Words (Suggested by Author(s))	18. Distribution Statement
Indium Phosphide Gunn diodes Millimeter wave sources, Local Oscillators, Submillimeter wave sources, Space borne reliability of oscillators	

19. Security Classif. (of this report)	20. Security Classif. (of this page)	21. No. of pages	22. Price
UNCLASSIFIED	UNCLASSIFIED	107	

NASA FORM 1626 OCT 86